43334

National Library of Canada | Bibliothèque nationale du Canada | CANADIAN THESES ON MICROFICHE | THÈSES CANADIENNES SUR MICROFICHE

NAME OF AUTHOR/NOM DE L'AUTEUR STANLEY JOHN BACKS

TITLE OF THESIS/TITRE DE LA THÈSE NUCLEAR MAGNETIC RESONANCE STUDIES OF THE SOLUTION CHEMISTRY OF AQUEOUS TRIMETHYLLEAD AND ITS COMPLEXES WITH SULFHYDRYL LIGANDS

UNIVERSITY/UNIVERSITÉ UNIVERSITY OF ALBERTA

DEGREE FOR WHICH THESIS WAS PRESENTED/ GRADE POUR LEQUEL CETTE THÈSE FUT PRÉSENTÉE MASTER of SCIENCE

YEAR THIS DEGREE CONFERRED/ANNÉE D'OBTENTION DE CE GRADE 1979

NAME OF SUPERVISOR/NOM DU DIRECTEUR DE THÈSE DR. DALLAS L. RABENSTEIN

Permission is hereby granted to the NATIONAL LIBRARY OF CANADA to microfilm this thesis and to lend or sell copies of the film.

The author reserves other publication rights, and neither the thesis nor extensive extracts from it may be printed or otherwise reproduced without the author's written permission.

*L'autorisation est, par la présente, accordée à la BIBLIOTHÈQUE NATIONALE DU CANADA de microfilmer cette thèse et de prêter ou de vendre des exemplaires du film.*

*L'auteur se réserve les autres droits de publication; ni la thèse ni de longs extraits de celle-ci ne doivent être imprimés ou autrement reproduits sans l'autorisation écrite de l'auteur.*

DATED/DATÉ JUNE 25, 1979 SIGNED/SIGNÉ [signature]

PERMANENT ADDRESS/RÉSIDENCE FIXÉ BOX 874
HIGH PRAIRIE, ALTA.
T0G 1E0

NL-91 (3-74)

National Library of Canada

Cataloguing Branch
Canadian Theses Division

Ottawa, Canada
K1A 0N4

Bibliothèque nationale du Canada

Direction du catalogage
Division des thèses canadiennes

## NOTICE

The quality of this microfiche is heavily dependent upon the quality of the original thesis submitted for microfilming. Every effort has been made to ensure the highest quality of reproduction possible.

If pages are missing, contact the university which granted the degree.

Some pages may have indistinct print especially if the original pages were typed with a poor typewriter ribbon or if the university sent us a poor photocopy.

Previously copyrighted materials (journal articles, published tests, etc.) are not filmed.

Reproduction in full or in part of this film is governed by the Canadian Copyright Act, R.S.C. 1970, c. C-30. Please read the authorization forms which accompany this thesis.

THIS DISSERTATION
HAS BEEN MICROFILMED
EXACTLY AS RECEIVED

## AVIS

La qualité de cette microfiche dépend grandement de la qualité de la thèse soumise au microfilmage. Nous avons tout fait pour assurer une qualité supérieure de reproduction.

S'il manque des pages, veuillez communiquer avec l'université qui a conféré le grade.

La qualité d'impression de certaines pages peut laisser à désirer, surtout si les pages originales ont été dactylographiées à l'aide d'un ruban usé ou si l'université nous a fait parvenir une photocopie de mauvaise qualité.

Les documents qui font déjà l'objet d'un droit d'auteur (articles de revue, examens publiés, etc.) ne sont pas microfilmés.

La reproduction, même partielle, de ce microfilm est soumise à la Loi canadienne sur le droit d'auteur, SRC 1970, c. C-30. Veuillez prendre connaissance des formules d'autorisation qui accompagnent cette thèse.

LA THÈSE A ÉTÉ
MICROFILMÉE TELLE QUE
NOUS L'AVONS REÇUE

NL-339 (3/77)

T H E  U N I V E R S I T Y  O F  A L B E R T A

# NUCLEAR MAGNETIC RESONANCE STUDIES OF THE SOLUTION CHEMISTRY OF AQUEOUS TRIMETHYLLEAD AND ITS COMPLEXES WITH SULFHYDRYL LIGANDS

by

© STANLEY JOHN BACKS

A THESIS

SUBMITTED TO THE FACULTY OF GRADUATE STUDIES AND RESEARCH

IN PARTIAL FULFILMENT OF THE REQUIREMENTS FOR THE DEGREE

OF MASTER OF SCIENCE

DEPARTMENT OF CHEMISTRY

EDMONTON, ALBERTA

FALL, 1979

THE UNIVERSITY OF ALBERTA

FACULTY OF GRADUATE STUDIES AND RESEARCH

The undersigned certify that they have read, and recommend to the Faculty of Graduate Studies and Research, for acceptance, a thesis entitled NUCLEAR MAGNETIC RESONANCE STUDIES OF THE SOLUTION CHEMISTRY OF AQUEOUS TRIMETHYLLEAD AND ITS COMPLEXES WITH SULFHYDRYL LIGANDS submitted by STANLEY JOHN BACKS in partial fulfilment of the requirements for the degree of Master of Science.

Dalla L Rabenstein

D. L. Rabenstein (supervisor)

F. F. Cantwell

H. J. Kass (External Examiner)

DATE June 20, 1979

To my parents

and

to my Kathy

## ABSTRACT

The aqueous solution chemistry of trimethyllead(IV) and of the trimethyllead(IV) complexes of selected organic ligands has been investigated by proton magnetic resonance spectroscopy. The formation constants for the $(CH_3)_3Pb^+$ complexes of hydroxide ion and of the various sulfhydryl and carboxyl functional groups of 2-mercaptoethanol, glycine, N-acetyl-D,L-penicillamine, D,L-penicillamine, L-cysteine and glutathione were determined from the pH dependence of the chemical shift of the methyl protons of trimethyllead. One-to-one stoichiometry was dominant in all experimental cases. In addition, weak two-to-one metal-to-ligand complexes were observed for the trimethyllead complexes of hydroxide ion and of the sulfhydryl groups of 2-mercaptoethanol and glutathione. No evidence of amino group complexation by trimethyllead was found. The formation constants of the carboxylate complexes and of the various two-to-one metal-to-ligand complexes are small, while those of the sulfhydryl complexes of one-to-one stoichiometry are generally several orders of magnitude higher. The extent of complex formation is strongly pH dependent due to the competitive effects of ligand functional group protonation at neutral or low pH and $(CH_3)_3PbOH$ formation at high pH. This pH dependence is illustrated by calculations of the species distributions and the conditional formation

constants of the various complexes as functions of pH. The trimethyllead chemical shifts of the sulfhydryl and carboxylate complexes are found further upfield and the formation constants increase as the $pK_a$ of the ligand functional group increases. To some extent, other factors such as steric and electrostatic effects also appear to influence these parameters.

ACKNOWLEDGEMENTS

I wish to express my sincere thanks to Dr. D. L. Rabenstein for his guidance, encouragement and patience during the course of my research.

I also wish to express my appreciation of the indispensable advice and assistance provided by Dr. C. A. Evans during a portion of my work.

I am indeed grateful to my colleagues in the research group, past and present, for their valuable advice and for many helpful discussions. Deserving of special thanks for their unfaltering encouragement and support are my friends and family, especially those to whom this volume is dedicated.

Sincere thanks are also extended to Mrs. L. Ziola for her helpfulness and her excellent secretarial work.

The financial support of a Water Resources Research Support Program Grant from the Inland Waters Directorate, Environment Canada and the University of Alberta is gratefully acknowledged.

TABLE OF CONTENTS


| CHAPTER | | PAGE |
|---|---|---|
| | LIST OF TABLES | xii |
| | LIST OF FIGURES | xiii |
| I. | INTRODUCTION | 1 |
| | A. Sources and Toxic Action of Trimethyllead | 2 |
| | 1. Trimethyllead in the Environment | 2 |
| | 2. Trimethyllead Toxicology | 4 |
| | B. The Coordination Chemistry of Trimethyllead | 7 |
| | 1. The Structure and Bonding of Trimethyllead Complexes | 7 |
| | 2. Formation Constants of Trimethyllead Complexes in Aqueous Solution | 11 |
| | C. The Present Study | 15 |
| II. | EXPERIMENTAL | 16 |
| | A. Chemicals | 16 |
| | B. Preparation and Standardization of Trimethyllead Perchlorate Solutions | 17 |
| | C. Preparation and Standardization of Ligand Solutions | 22 |
| | D. pH Measurements | 26 |
| | E. Proton Nuclear Magnetic Resonance Measurements | 26 |
| | F. Carbon-13 Nuclear Magnetic Resonance Measurements | 27 |
| | G. Solutions for Nuclear Magnetic Resonance Measurements | 28 |

CHAPTER PAGE

H. Determination of Formation Constants by NMR Spectroscopy ..... 30

I. Determination of Acid Dissociation Constants of Selected Ligands ..... 33

1. Determination by NMR Measurements ..... 33

2. Determination by pH Titration ..... 34

III. TRIMETHYLLEAD SPECIES AND EQUILIBRIA IN AQUEOUS SOLUTION ..... 37

A. The Stability of Trimethyllead in Aqueous Solution ..... 37

1. Introduction ..... 37

2. Results and Discussion ..... 38

B. The Acid-Base Chemistry of Trimethyllead ..... 40

1. Introduction ..... 40

2. Results and Discussion ..... 42

(a) Determination of Species Present in Aqueous Trimethyllead Solutions .. 44

(b) Determination of the Formation Constants of Trimethyllead Hydroxide Complexes ..... 47

IV. THE TRIMETHYLLEAD COMPLEXES OF SELECTED THIOLS AND AMINO ACIDS ..... 56

A. Introduction ..... 56

B. Results ..... 57

1. 2-Mercaptoethanol Complexes ..... 57

CHAPTER PAGE

(a) The Acid Dissociation Constant of 2-Mercaptoethanol ..... 57

(b) The 2-Mercaptoethanol Complexes of Trimethyllead ..... 62
*(i) Qualitative Observations* ..... 62
*(ii) Derivation of a Mathematical Model for the 2-Mercapto-ethanol-Trimethyllead System*.. 65
*(iii) Computer Optimization of Formation Constants and Chemical Shifts of Trimethyllead Complexes* ..... 70
*(iv) Computed Results* ..... 73

2. Glycine Complexes ..... 74

(a) The Acid Dissociation Constants of Glycine ..... 74

(b) The Glycine Complexes of Trimethyl-lead ..... 77

3. N-Acetyl-D,L-Penicillamine Complexes ..... 81

(a) The Acid Dissociation Constants of N-Acetyl-D,L-Penicillamine ..... 81

(b) The N-Acetyl-D,L-Penicillamine Complexes of Trimethyllead ..... 83

4. D,L-Penicillamine Complexes..... 88

(a) The Macroscopic Acid Dissociation Constants of D,L-Penicillamine ..... 88

(b) The Microscopic Acid Dissociation Constants of D,L-Penicillamine ..... 94

(c) The D,L-Penicillamine Complexes of Trimethyllead ..... 96

5. L-Cysteine Complexes .....103

(a) The Macroscopic Acid Dissociation Constants of L-Cysteine .....103

(b) The Microscopic Acid Dissociation Constants of L-Cysteine .....104

CHAPTER PAGE

(c) The L-Cysteine Complexes of Trimethyllead ..... 107

6. Glutathione Complexes ..... 111

(a) The Acid Dissociation Constants of Glutathione ..... 111

(b) Glutathione Complexes of Trimethyllead ..... 115

*(i) Proton NMR Results* ..... 115
*(ii) Carbon-13 NMR Results* ..... 120

C. Discussion ..... 125

1. The pH Dependence of the Complexation of Trimethyllead by Organic Ligands ..... 128

(a) Conditional Formation Constants as Functions of pH ..... 128

(b) Species Distributions as Functions of pH ..... 136

2. Other Factors Influencing the Complexation of Trimethyllead by Organic Ligands ..... 145

3. Conclusions ..... 155

BIBLIOGRAPHY ..... 156

## LIST OF TABLES


| Table | Description | Page |
|---|---|---|
| I | Measured Formation Constants of Aqueous Trimethyllead Complexes | 12 |
| II | Selected Macroscopic $K_a$ Values of D,L-Penicillamine | 91 |
| III | Selected Macroscopic $K_a$ Values of L-Cysteine | 105 |
| IV | Ionization Constants of Glutathione | 114 |
| V | Formation Constants of the Trimethyllead, Proton, $Pb^{++}$ and Methylmercury Complexes with the Sulfhydryl Groups of Several Organic Ligands and the Chemical Shifts vs. DSS of the Trimethyllead Complexes | 126 |
| VI | Formation Constants, $pK_a$ Values and Chemical Shifts of the Carboxylate Complexes and the Two to One Sulfhydryl Complexes of Trimethyllead | 127 |

## LIST OF FIGURES


| Figure | Description | Page |
|---|---|---|
| 1. | Proton nmr spectrum of the methyl groups of trimethyllead in 0.140 M solution at approximately neutral pH. | 41 |
| 2. | pH dependence of the chemical shift of the methyl protons of trimethyllead in a 0.0100 M aqueous solution at 0.3 M ionic strength (maintained with $NaClO_4$). | 43 |
| 3. | pH dependence of the trimethyllead species distribution in a 0.100 M aqueous solution, calculated using $K_1$ and $K_2$ as in the text. | 52 |
| 4. | pH dependence of the trimethyllead species distribution in a $5.00 \times 10^{-3}$ M aqueous solution, calculated using $K_1$ and $K_2$ as in the text. | 53 |
| 5. | pH dependence of the chemical shift of the $-OCH_2-$ and the $-CH_2S-$ multiplet resonances for a 0.139 M solution of 2-mercaptoethanol at 25°C and 0.3 M ionic strength (maintained with $NaClO_4$). | 61 |
| 6. | pH dependence of the chemical shift of trimethyllead in a sulfhydryl-free 0.0100 M aqueous solution (Δ) and in solutions of 0.0100 M trimethyllead and 0.0200 M 2-mercaptoethanol (●), 0.0100 M trimethyllead and | 63 |

| Figure | Description | Page |
|---|---|---|
| | 0.00970 M 2-mercaptoethanol (◆), and 0.0200 M trimethyllead and 0.0100 M 2-mercaptoethanol (■). Ionic strength was controlled at 0.3 M with $NaClO_4$ and temperature was 25°C. | |
| 7. | The dependence of the chemical shift of trimethyllead upon the ratio of 2-mercaptoethanol to trimethyllead in solution at pH 8.0. The concentration of ligand was 0.00887 M except at the ratio of zero to one. The ionic strength was maintained at 0.3 M with $NaClO_4$ and the temperature was 25°C. | 64 |
| 8. | Flow chart of the computer procedure employed to optimize the formation constants and chemical shifts of the 2-mercaptoethanol complexes of trimethyllead. | 71 |
| 9. | pH dependence of the chemical shift of the methylene protons of glycine in a 0.100 M solution at 25°C and 0.3 M ionic strength (maintained with $NaClO_4$). | 75 |
| 10. | pH dependence of the chemical shift of trimethyllead at 25°C and 0.3 M ionic strength (maintained with $NaClO_4$) in a solution of 0.0100 M trimethyllead only (△) and in a solution containing 0.0100 M trimethyllead and 0.100 M glycine (◆). | 78 |

| Figure | Description | Page |
|---|---|---|
| 11. | pH dependence of the chemical shift of trimethyllead at 25°C and 0.3 M ionic strength (maintained with $NaClO_4$) in solutions of 0.0100 M trimethyllead only (Δ), 0.0100 M trimethyllead and 0.0198 M N-acetyl-D,L-penicillamine (◆), and 0.0100 M trimethyllead and 0.0395 M N-acetyl-D,L-penicillamine (■). | 85 |
| 12. | pH dependence of the chemical shift of trimethyllead at 25°C and 0.3 M ionic strength (maintained with $NaClO_4$) in solutions of 0.0100 M trimethyllead only (Δ), 0.00498 M trimethyllead and 0.00996 M D,L-penicillamine (◆), and 0.00500 M trimethyllead and 0.0199 M D,L-penicillamine (●). | 97 |
| 13. | pH dependence of the chemical shift of the methyl protons of D,L-penicillamine at 25°C and 0.3 M ionic strength (maintained with $NaClO_4$) in a solution of 0.00498 M trimethyllead and 0.00996 M D,L-penicillamine. | 98 |
| 14. | pH dependence of the chemical shift of trimethyllead at 25°C and 0.3 M ionic strength (maintained with $NaClO_4$) in solutions of 0.0100 M trimethyllead only (Δ), 0.00499 M trimethyllead and 0.00949 M L-cysteine (◆) | 108 |

| Figure | Description | Page |
|---|---|---|
| | and 0.00502 M trimethyllead and 0.0190 M L-cysteine (●). | |
| 15. | Microscopic ionization scheme for glutathione, considering only the predominant species present (124). See text for labelling of the acidic groups and definition of the subscripts. | 113 |
| 16. | pH dependence of the chemical shift of trimethyllead at 25°C and 0.3 M ionic strength (maintained with $NaClO_4$) in solutions of 0.0100 M trimethyllead only (△), 0.00501 M trimethyllead and 0.00973 M glutathione (●), 0.00501 M trimethyllead and 0.0194 M glutathione (◆) and 0.0749 M trimethyllead and 0.146 M glutathione (■). | 116 |
| 17. | Microscopic ionization and trimethyllead complexation scheme for glutathione in solutions of low metal to ligand ratios. | 118 |
| 18. | pH dependence of the carbon-13 chemical shift of selected carbons of glutathione at 25°C in a solution (117,128) of 0.21 M glutathione only (dashed lines) and at 0.4 M ionic strength (maintained with $NaClO_4$) in a solution of 0.146 M glutathione and 0.0947 M trimethyllead (circles). | 122 |

| Figure | Description | Page |
|---|---|---|
| | Positive chemical shifts indicate the resonances are upfield of dioxane. | |
| 19. | pH dependence of the carbon-13 chemical shift of selected carbons of glutathione at 25°C in a solution (117,128) of 0.21 M glutathione only (dashed lines) and at 0.4 M ionic strength (maintained with $NaClO_4$) in a solution of 0.146 M glutathione and 0.0947 M trimethyllead (circles). Positive chemical shifts indicate the resonances are upfield of dioxane. | 123 |
| 20. | pH dependence of the carbon-13 chemical shift (vs. dioxane) of 0.0947 M trimethyllead in solution with 0.146 M glutathione at 25°C and 0.4 M ionic strength (maintained with $NaClO_4$). Positive chemical shifts indicate the resonances are upfield of dioxane. | 124 |
| 21. | Conditional formation constants of the 2-mercaptoethanol complexes of trimethyllead as functions of pH at 25°C and 0.3 M ionic strength. | 130 |
| 22. | Conditional formation constants of the glycine complexes of trimethyllead as functions of pH at 25°C and 0.3 M ionic strength. | 131 |

| Figure | Description | Page |
|---|---|---|
| 23. | Conditional formation constants of the N-acetyl-D,L-penicillamine complexes of trimethyllead as functions of pH at 25°C and 0.3 M ionic strength. | 132 |
| 24. | Conditional formation constants of the D,L-penicillamine complexes of trimethyllead as functions of pH at 25°C and 0.3 M ionic strength. | 133 |
| 25. | Conditional formation constants of the L-cysteine complexes of trimethyllead as functions of pH at 25°C and 0.3 M ionic strength. | 134 |
| 26. | Conditional formation constants of the glutathione complexes of trimethyllead as functions of pH at 25°C and 0.3 M ionic strength. | 135 |
| 27. | pH dependence of the trimethyllead (upper plot) and 2-mercaptoethanol (lower plot) species distribution in a solution containing 0.005 M trimethyllead and 0.010 M ligand at 25°C and 0.3 M ionic strength. Symbols are defined as in Equations 13 and 40. | 138 |
| 28. | pH dependence of the trimethyllead (upper plot) and glycine (lower plot) species distribution in a solution containing 0.005 M | 139 |

| Figure | Description | Page |
|---|---|---|
| | trimethyllead and 0.010 M ligand at 25°C and 0.3 M ionic strength. Symbols are defined as in Equations 13 and 55 - 60. | |
| 29. | pH dependence of the trimethyllead (upper plot) and N-acetyl-D,L-penicillamine (lower plot) species distribution in a solution containing 0.005 M trimethyllead and 0.010 M ligand at 25°C and 0.3 M ionic strength. Sumbols are defined as in Equations 13 and 66. | 140 |
| 30. | pH dependence of the trimethyllead (upper plot) and D,L-penicillamine (lower plot) species distribution in a solution containing 0.005 M trimethyllead and 0.010 M ligand at 25°C and 0.3 M ionic strength. Symbols are defined as in Equations 13 and 87. | 141 |
| 31. | pH dependence of the trimethyllead (upper plot) and L-cysteine (lower plot) species distribution in a solution containing 0.005 M trimethyllead and 0.010 M ligand at 25°C and 0.3 M ionic strength. Symbols are defined as in Equations 13 and 97. | 142 |
| 32. | pH dependence of the trimethyllead (upper plot) and glutathione (lower plot) species distribution in a solution containing | 143 |

| Figure | Description | Page |
|---|---|---|
| | 0.005 M trimethyllead and 0.010 M ligand at 25°C and 0.3 M ionic strength. Symbols are defined as in Equation 13 and Figure 17. | |
| 33. | The dependence of the logarithm of the trimethyllead complex formation constant upon the $pK_a$ values of the respective free ligands. Complexes shown are those studied in this work (○) and in references 62 (◇) and 63 (□). | 147 |
| 34. | The dependence of the chemical shift of the trimethyllead methyl protons in certain trimethyllead complexes upon the $pK_a$ values of the respective free ligands. Complexes shown are those studied in this work (○) and in references 62 (◇) and 63 (□). | 153 |

# CHAPTER I

## INTRODUCTION

Inorganic lead, in the forms of metallic lead and lead salts, has been familiar to mankind since ancient times. In contrast, compounds which include a lead-carbon bond were unknown until 1853, when Loewig published a series of papers describing the synthesis of several organolead compounds (1,2,3). Included were the first reports of organolead salts of the type $R_3PbX$, X being an inorganic anion. In 1860, Klippel prepared a number of similar compounds using organic anions (4). From these origins, organolead chemistry has developed into one of the largest areas of organometallic chemistry, exceeded only by those of tin, silicon and mercury (6). This prominence is primarily due to the utility (and hence, large scale production) of various organolead compounds as antiknock additives for internal combustion engine fuels (7), a property first reported in 1922 (8).

The most recent comprehensive reviews of organolead chemistry (5,9) and the annual reviews published by the Journal of Organometallic Chemistry demonstrate the preponderance of synthetic and non-aqueous chemistry in the organolead literature. Relatively little is understood of the aqueous coordination chemistry of organolead compounds; this is especially true of the cationic

triorganolead species. However, recent studies of the environmental, toxicological and chemical behaviour of such compounds have emphasized the need for a greater understanding of the properties of aqueous triorganolead. Partial fulfillment of this need is presented in this thesis, a study of the aqueous solution chemistry of trimethyllead (the simplest of the triorganolead cations) and of its complexes with a number of organic ligands.

## A. Sources and Toxic Action of Trimethyllead

### 1. Trimethyllead in the Environment

Several independent processes are thought to be responsible for the environmental formation and accumulation of triorganolead compounds. Atmospheric contamination with organolead compounds arises primarily from the vaporization of unburned gasoline additives (10,11), the main sources being open-air transfer of fuel between containers and incomplete combustion of fuel and waste oil. In addition, organolead compounds are being employed as biocidal agents, as chemical catalysts and as stabilizers for PVC plastics, as well as in lubricating oils, in electroplating processes and in a number of polymerization procedures (10,12). The manufacture, use and ultimate disposal of such products results in further contamination of the atmosphere, soils and natural waters.

Triorganolead compounds form only a portion of the

total organolead released to the environment. However, some of the other organolead compounds are thermodynamically unstable (13), being decomposed by light or by air oxidation at fairly low temperatures (14). Toxic triorganolead compounds are rather stable intermediates in such decompositions.

It should also be noted that organolead compounds account for only a fraction of all lead pollution. Extensive commercial use of lead in many forms (10) has resulted in significant environmental concentrations of inorganic lead. A major contributing factor is the complete combustion of organolead gasoline additives, with the resultant formation of inorganic lead compounds (12). Indeed, only a few percent of the total lead in urban atmospheres is organolead; the remainder is inorganic lead particulate matter (15). However, many of these lead compounds can be methylated by mixed microbial communities in lake sediments (16-18); a general mechanism for lead biomethylations has been proposed (19). Since most of the lead released by man eventually is trapped in soils and sediments (20) where such microbes flourish, appreciable amounts of trimethyllead and tetramethyllead may be formed in this way. In addition, tri- and tetraorganolead compounds may be produced by disproportionation of diorganoleads (18).

The multiplicity of interconversion mechanisms of

organic and inorganic lead compounds has caused significant uncertainty in the estimates of environmental triorganolead concentrations. Nonetheless, these compounds are sufficiently toxic to warrant concern, especially since higher concentrations are expected in densely populated areas (10,11,20).

## 2. Trimethyllead Toxicology

Inorganic lead poisoning is relatively common and its toxic effects and treatment with chelating agents have been well documented (11). In contrast, the incidence of acute organolead poisoning is low; hence, much less is understood of its toxicology and treatment. It is known, however, that standard chelation therapy with 2,3-dimercaptopropanol (BAL), EDTA or penicillamine is ineffective (21-24) except for cases of diorganolead poisoning, which respond to treatment with BAL (23,24). Almost nothing is known of the effects of long term low level exposure to organoleads (11,21).

Tetra- and triorganolead compounds induce distinctive toxic effects unrelated to the toxicity of inorganic lead (22). Tetraorganoleads appear to be relatively inert in themselves, but considerable evidence indicates that "in vivo" decomposition of these compounds occurs (primarily in the liver), forming triorganolead salts, the ultimate toxic agents (21-29). Hence, absorption of

tetraorganolead compounds through ingestion, inhalation or skin contact will result in symptoms identical to those of triorganolead poisoning.

The toxic effects of triorganoleads appear to vary according to the degree of lipophilicity of the organolead cation and of the neutral complex (25). It is thought that the primary effect of the relatively hydrophilic trimethyllead species is to promote increased exchange of mitochondrial hydroxide ions for extramitochondrial chloride ions, resulting in swelling and altered organelle function (25,30). Other documented effects include inhibition of mitochondrial oxidative phosphorylation (that is, synthesis of ATP), inhibition of ATP-coupled enzymes which transport sodium and calcium ions, inhibition of glutathione transferases and alteration of mitochondrial membrane permeability (25,30,31). However, the relation of these effects to the dominant action of triorganoleads on the central nervous system is not well understood (25).

All of the above effects are observed primarily during acute triorganolead intoxication, but other physiological disturbances may result from much smaller doses. For example, trimethyllead is known to bind to the phosphate backbone of DNA (32). It is therefore not surprising that trialkylleads are somewhat mutagenic in certain plants and in larval fruit flies (33). No

teratogenicity has been found for such compounds (34), but studies confirming this have not been performed. In addition, low doses of tetraethyllead are carcinogenic towards mice (35); paradoxically, lethally high doses were reported to have a regressive effect on mouse tumors (36). In man, it has been determined that long term contact with tetraethyllead inhibits spermatogenesis (37) and may also result in profound changes in the hemopoietic system (38).

To date, no efficacious therapeutic agent for triorganolead poisoning has been demonstrated conclusively. (An early report claiming dramatic improvement with a mixture of sodium trithiolactate and sodium thiolactate (39) remains unconfirmed.) Fortunately, organolead poisoning is relatively self-limiting in duration: continuous supportive care allows eventual full recovery (21). The development of a rapid and effective therapy is nonetheless an important end, but the prerequisite means to this are a deeper understanding of both the toxic mechanisms and the coordination chemistry of triorganolead compounds.

## B. The Coordination Chemistry of Trimethyllead

### 1. The Structure and Bonding of Trimethyllead Complexes

It is well established that tetramethyllead and other $R_4Pb$ compounds are tetrahedral (40,41). However, cleavage of one lead-carbon bond produces the trimethyllead cation, $(CH_3)_3Pb^+$, which may assume a variety of structures depending on the number and kind of Lewis base molecules coordinated to the lead atom. When only one base is bonded to each cation, as occurs for solutions of trimethyllead salts in non-coordinating solvents, the complexes are four-coordinate pseudotetrahedral monomers (42-44).

In most cases, however, the favored geometry of trialkylleads is five-coordinate trigonal bipyramidal (tbp). Indeed, solid state trimethyllead complexes of one to one stoichiometry commonly exist as polymeric chains of tbp units, with the anions bridging between planar trimethyllead moieties. Examples include the trimethyllead complexes with halides (42,45), methoxide (45), formate, acetate, monochloroacetate and imidazole (43,46), cyanide (48), thiocyanate (44) and several other donor species (49-52). Exceptions to this rule, such as the monomeric thio- and dithioacetate complexes (43), are very uncommon in the literature. X-ray crystallographic studies have confirmed the tbp polymeric structure of solid trimethyllead acetate (53).

Trigonal bipyramidal symmetry is also favored in solutions of these complexes in strong donor solvents. In such solvents, the planar trimethyllead moiety is axially coordinated by two donor molecules, at least one of which is a molecule of solvent. A number of such coordination compounds of trimethyllead have been described (44,49,42,54-57).

The strength of the electron donors is a factor in complexations of this sort. For example, the work of Shier and Drago (57) on trimethyllead perchlorate in pyridine solution showed that the perchlorate anion is not coordinated directly to the lead atom as it is in the solid state, but is replaced in the inner coordination sphere by a second pyridine molecule. Hence, a strong donor solvent molecule may displace the anion of a solid complex to the outer coordination sphere during solvation (58). Water is another solvent which may behave in this manner (52).

Less polar, less strongly coordinating solvents also tend to preserve tbp symmetry in trimethyllead complexes, but by coordination of only one solvent molecule to the lead atom (47). Here the anion remains in the inner sphere of the complex. Little or no solvent coordination occurs in the non-polar solvents, resulting in a tetrahedral trimethyllead-ligand complex (52). However, perfect tbp and tetrahedral conformations are observed

only for certain complexes in the strongest and weakest donor solvents, respectively. Intermediate distorted symmetries may also occur, depending on the differences in donor properties of the ligand and the solvent (59,60).

Water is an almost ideal polar solvent for trimethyllead cations, as it has the necessary qualities of good donor characteristics and a high dielectric constant (13). In aqueous solution the $(CH_3)_3Pb$(IV) moiety is therefore planar (61) and is assumed to be axially coordinated by two water molecules (62). One of these solvating water molecules may be displaced by certain ligands (58,62,63), often without altering the symmetry significantly. (For simplicity, any such waters of solvation are omitted from the molecular formulae of the various aqueous trimethyllead species throughout this thesis.) A consequence of this model is that chelate formation with trimethyllead is not favored; this is consistent with the ineffectiveness of chelation therapy noted earlier.

The symmetry of complexed trimethyllead is a function of the types and strengths of the various metal-ligand bonds. The methyl groups of the aquated trimethyllead cation are coplanar because the lead s-orbital tends to concentrate in the bonds to these, the least electronegative substituents (57). The lead-carbon bonds are therefore essentially $sp^2$ hybridized, with 33% s-character in each bond (55). The axial bonds to the water molecules

are formed from the lead $p_z$ and $d_{z2}$ orbitals, which possess the appropriate orientation (60). The absence of s-character from the axial bonding orbitals results in longer, weaker and more polarized bonds to the water molecules than to the methyl groups (55).

There are thus two distinct types of metal bonding in tbp complexes of trimethyllead: the kinetically stable, $sp^2$ hybridized and relatively covalent lead-carbon bonds and the labile, relatively polar and $p_z + d_{z2}$ hybridized bonds to the electronegative donor molecules (9,13,52). However, the nature and hence the symmetry of these bonds is dependent on the characteristics of the ligands. The bonds to "hard" bases (as defined by Pearson (64)) have a high degree of ionic character, whereas those to "soft" bases are more covalent (13,52). Distortion of tbp symmetry towards tetrahedral arises from strongly covalent ligand bonding, which requires transfer of s-character away from the lead-carbon bonds to the lead-ligand bond in question. The lead orbitals become increasingly $sp^3$ hybridized and d orbital participation is concurrently reduced. In addition, the symmetry may be affected by possible $p\pi$-$d\pi$ and hyperconjugative interactions which have been reported for trimethyllead complexes with sulfur functional groups (65-67) and unsaturated systems (68,69), although such effects are negligible with relatively "hard" Lewis base complexes (70,71). Steric and lipo-

philic interactions of ligand substituents with the trimethyllead methyl groups may also affect the symmetry as well as the strength of ligand-metal bonding. (Such properties come into prominence in the biochemistry of trimethyllead; selective binding to macromolecules is thought to depend in part on the presence of special tertiary structures (25).)

For the purposes of this thesis, the symmetry and coordination chemistry of trimethyllead can be summarized rather simply. The aquated trimethyllead cation is tbp in symmetry, with one water molecule coordinated in each of the axial positions. Complex formation involves the displacement of at least one of these water molecules by another ligand. Depending on the donor, the tbp symmetry may be distorted to some extent, but the central lead atom will almost always remain pentacoordinated, with the labile ligands positioned axially.

## 2. Formation Constants of Trimethyllead Complexes in Aqueous Solution

Quantification of the binding of aqueous trimethyllead by various ligands has been the subject of very few published studies. The results of these determinations are summarized in Table I. Included are results from Chapter III of this thesis, which formed part of a recent publication (62).

TABLE I: MEASURED FORMATION CONSTANTS OF AQUEOUS TRIMETHYLLEAD COMPLEXES

| LIGAND | METHOD | TEMP (°C) | MEDIUM | FORMATION CONSTANT | REFERENCE |
|---|---|---|---|---|---|
| $OH^-$ | glass el. | ? | ? | $3.5 \times 10^4$ [a] | 32 |
| " | " | 25 | 0.1 M $KNO_3$ | $5.0 \times 10^5$ [a] | 72 |
| " | nmr | " | 0.3 M $NaClO_4$ | $7.34 \times 10^4$ [b] | 62 |
| TMLOH[c] | " | " | " | $3.12 \times 10^1$ [b] | 62 |
| $HPO_4^{2-}$ | " | " | " | 75 | 63 |
| $SO_3^{2-}$ | " | " | " | 18.8 | 63 |
| $SeO_3^{2-}$ | " | " | " | 90 | 63 |
| $S_2O_3^{2-}$ | " | " | " | 138 | 63 |
| $SCN^-$ | " | " | 1.50 M $NaClO_4$ | 0.38 | 63 |
| " | anion exchange | " | 0 ? | 2.1 | 73 |
| $CO_3^{2-}$ | nmr | " | 0.3 M $NaClO_4$ | 396 | 63 |
| $I^-$ | " | " | " | 1.89 | 63 |
| $Br^-$ | " | " | " | 1.95 | 63 |
| $Cl^-$ | " | " | " | 1.22 | 63 |
| " | Ag/AgCl el. | " | 1 M $NaClO_4$ | 2.1 | 74 |
| $F^-$ | quinhydrone el. | " | " | 6.5 | 75 |

(cont'd)

TABLE I (con't)

| LIGAND | METHOD | TEMP (°C) | MEDIUM | FORMATION CONSTANT | REFERENCE |
|---|---|---|---|---|---|
| acetate | glass el. | " | " | 3.5 | 76 |
| " | " | ? | ? | 16.5 | 32 |
| " | DC conductivity | ? | ? | 18.6 | 32 |
| " | nmr | 25 | 0.3 M $NaClO_4$ | 9.3 | 62 |
| pivalate | " | " | " | 16.6 | 62 |
| propionate | " | " | " | 12.0 | 62 |
| formate | " | " | " | 7.2 | 62 |
| acetylglycine | " | " | " | 6.6 | 62 |
| chloroacetate | " | " | " | 3.3 | 62 |
| DNA phosphate | eqm. dialysis | ? | ? | 8.65 | 32 |

(a) Calculated from the reported $pK_a$ of the aquated trimethyllead cation. Both values are in some doubt.

(b) Reported in detail later in this thesis.

(c) The aquated trimethyllead hydroxide complex.

The results in Table I and the corresponding published comments invite several conclusions regarding trimethyllead complexes. With the exception of hydroxide the affinity of these ligands for trimethyllead is small relative to that of water. Hence, water is the only ligand known to form two to one ligand to metal complexes with trimethyllead in aqueous solution. However, a second trimethyllead cation may bind, albeit weakly, to the coordinated donor atom of a relatively strong one-to-one complex such as trimethyllead hydroxide. In addition, a direct correlation has been proposed to exist between trimethyllead binding constants and ligand basicity (77); in the absence of other factors, strongly basic ligands should prove to be the most effective complexing agents for trimethyllead, a Lewis acid. This correlation will be examined in Chapter IV of this thesis.

A number of the ligands in Table I are present in biological fluids. At physiological pH levels, there will be significant fractions of trimethyllead complexed by each of these, even those with small formation constants (63). The presence of such complexes may account in part for the unique biological properties of trimethyllead (25).

## C. The Present Study

Triorganolead systems have been studied extensively in recent years by means of various nmr techniques (44,49, 54-57,59,62,63,67,69,77-83). Several of these studies have demonstrated that the nmr chemical shift of trimethyllead protons provides a sensitive probe of the extent of complex formation (62,63,77). The variation of this chemical shift with pH was employed in this thesis to determine the equilibrium formation constants of aqueous trimethyllead with hydroxide and with various organic ligands. Details of this technique will be presented in the appropriate sections of this thesis.

Complexes of trimethyllead with ligands containing sulfhydryl groups form the majority of the species studied. Several factors influenced the selection of ligands: sulfhydryl groups are common in biological systems, they are relatively basic when deprotonated and such ligands have been found to complex very strongly with methylmercury (84), the central metal atom of which is isoelectronic with that of trimethyllead. A major factor in choosing sulfhydryl ligands is that $Pb^{2+}$ is strongly complexed by sulfhydryl groups.

This work marks the conclusion of a program of research directed towards quantitatively characterizing the aqueous coordination chemistry of trimethyllead.

# CHAPTER II

# EXPERIMENTAL

## A. Chemicals

Glycine (AnalaR, British Drug Houses Chemicals Ltd.), 2-mercaptoethanol (Eastman Kodak Co.), N-acetyl-D,L-penicillamine (Sigma Chemical Co.), D,L-penicillamine (Aldrich Chemical Co.), L-cysteine (Nutritional Biochemicals Corp.), reduced glutathione (Sigma Chemical Co.) and t-butanol (J. T. Baker Chemical Co.) were used as received. In some cases, the above reagents or their solutions were standardized as described below. Trimethyllead acetate (Ventron Alfa Products) was the only water soluble form of trimethyllead commercially available. To avoid interference due to acetate complexation of trimethyllead (62,77), the trimethyllead acetate was converted to a trimethyllead perchlorate stock solution. The purification by ion exchange and the standardization by pH titration of this solution is described below.

All other chemicals were of the highest grade commercially available and were used without further purification or standardization. Doubly distilled water was used exclusively in all stages of solution preparation and as a final rinse in the cleaning of all glassware.

B. Preparation and Standardization of Trimethyllead Perchlorate Solutions

Ion exchange has been used to remove acetate from methylmercuric hydroxide solutions (85) and a similar method was developed for the conversion of trimethyllead acetate to trimethyllead perchlorate. A column of Dowex 2-X8 anion exchange resin was prepared for use by first washing with 0.5 M hydrochloric acid and doubly distilled water to remove residual impurities, and then regenerating with 0.5 M sodium hydroxide. A freshly prepared solution of approximately 0.25 M trimethyllead acetate was filtered under vacuum through a Nalgene disposable filter unit of 0.2 μm pore size to remove an insoluble fraction. These filter units were found to release a yellowish impurity (possibly a membrane binding agent) into the filtrate when basic solutions were filtered. Therefore, all filter units were rinsed several times before use by drawing 0.5 M sodium hydroxide, followed by doubly distilled water, through the filter until the filtrate was colorless. Proton magnetic resonance spectra of the resultant solutions showed no unexpected resonances.

The filtrate was then passed several times through the anion exchange column; the number of passes required depended on the volume of stock solution to be prepared and on the capacity of the column. The eluate was filtered through fresh Nalgene filter units after each pass to

remove a cloudy white precipitate which formed soon after elution. This precipitate was thought to be trimethyllead hydroxide (the hydroxides of most cations are less soluble than the corresponding acetates and in addition, the original trimethyllead acetate solution was near saturation before the exchange of ions took place in the column). The eluate was filtered to eliminate the possibility of co-precipitation of residual trimethyllead acetate. Precipitate also appeared after the final pass through the column, but dissolved completely below pH 9.7 as the pH was adjusted with perchloric acid.

The column was regenerated between passes with 0.5 M sodium hydroxide. The proton magnetic resonance spectrum, at high amplitude, of a sample was taken after each pass to test for the presence of residual acetate. These pmr samples were first acidified with concentrated perchloric acid; in basic solution a satellite resonance of trimethyllead partially obscures the small acetate resonance. In acidic solution, the resonance of the methyl protons of the resultant acetic acid is located approximately 0.84 ppm downfield from the tert-butyl resonance of t-butanol and it is detectable at concentration levels of greater than approximately 0.001 M with the nmr instrument used in this research. When the acetic acid resonance fell below this detection limit in the presence of 0.2 M trimethyllead perchlorate, the solution was

refiltered through a fresh Nalgene unit, neutralized to between pH 5 and 7, and stored tightly sealed in the absence of light (21).

The stock solution of trimethyllead perchlorate was standardized by titration with sodium hydroxide using a Mettler DV11 Automatic Titrator, using a glass electrode to locate the endpoint. To ensure complete neutralization of all the trimethyllead hydroxide present in solution, the initial pH was first reduced to a value between pH 2 and 3 using concentrated perchloric acid. The solution is thus a mixture of a strong acid ($HClO_4$) and a weak acid ($(CH_3)_3Pb^+$), which yields a titration curve with two inflection points. Titration of the added perchloric acid gives a sharp inflection point at pH 5 and the $(CH_3)_3Pb^+$ a less well defined inflection point at approximately pH 10.4. The exact position of the trimethyllead endpoint was determined using a second derivative plot of the titration curve (86). The titration with base converted the trimethyllead from $(CH_3)_3Pb^+$ to $(CH_3)_3PbOH$. Consequently, the amount of sodium hydroxide added between the first and second endpoints provided the concentration of trimethyllead in the stock solution.

During the period of development of this technique, the existence of a third species of trimethyllead in aqueous solution (i.e., the dimer, $((CH_3)_3Pb)_2OH^+$) was suspected (77). Verification of the accuracy of the

potentiometric technique was therefore required. This was accomplished by determining the trimethyllead concentration of several stock solutions with atomic absorption spectroscopy (62,77), and with EDTA titrations of aliquots following conversion to $Pb^{2+}$. The atomic absorption results tended to be slightly higher than the trimethyllead concentrations obtained by potentiometry, but the agreement was within experimental error, supporting the potentiometric standardization. Further confirmation of the accuracy of the potentiometric method was obtained with the reduction-EDTA titration method, which also gave results identical within experimental error to those of potentiometry.

The procedure used in the reduction-EDTA titration method involved the digestion of aliquots (typically 5.00 ml) of the stock solution with 15 ml of aqua regia (one part concentrated nitric acid plus four parts concentrated hydrochloric acid) for about four hours to ensure complete reduction of $(CH_3)_3Pb^+$ to $Pb^{2+}$. The sides and cover of the reaction vessel were periodically rinsed down with concentrated nitric acid. The solutions were then evaporated to one half of their original volumes. Several volumes of nitric acid were added during a period of several hours of gentle heating in order to evaporate chloride (as $HCl_{(g)}$) which causes precipitation of $PbCl_2$. The resultant acidified $Pb(NO_3)_2$ solutions were adjusted to

approximately neutral pH with solid sodium hydroxide pellets. The pH value was followed with a combination glass electrode. This solution was titrated with standardized EDTA using hexamine buffer and xylenol orange indicator (87). The EDTA solution was standardized by titration with a $ZnSO_4$ solution of accurately known concentration in the presence of xylenol orange indicator (87).

It was necessary to modify slightly Vogel's (87) procedure for the titration of $Pb^{2+}$. The quantity of hexamine specified did not always provide sufficient buffer capacity to prevent a decrease in pH such that suboptimal levels were reached during the course of the titration. This drop in pH is due to the release of protons from disodium EDTA during complexation. Continuous monitoring of pH with a small combination glass electrode, together with further addition of solid sodium hydroxide as required to maintain a pH of about 6, ensured consistently good indicator endpoints.

The three independent procedures yield identical results within experimental error, supporting the validity of these methods. The presence of a small amount of the dimeric species, $((CH_3)_3Pb)_2OH^+$, was not found to interfere in the pH titrations at the concentrations used here. (It is now known (and detailed in Chapter III) that this species is significant only in the neutral pH regions, and readily reacts with a further hydroxide ion. At the

end point, all trimethyllead in solution is present as trimethyllead hydroxide; thus, a one to one stoichiometry will be preserved in titrations of $(CH_3)_3Pb^+$ with hydroxide). Since the potentiometric method is quite convenient and yields the most precise results, it was the method of choice for the standardization of succeeding preparations of trimethyllead.

C. Preparation and Standardization of Ligand Solutions

All solutions in this and subsequent sections were prepared with doubly distilled water which had been freshly boiled and cooled under a stream of argon (to prevent the reabsorption of oxygen and carbon dioxide). All pipets were calibrated by a standard method (89).

Liquid 2-mercaptoethanol (nominally 98% pure) was the source of the mercaptoethanol ligand. A 5.00 ml aliquot of the liquid was diluted to 100 ml with water. A 2.00 ml aliquot of the dilute solution was added to 140 ml of water, to which sufficient crystalline sodium perchlorate had been added to give a final ionic strength ($\mu$) of 0.3 M. The concentration of ligand in the final solution was approximately 0.012 M. Concentrated perchloric acid was added dropwise until the pH of the solution was between 2.6 and 3.0. The added acid contributed only about 0.01 M to the final ionic strength. The resultant solution was titrated with standard 0.12 M sodium hydroxide using a Mettler

DV11 Autotitrator. Titrant was added in small increments in the regions of the endpoints and near the half-neutralization point of 2-mercaptoethanol to define these regions as well as possible. The titration curve was followed with a glass electrode. As with the standardization of trimethyllead, the solution was a mixture of a strong acid (perchloric acid) and a weak acid (2-mercaptoethanol), thus giving two inflection points in the curve. The sharply defined inflection point at pH 5 was due to $HClO_4$ while the less distinct break at pH 10.6 was due to the ligand. The positions of the endpoints were determined using a second derivative plot of the titration curve (86). The amount of sodium hydroxide added between the two endpoints provided the concentration of 2-mercaptoethanol in the dilute solution, and hence, in the concentrated liquid. Ten replicates gave a median purity of 97.2 % ± 0.6%.

A proton magnetic resonance integration experiment was performed to determine the species present in the concentrated liquid 2-mercaptoethanol. Six replicates of the integration curves of the neat liquid 2-mercaptoethanol spectrum were obtained on a Varian HA-100 spectrometer. Ratios of the heights of the integration waves were compared, and the results obtained were consistent with a solution composed of 97% $HOCH_2CH_2SH$, 1.5% $HOCH_2CH_2SSCH_2CH_2OH$ and 1.5% $H_2O$. Neither impurity inter-

feres with the nmr determination of the formation constants for the complexation of $(CH_3)_3Pb^+$ by the sulfhydryl group of 2-mercaptoethanol, provided that standardized solutions are used. The nmr integration experiment also confirms the accuracy of the pH titration standardization. The determination of the acid dissociation constant of the ligand thiol group from the titration data is described in section I of this chapter.

N-acetyl-D,L-penicillamine was standardized using a method similar in most respects to that used for 2-mercaptoethanol. The significant differences were that the ligand was added directly to the titration mixture as a crystalline solid and no perchloric acid was required. The ligand carboxylic acid group provided a good endpoint at pH 7, while the sulfhydryl group endpoint was of no use, being poorly defined in the high pH region. To obtain the desired information, it was assumed that the concentration of carboxylic acid groups equalled that of the sulfhydryl groups. Hence, the volume of standard sodium hydroxide required to titrate to the first endpoint was used to calculate the purity (in terms of the sulfhydryl group) of the crystalline solid. Four replicates gave a median value of 99.1 ($\pm$ 0.4) %. These results were corroborated by several determinations of sulfhydryl purity using the standardization procedure described by Benesch and Benesch (90). In this procedure, the reaction of the reduced ligand thiol groups with

iodoacetamide stoichiometrically releases into solution the protons of all such groups. The concentration of the protons released is determined by appropriate titrimetric measurements (90). This procedure gave a median result of 98.7 (± 1.0) %, which confirms the accuracy of the pH titration technique within experimental error.

The purity of the reduced sulfhydryl group of the glutathione employed in this study was determined by titration with coulometrically generated iodine in acetate buffer using biamperometric endpoint detection (91). Five replicates gave a purity with respect to the -SH group of 97.3 (± 0.5) % (93). The purities of the -SH groups of L-cysteine and D,L-penicillamine were determined by titration with coulometrically generated bromine in 1 M hydrochloric acid using biamperometric endpoint detection (92). Five replicates gave a purity for cysteine of 95.0% ± 0.5% and for penicillamine of 99.6% ± 0.4% (93).

The sodium hydroxide solutions used in all phases of this work were prepared under an atmosphere of argon using the carefully degassed water described at the beginning of this section. Standardization of these solutions was accomplished by titration against known amounts of primary standard potassium hydrogen phthalate (88). The standard sodium hydroxide stored in the autotitrator reservoir was protected from atmospheric carbon dioxide by means of an Ascarite-containing tube on the only air inlet. This

stock solution was restandardized carefully before each use, even though its molarity was found to be stable for several weeks.

D. pH Measurements

pH Measurements were carried out at 25 ± 1 °C with an Orion Model 701 digital pH meter equipped with a standard full pH range glass electrode and a silver/silver chloride reference electrode in which saturated sodium sulfate was used as the electrolyte solution. This reference electrode was used rather than the standard Ag/AgCl reference electrode with potassium chloride electrolyte to avoid problems resulting from the precipitation of potassium perchlorate in the reference electrode fiber junction. Fisher Certified Buffer solutions having pH values of 4.01, 7.00 and 10.00 at 25°C (potassium hydrogen phthalate, potassium phosphate and potassium borate/potassium carbonate, respectively) were used to standardize the pH meter.

E. Proton Nuclear Magnetic Resonance Measurements

Proton nmr spectra were obtained on a Varian A-60-D high resolution spectrometer at a probe temperature of 25 ± 1°C. The temperature of the probe was determined by measuring the potential of a copper vs. constantan thermocouple inserted in the probe.

Spectra were recorded at sweep rates of 0.2 Hz/sec

for the chemical shift measurements. Reported data are the median of three scans. Chemical shifts were measured relative to the tert-butyl resonance of t-butanol (TBA) or the central resonance of tetramethylammonium (TMA) cation, but are reported relative to the methyl resonance of sodium 2,2-dimethyl-2-silapentane-5-sulfonic acid (DSS). Positive shifts correspond to resonances of protons less shielded than the methyl protons of DSS. The tert-butyl resonance of TBA is 1.243 ppm downfield from the methyl resonance of DSS; the central resonance of TMA is 3.175 ppm downfield from DSS.

The sweep widths of the nmr recorder were calibrated by a sideband procedure. A Hewlett-Packard Model 200 AB audio oscillator was used to provide sideband signals from tetramethylsilane (12% in chloroform). The frequency of the sideband was counted with a Hewlett-Packard Model 5307A High Resolution Counter. For recorder calibration, the shift of the sideband from the main signal (as indicated by the calibration lines of the recorder paper) was matched to the counted frequency generated by the audio oscillator.

F. Carbon-13 Nuclear Magnetic Resonance Measurements

Carbon-13 nmr spectra were obtained using a Varian HA-100 spectrometer operating at a frequency of 25.1 MHz and equipped with a Digilab FTS/NMR-3 Data System. The pulsed Fourier transform mode was used with proton de-

coupling. For each free induction decay signal, 8 K data points were collected in the computer. The spectra were time averaged using 500 accumulations in all cases except one, where 4 K accumulations were required to measure the $^{207}Pb$ - $^{13}C$ coupling constant at pH 5.0. These accumulations gave adequate signal-to-noise ratios in each case. The deuterium resonance from $C_6D_6$ in a coaxial capillary served as the lock signal. The frequency range of the transformed spectra was 5000 Hz. Chemical shifts are reported in ppm relative to the carbon-13 resonance of the 1,4-dioxane added as an internal reference. The resonance of 1,4-dioxane is 67.73 ppm downfield from the tetramethylsilane carbon-13 resonance. Positive chemical shifts correspond to less shielding than in 1,4-dioxane. The chemical shift measurements are considered accurate to within 0.05 ppm. For all measurements the sample temperature was 25 ± 1°C as measured with a standard thermocouple.

G. Solutions for Nuclear Magnetic Resonance Measurements

Solutions used in the nuclear magnetic resonance measurements were prepared in carefully degassed doubly distilled water from buret-delivered aliquots of stock trimethyllead perchlorate. The ligand was weighed into the mixture as a solid or an aliquot of ligand solution was added to the mixture by buret or pipet. The concentration of trimethyllead in the solutions from which nmr measurements

were determined was 0.005 M to 0.075 M. Ratios of ligand to trimethyllead varied between 0.5 and 10 to 1, but typically were either 2 or 4 to 1. Tert-butanol was added as an internal chemical shift reference for the trimethyllead resonance, at a concentration about two-thirds that of trimethyllead. Tetramethylammonium nitrate was used as the internal standard instead of TBA only for those ligand shift measurements where TMA allowed the use of a narrower nmr sweep width. The concentration of TMA was typically less than 0.01 M. In all cases, the ionic strength was maintained at approximately 0.3 M with sodium perchlorate.

In the experiments which measured chemical shift as a function of pH, the ionic strength of the solution was first adjusted to 0.3 M and then samples were withdrawn as the pH was varied. Variations in ionic strength caused by change in the chemical species in solution are small (typically $\pm$ 0.02 M) relative to the background ionic strength. The solutions were initially made acidic to about pH 2.5, using a measured amount of perchloric acid. Then sodium hydroxide was added and samples were withdrawn at appropriate pH intervals until approximately pH 12.5 was reached. Usually twenty-one to twenty-five 0.4 ml samples were required to cover this pH range. Concentrated perchloric acid (70%) and deoxygenated carbonate-free sodium hydroxide solutions were used to adjust the pH. Since compounds containing thiol groups are subject to

air oxidation, and since high pH samples absorb atmospheric carbon dioxide (causing downward pH drift), all possible stages of the solution preparation and sampling were performed under a stream of argon. Nmr spectra were obtained immediately after sample preparation or after overnight storage of samples under argon at 1°C.

In the mole ratio experiment of trimethyllead vs. 2-mercaptoethanol, each sample solution was made separately with varying ligand to trimethyllead ratios, but at constant pH and ionic strength. The ratio of ligand to trimethyllead in these solutions ranged from 0.0 to 6.1. The ionic strength of all samples was held at approximately 0.3 M with sodium perchlorate. The pH in all cases was adjusted to 8.0; very little base was added.

The solutions for carbon-13 nuclear magnetic resonance spectroscopy were prepared in a manner similar to that for the proton nmr experiments, except that dioxane was used as the internal standard. The concentration of dioxane was about 0.04 M, the trimethyllead was 0.0947 M, the glutathione was 0.146 M and the perchlorate was approximately 0.17 M (added as 70% $HClO_4$) giving a $\mu$ of 0.4 M.

H. Determination of Formation Constants by NMR Spectroscopy

The formation constants of the trimethyllead complexes were calculated from the chemical shift of the methyl

protons of trimethyllead in solutions of known pH and known trimethyllead and ligand concentrations.

All the systems studied in this thesis were found to be labile; that is, the trimethyllead moiety is exchanging between its various forms (aquated, hydroxy-complexed and ligand-complexed) at a rate which is fast on the nmr time scale. Thus, a single sharp resonance is observed for the methyl protons of trimethyllead. The observed chemical shift of this resonance is the weighted average of the chemical shifts of the various trimethyllead species. This is expressed by the following relation:

$$\delta_{OBS} = \sum_i P_i \delta_i \qquad (1)$$

where $\delta_{OBS}$ represents the observed, exchange averaged chemical shift of trimethyllead, $P_i$ is the fraction of the $i^{th}$ trimethyllead species in solution and $\delta_i$ is the chemical shift of that species.

The formation constants and the chemical shifts of the complexes were obtained from pH vs chemical shift experiments by curve-fitting the data to Equation 1. The curve-fitting program used was generously supplied by Drs. J. L. Dye and V. A. Nicely of Michigan State University. This program, KINET, has been described in the literature (94). A user-supplied subroutine is required to describe the model to be fitted to the data. To use Equation 1, it is first necessary to solve for the

various fractions, $P_i$. The fractions are calculated from the equations for the formation constants and the mass balance equations for trimethyllead and ligand. Manipulation of the i equations to eliminate all fractions but one, $P_x$, gives a polynomial in $P_x$. The coefficients of $P_x$ in this polynomial are in terms of the formation constants, the concentrations of hydrogen ion or hydroxide ion, and the total concentrations of trimethyllead and of ligand. Solution of this polynomial for $P_x$ was achieved iteratively using the Library Subroutine DRTMI, which is part of the IBM Scientific Subroutine Package (SSP Library). With this value for $P_x$ at a particular pH, the other fractions were calculated using the appropriate formation constant equations. The numerical values for these fractions were used to calculate a chemical shift with Equation 1. This entire process was repeated for each data point. The sum of the squares of the differences between each predicted chemical shift and the corresponding observed chemical shift was minimized by the program KINET. It accomplished this by systematically varying the initial estimates for the unknown formation constants and chemical shifts until the predicted and observed curves converged. The values of the unknown parameters at convergence were considered accurate only if all the error indicators calculated by KINET were small. In order to determine accurate formation constants by the above method, it was

necessary to have in solution a significant fractional concentration of each form of trimethyllead in some portion of the observed pH range. Those complexes which did not meet this criterion, or whose chemical shift was similar to that of a species in plentiful supply, received from KINET large error estimates for their best-fit formation constants and chemical shifts.

Examples of the above procedure are described in detail in Chapters III and IV.

## I. Determination of Acid Dissociation Constants of Selected Ligands

### 1. Determination by NMR Measurements

It is well known that the shifts of carbon-bonded protons close to acidic functional groups are sensitive to the deprotonation of that functional group (95): the method outlined in the previous section is applicable to the determination of $K_a$ for organic acids (96). The acid dissociation constants of selected ligands were calculated from the pmr chemical shift of the ligand resonances in solutions of known pH and ligand concentrations. The method is similar to that described above for the determination of formation constants, with only minor differences. Tetramethylammonium nitrate (0.002 M) was used as the internal standard. Somewhat higher concentrations of

ligand (approximately 0.15 M) were required due to the lower intensity of the ligand methylene resonances compared to the degenerate methyl resonances of trimethyllead. Therefore, the ionic strength was somewhat more difficult to maintain at the desired value of 0.3 M. The presence of multiple ligand resonances with chemical shifts sensitive to deprotonation allowed separate determinations of the acid dissociation constant with each resonance. These results were averaged to give the value used in this work.

Further details of each acid dissociation constant determination are described in Chapter IV.

2. Determination by pH Titration

The acid dissociation constants of two of the dibasic ligands were obtained by potentiometric titration using a glass electrode. The titrations were carried out under argon using degassed sodium hydroxide as detailed in the previous sections in this chapter. The ionic strength was controlled at 0.3 M with crystalline sodium perchlorate.

Both ligands titrated were dibasic acids, but the estimated $pK_a$ values were quite different, thus warranting different experimental procedures. 2-Mercaptoethanol was thought to have a $pK_1$ of approximately 9 and a $pK_2$ of above 14. It may be argued that such a high value for $pK_2$ effectively renders 2-mercaptoethanol a monobasic

acid in water; hence, $pK_2$ was ignored. The procedure was therefore as follows. Initially, the pH was reduced to below 3 using concentrated perchloric acid. Titration of the perchloric acid yields a sharp inflection point at pH 5.5 and titration of the sulfhydryl group of the ligand gives a less well-defined inflection point at about pH 10.6. The acid dissociation constant, which is defined by Equations 2 and 3, was determined

$$H_2L \rightleftarrows H^+ + HL^- \tag{2}$$

$$K_1 = \frac{[H^+][HL^-]}{[H_2L]} \tag{3}$$

from the pH data between the two inflection points.

N-acetyl-D,L-penicillamine was thought to have a $pK_1$ of about 3 and a $pK_2$ of approximately 10. Therefore, no perchloric acid was added: a weighed amount of dry crystalline ligand was dissolved and titrated as detailed in section C above. $K_1$ and $K_2$, as defined by Equations 2 to 5 inclusive,

$$HL^- \rightleftarrows H^+ + L^{2-} \tag{4}$$

$$K_2 = \frac{[H^+][L^{2-}]}{[HL^-]} \tag{5}$$

were determined from the pH titration data between the start and the first inflection point, and between the two inflec-

tion points, respectively. In all cases, the exact positions of the endpoints were determined by second derivative plots (86). All pH titration experiments were designed to minimize dilution errors and activity corrections, using the methods described by Albert and Serjeant (97).

# CHAPTER III

## TRIMETHYLLEAD SPECIES AND EQUILIBRIA IN AQUEOUS SOLUTION

At the initiation of this research, no detailed information was available regarding the stability of trimethyllead in aqueous solution or the nature of the aqueous acid-base equilibria of trimethyllead. In section A of this chapter, the results of a long-term study of the stability of aqueous trimethyllead at various pH levels are reported. In section B, nuclear magnetic resonance results are described for the aqueous acid-base solution chemistry of trimethyllead. The aqueous species are identified and constants for the equilibria between the various species are determined. The research described in section B was performed in collaboration with Dr. T. L. Sayer, E. K. Millar and Dr. C. A. Evans (62).

### A. The Stability of Trimethyllead in Aqueous Solution

#### 1. Introduction

In aqueous solution, the methyllead compounds $(CH_3)_3PbX$ and $(CH_3)_2PbX_2$ redistribute according to the following reaction scheme (18):

$$4(CH_3)_3PbX \rightleftarrows 2(CH_3)_2PbX_2 + 2(CH_3)_4Pb \qquad (6)$$

$$2(CH_3)_2PbX_2 \rightarrow (CH_3)_3PbX + CH_3X + PbX_2 \qquad (7)$$

$$3(CH_3)_3PbX \rightarrow 2(CH_3)_4Pb + CH_3X + PbX_2 \qquad (8)$$

Reaction 7 is much faster than 6 and the rate of both reactions depends on the nature of the anion X (98,99). The perchlorate anion used extensively in the present study was shown to produce a much lower rate constant for reaction 7 than did many common anions (98), especially under the conditions employed in this work. The overall stoichiometry of the disproportionation of trimethyllead can be described by reaction 8.

The comparatively low rate constant of reaction 6 seems to indicate that trimethyllead (and especially trimethyllead perchlorate) is relatively stable at room temperature (18). Nonetheless, the occurrence of reactions 6 through 8 as well as other observations (52) cast some doubt on the exact composition and practical stability of the trimethyllead perchlorate stock solutions used in this work. Therefore, a study to determine the long term stability of the lead-carbon bonds towards hydrolysis at several pH levels was completed.

## 2. Results and Discussion

Solutions of 0.185 M trimethyllead at pH levels of 0.9, 2.0, 7.1 and 11.0 were tested periodically for the presence of Pb(II) ions using chemical spot tests. Sodium rhodizonate was used as detailed by Feigl and Anger (100); this method was sensitive to inorganic lead at concentrations greater than approximately $10^{-4}$ M. Since the indicator

was inactive at high pH, the alkaline sample spots were neutralized before testing using the tartrate buffer described in the reference above. Quantitative results were obtained by comparing the test results with those of a fresh series of standard lead(II) nitrate solutions, which ranged in concentration from $10^{-1}$ M to $10^{-5}$ M. After 28 months of monitoring, the results indicated that the concentration of inorganic lead was less than $10^{-4}$ M in solutions at neutral pH. This corresponded to less than one part per thousand decomposition of trimethyllead perchlorate to inorganic lead. Lead(II) ions were found to be present at levels of approximately $10^{-2}$ M in pH 0.9 solutions, between $10^{-2}$ M and $10^{-3}$ M in pH 2.0 solutions and between $10^{-3}$ and $10^{-4}$ M in pH 11.0 solutions.

These results were corroborated by the comparison of the integrated proton nmr intensities of the above samples during the initial five month experimental period. No new resonances appeared as time progressed. In addition, the intensity measurements of the methyl resonance of trimethyllead relative to those of the internal standard tert-butanol were consistent with the spot test results within experimental error. Neutral pH was thus found to be the most favorable for prolonged stability of trimethyllead perchlorate in aqueous solution.

Taken together, these results established that aqueous solutions of trimethyllead perchlorate do not decompose

significantly, even over long periods of time, under the conditions employed in the above experiments. Hence, these conditions were met in the storage of all trimethyllead stock solutions: the maintenance of darkness under an inert atmosphere (14) at neutral pH, the use of the perchlorate anion only and the use of concentrations of trimethyllead below the observed maximum of about 0.2 M. For shorter periods of time, certainly on the time scale of the experiments described later in this thesis, trimethyllead in aqueous solution appeared to be stable to hydrolysis of the lead-carbon bond even at extremes of pH.

## B. The Acid-Base Chemistry of Trimethyllead

### 1. Introduction

The proton nuclear magnetic resonance spectrum of trimethyllead in aqueous solution consists of a methyl singlet flanked symmetrically by two less intense satellite peaks. Figure 1 shows a typical spectrum at approximately neutral pH. The singlet is due to the protons of the methyl groups bound to those lead atoms having a nuclear spin of zero, while the satellites are due to the protons of the methyl groups bonded to $^{207}Pb$, the isotope having a nuclear spin of one-half (22.6% natural abundance).

The observed chemical shift, $\delta_{OBS}$, is given by the position of the central resonance, measured from the

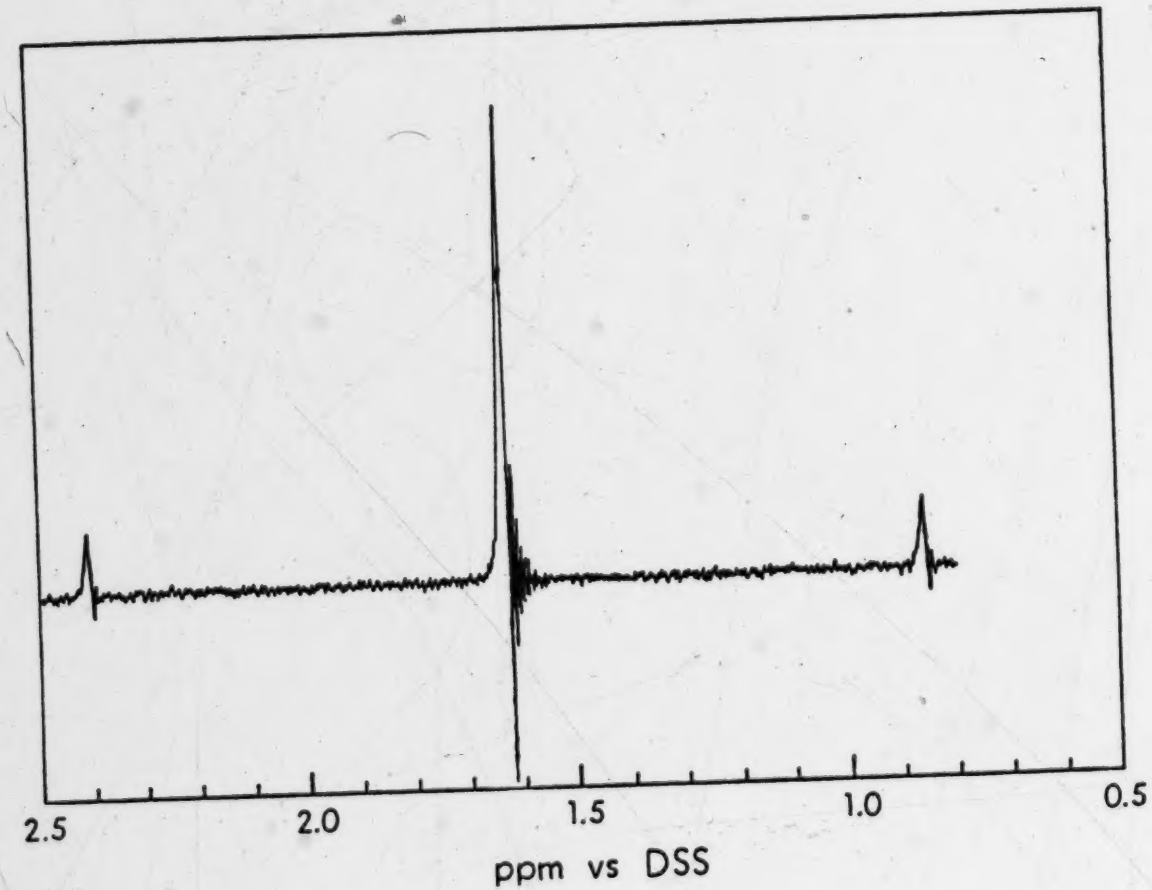


Figure 1. Proton nmr spectrum of the methyl groups of trimethyllead in 0.140 M solution at approximately neutral pH.

resonance of a chemical shift standard. The lead-proton spin-spin coupling constant, $J_{^{207}Pb-^{1}H}$, is given by the separation of the satellite lines. Both the chemical shift of the methyl singlet and the coupling constant are dependent upon the nature of the ligands coordinated to the trimethyllead in solution. In aqueous solutions of trimethyllead containing no coordinating ligands other than water and hydroxide ion, the chemical shift and the coupling constant are both pH dependent. The chemical shift of the central resonance of trimethyllead perchlorate in aqueous solution at a concentration of 0.0100 M is shown as a function of pH in Figure 2. (The ionic strength was maintained at 0.3 M with $NaClO_4$.) The coupling constant of trimethyllead varies from 77 Hz to 79 Hz over a similar pH range (62,77). The pH dependence is due to the formation of trimethyllead hydroxide complexes as the concentration of hydroxide ion is increased. No evidence exists for the coordination of more than one hydroxide ion per trimethyllead cation up to at least pH 12. Indeed, the available data indicate that essentially all the trimethyllead is present as $(CH_3)_3PbOH$ at high pH.

## 2. Results and Discussion

The aqueous species of trimethyllead and the equilibrium constants for these species were determined from chemical shift vs. pH data of the type displayed in Figure 2. The

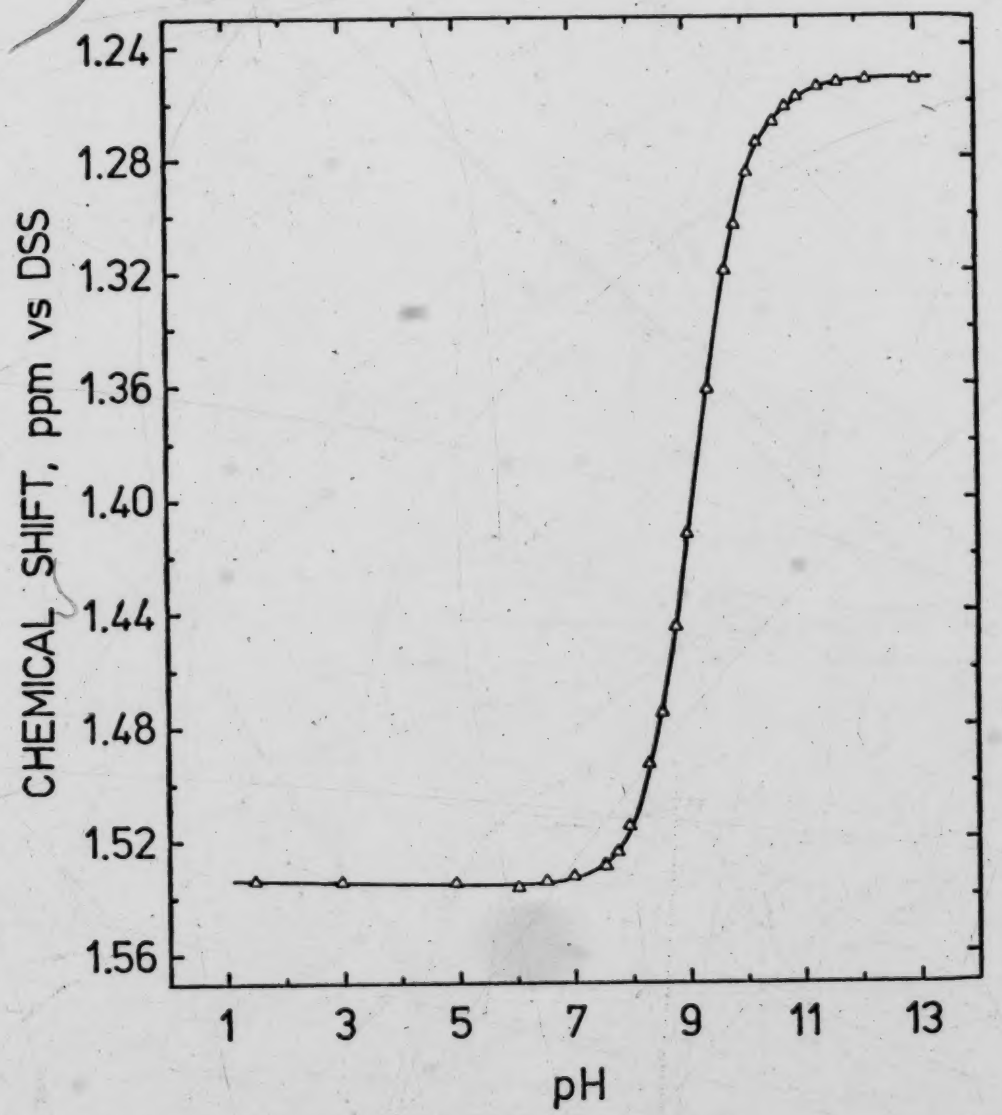


Figure 2. pH dependence of the chemical shift of the methyl protons of trimethyllead in a 0.0100 M aqueous solution at 0.3 M ionic strength (maintained with $NaClO_4$).

experimental solutions possessed total trimethyllead concentrations ranging from $5 \times 10^{-3}$ M to $2 \times 10^{-1}$ M. At each pH of a solution, the accepted chemical shift value was commonly the median of three measurements.

Lead-proton spin-spin coupling constant data were not used to determine the trimethyllead species and equilibrium constants. The small relative change in the coupling constant over the entire range of pH provided data of poor sensitivity towards ligand complexation: accurate results could not be obtained from such information. These data contrasted with the data obtained from the analogous methylmercury system (85). Both the mercury(199)-proton spin-spin coupling constants and the chemical shift data could be used to obtain precise results, because both were quite sensitive to ligand complexation.

(a) Determination of Species Present in Aqueous Trimethyllead Solutions. Initially, it was assumed that a simple acid-base equilibrium existed between $(CH_3)_3Pb^+$ and $(CH_3)_3PbOH$, and that no other species of trimethyllead was present. This system is represented by the following equations:

$$(CH_3)_3Pb^+ + OH^- \rightleftarrows (CH_3)_3PbOH \qquad (9)$$

$$K_1 = \frac{[(CH_3)_3PbOH]}{[(CH_3)_3Pb^+]a_{OH^-}} \qquad (10)$$

where $a_{OH^-}$ is the hydroxide ion activity and $K_1$ is the formation constant of $(CH_3)_3PbOH$. The limiting chemical shift at a pH of less than 2 was taken to be the shift of pure $(CH_3)_3Pb^+$ and that at a pH of greater than 12 was taken to be the shift of pure $(CH_3)_3PbOH$. In dilute solutions of trimethyllead, this model agreed well with the observed chemical shift data. However, the displacement of the chemical shift curve for solutions of higher trimethyllead concentration, especially in the neutral and moderately basic pH regions, indicated the presence of a third species of intermediate chemical shift. In addition, this concentration dependence suggested that the equilibria between this third species and the two above-mentioned species were asymmetric; the position of an asymmetric equilibrium would indeed favor the simpler species $(CH_3)_3Pb^+$ and $(CH_3)_3PbOH$ at lower total trimethyllead concentrations.

The aqueous methylmercury system, which has been described in detail (85,101), was thought to be analogous to that of aqueous trimethyllead in many respects. It was determined in those studies that an important species in the acid-base chemistry of methylmercury is the dimer $(CH_3Hg)_2OH^+$. The asymmetrical nature of the equilibria observed in the methylmercury system is for the most part due to this species. Hence, a model of the trimethyllead system including the analogous dimeric species $((CH_3)_3Pb)_2OH^+$ was tested. This model, as described by Equations 9

through 12, gave the best fit to the observed chemical shift data of all the models examined.

$$(CH_3)_3Pb^+ + (CH_3)_3PbOH \rightleftharpoons ((CH_3)_3Pb)_2OH^+ \qquad (11)$$

$$K_2 = \frac{[((CH_3)_3Pb)_2OH^+]}{[(CH_3)_3Pb^+][(CH_3)_3PbOH]} \qquad (12)$$

$K_1$ and $K_2$ are the formation constants for the mononuclear and dinuclear hydroxide complexes, respectively. No evidence was found for the existence of a fourth trimethyllead species analogous to the species $(CH_3Hg)_3O^+$ described for the methylmercury system (101).

The dinuclear species $((CH_3)_3Pb)_2OH^+$ was therefore considered to form only by the association of $(CH_3)_3Pb^+$ and $(CH_3)_3PbOH$ as represented by Equation 11. Each trimethyllead moiety in the dimeric species is thought to share a single hydroxide ion with the other; hence, the methyl protons of the dimer would be shielded by an amount intermediate to that of the uncomplexed $(CH_3)_3Pb^+$ and the singly-complexed $(CH_3)_3PbOH$. As a result, the dinuclear species would be expected to have a chemical shift intermediate to those of the two mononuclear species. This, together with the asymmetric equilibrium of Equation 11, fitted well with the observed concentration dependence of the experimental data. The validity of this model was confirmed and $K_1$ and $K_2$ were evaluated as well, by comparing the observed chemical shift vs pH curves to

curves calculated from this model by computer.

Other models, in which either the species $((CH_3)_3Pb)_2O$ or $((CH_3)_3PbOH)_2$ were included, gave poor fits. The oxonium species $((CH_3)_3Pb)_3O^+$ was not considered due to the low value (0.7 $M^{-1}$) estimated for the formation constant of $(CH_3Hg)_3O^+$ in the analogous methylmercury system (101); the measurable formation constants of trimethyllead complexes were found to be consistently several orders of magnitude lower than those of the corresponding methylmercury complexes.

(b) Determination of the Formation Constants of Trimethyllead Hydroxide Complexes. The formation constants $K_1$ and $K_2$, as defined by Equations 10 and 12, and the chemical shift of the dinuclear species $((CH_3)_3Pb)_2OH^+$, $\delta_{TMLD}$, were determined by computer curve-fitting of the observed chemical shift data to the model curve calculated as described below.

The exchange of the trimethyllead moiety between its various aquated forms is fast on the nmr time scale; hence, the observed chemical shift of its central resonance (or its coupling constant) is an average of the chemical shifts (or coupling constants) of the various trimethyllead species in solution, weighted according to their individual populations. This relationship is described by Equation 1. For the model of the aqueous trimethyllead system described

by Equations 9 through 12, Equation 1 becomes

$$\delta_{OBS} = P_{TML}\delta_{TML} + P_{TMLOH}\delta_{TMLOH} + P_{TMLD}\delta_{TMLD} \quad (13)$$

where TML, TMLOH and TMLD refer to the species $(CH_3)_3Pb^+$, $(CH_3)_3PbOH$ and $((CH_3)_3Pb)_2OH^+$, respectively. P refers to the fraction of the total trimethyllead present in each of the forms and $\delta$ is the chemical shift of that form. The fractions are defined as

$$P_{TML} = [(CH_3)_3Pb^+]/TMLT \quad (14)$$

$$P_{TMLOH} = [(CH_3)_3PbOH]/TMLT \quad (15)$$

$$P_{TMLD} = 2[((CH_3)_3Pb)_2OH^+]/TMLT \quad (16)$$

where TMLT represents the total concentration of the trimethyllead moiety:

$$TMLT = [(CH_3)_3Pb^+] + [(CH_3)_3PbOH] + 2[((CH_3)_3Pb)_2OH^+] \quad (17)$$

The fractions $P_{TMLOH}$ and $P_{TMLD}$ can be expressed solely in terms of $K_1$, $K_2$, $a_{OH^-}$ and $P_{TML}$. The rearrangement of Equation 10 to Equation 18:

$$[(CH_3)_3PbOH] = K_1 a_{OH^-}[(CH_3)_3Pb^+] \quad (18)$$

followed by the division of both sides of Equation 18 by TMLT yields Equation 19.

$$P_{TMLOH} = K_1 a_{OH^-} P_{TML} \quad (19)$$

Similarly, $P_{TMLD}$ can be expressed as

$$P_{TMLD} = 2K_1K_2a_{OH^-}((CH_3)_3Pb^+)^2/TMLT \qquad (20)$$

Equation 14 allows substitution of $(TMLT \cdot P_{TML})^2$ for $((CH_3)_3Pb^+)^2$ to obtain Equation 21.

$$P_{TMLD} = 2K_1K_2a_{OH^-}(TMLT)P_{TML}^2 \qquad (21)$$

Substitution of Equations 19 and 21 into Equation 13 gives Equation 22.

$$\delta_{OBS} = P_{TML}\delta_{TML} + K_1a_{OH^-}P_{TML}\delta_{TMLOH} + 2K_1K_2a_{OH^-}(TMLT)P_{TML}^2\delta_{TMLD} \qquad (22)$$

$P_{TML}$ can be expressed in terms of $K_1$, $K_2$ and TMLT by manipulation of the mass balance equation for the trimethyllead moiety (Equation 17). Dividing both sides of Equation 17 by TMLT leads to Equation 23.

$$1 = P_{TML} + P_{TMLOH} + P_{TMLD} \qquad (23)$$

Substitution of Equations 19 and 21 into Equation 23, followed by a minor rearrangement, yields Equation 24.

$$2K_1K_2a_{OH^-}(TMLT)P_{TML}^2 + (1 + K_1a_{OH^-})P_{TML} - 1 = 0 \qquad (24)$$

Solution of this equation for $P_{TML}$ by the quadratic formula gives Equation 25.

$$P_{TML} = \frac{-(1 + K_1 a_{OH^-}) + ((1 + K_1 a_{OH^-})^2 + 8K_1K_2 a_{OH^-}(TMLT))^{1/2}}{4K_1K_2 a_{OH^-}(TMLT)} \quad (25)$$

The substitution of this equation into Equation 22 allows the evaluation of $K_1$, $K_2$ and $\delta_{TMLD}$ from the chemical shift data, over the pH range 0.5 to 13.0 and over the trimethyllead concentration range of $5 \times 10^{-3}$ M to $2 \times 10^{-1}$ M, using the non-linear least squares curve-fitting program KINET described by Dye and Nicely (94). The ionic strength was controlled at 0.3 M with sodium perchlorate. The chemical shifts of $(CH_3)_3Pb^+$ and $(CH_3)_3PbOH$ were taken to be the limiting shifts of the trimethyllead central resonance in sufficiently acidic and alkaline solutions, respectively.

The curve-fitting procedure required Equations 22 and 25. These were supplied in a subroutine to the curve-fitting program KINET. Using reasonable initial estimates for $K_1$, $K_2$ and $\delta_{TMLD}$, KINET calculated $P_{TML}$ with Equation 25 and then predicted a value, $\delta_{CALC}$, for the resultant chemical shift with Equation 22. This procedure was repeated at each data point to predict a chemical shift vs. pH curve for those particular values of $K_1$, $K_2$ and $\delta_{TMLD}$. The observed chemical shift data set (i.e., the observed curve) was compared to the calculated data set (i.e., the calculated curve) and the values of $K_1$, $K_2$ and

$\delta_{TMLD}$ were adjusted iteratively by KINET to minimize the sum of the squares of the residuals (SSR) over the entire data set, where

$$SSR = \sum_i (\delta_{i,CALC} - \delta_{i,OBS})^2 \qquad (26)$$

This procedure ultimately gave the values of $K_1$ = 7.34 ($\pm$ 0.1) x $10^4$ $M^{-1}$ and $K_2$ = 3.12 ($\pm$ 0.1) x $10^1$ $M^{-1}$ for the formation constants of trimethyllead hydroxide and trimethyllead dimer, where the uncertainties are the linear estimates of the standard deviation. The chemical shifts of the species are 1.535 ppm ($(CH_3)_3Pb^+$), 1.253 ppm ($(CH_3)_3PbOH$) and 1.327 ppm ($((CH_3)_3Pb)_2OH^+$), quoted from DSS (i.e., the methyl resonance of sodium 2,2-dimethyl-2-silapentane-5-sulphonic acid).

Due to the asymmetric nature of Equation 12 (that is, a dimer is formed), the fractional population of trimethyllead dimer in solution is a function of the total trimethyllead concentration. The species distribution as a function of pH, calculated using the above values for $K_1$ and $K_2$ and a value of 0.100 M for TMLT, is shown in Figure 3. The species distribution depicted by Figure 4 was calculated in a similar manner, except that TMLT (the total concentration of the trimethyllead moiety) was 5.00 x $10^{-3}$ M. At the latter concentration, the maximal fractional concentration of the trimethyllead moiety present as $((CH_3)_3Pb)_2OH^+$ is 0.07, compared to a value of 0.46

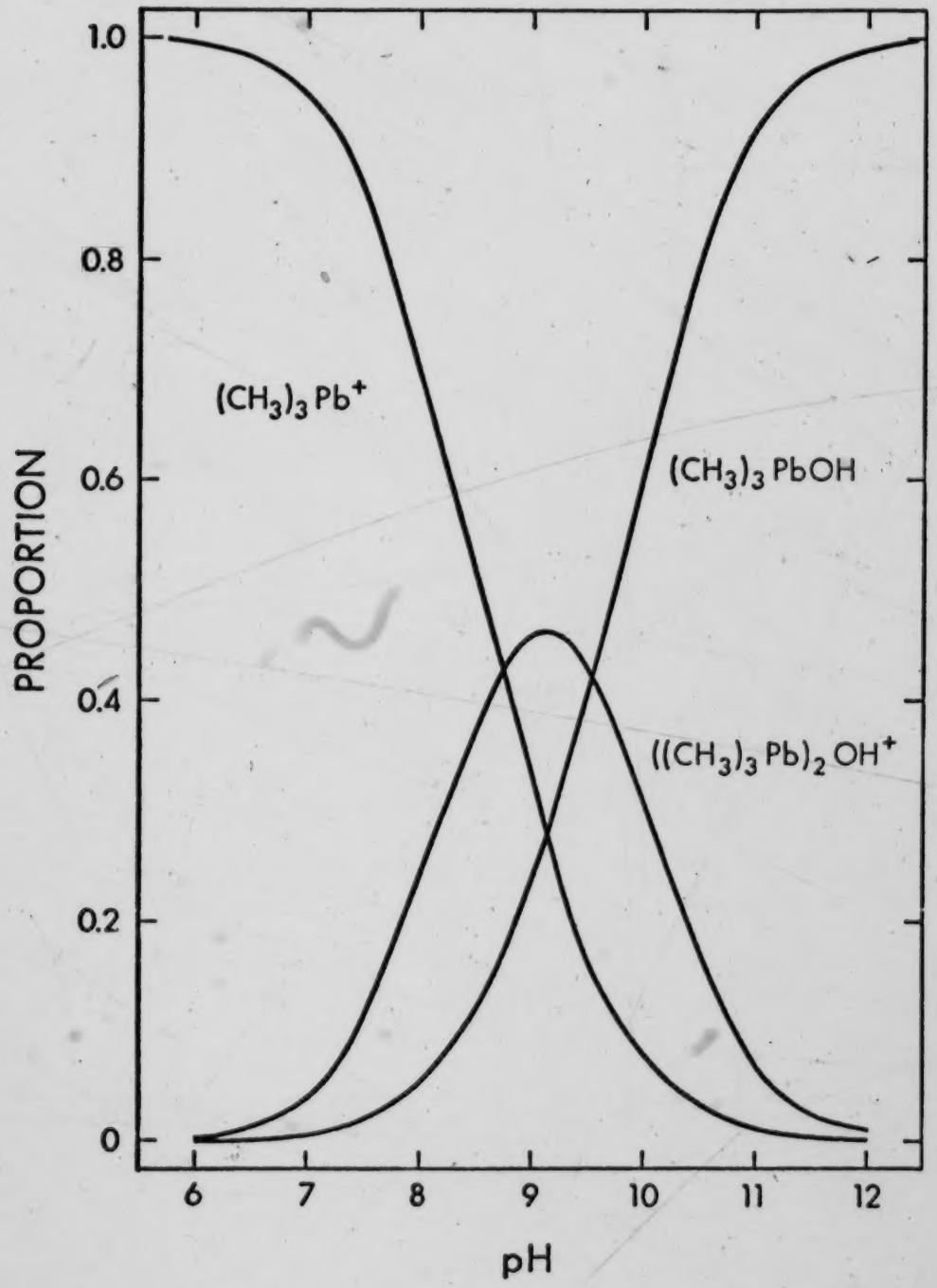


Figure 3. pH dependence of the trimethyllead species distribution in a 0.100 M aqueous solution, calculated using $K_1$ and $K_2$ as in the text.

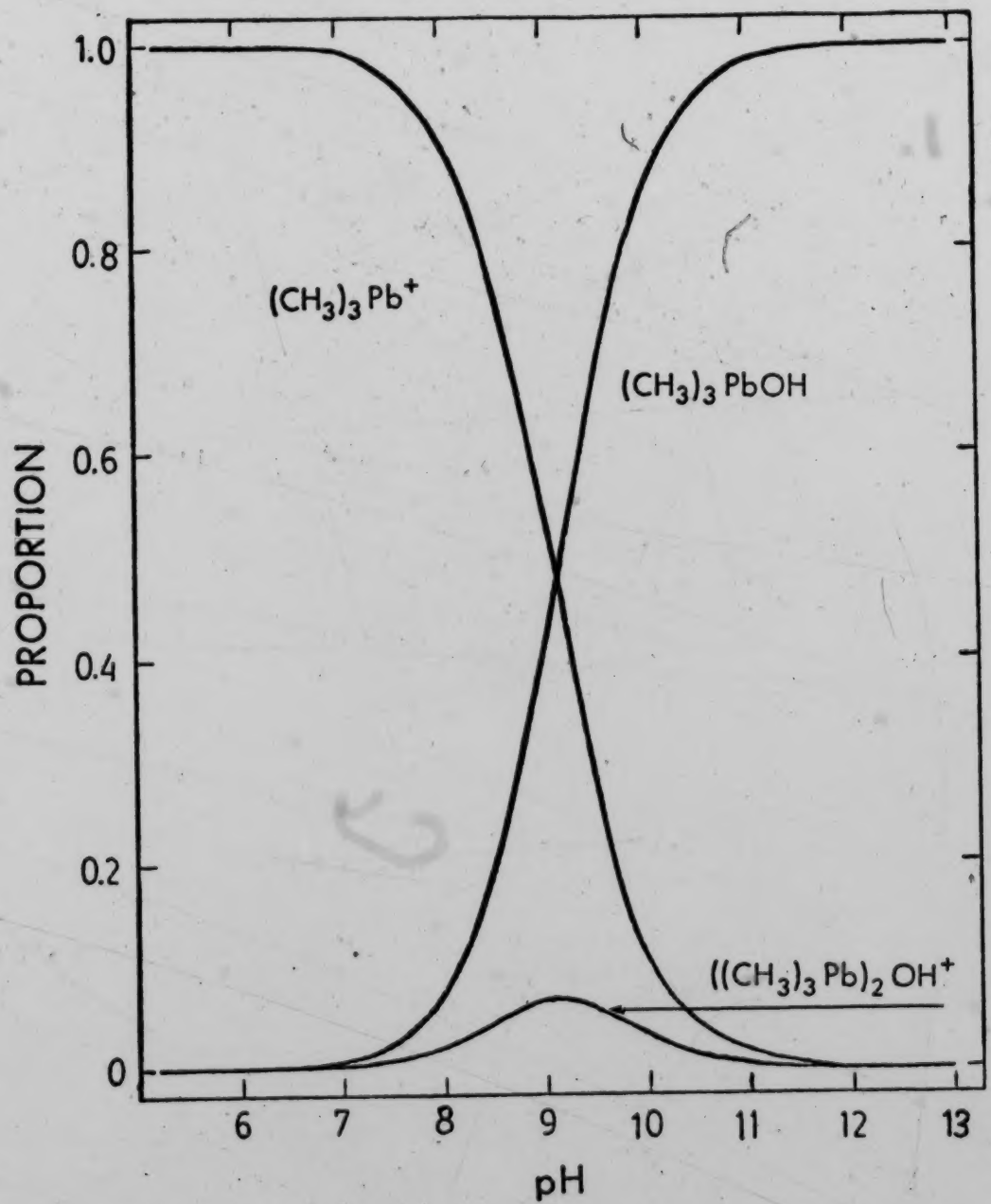


Figure 4. pH dependence of the trimethyllead species distribution in a $5.00 \times 10^{-3}$ M aqueous solution, calculated using $K_1$ and $K_2$ as in the text.

at the higher concentration. Since $K_1$ and $K_2$ were calculated from data acquired in solutions of 0.3 M ionic strength, these curves must be considered accurate only under similar conditions.

A very good fit of the calculated data to the observed data was obtained with the model described above. Thus, the previously mentioned analogy of the aqueous methylmercury equilibria (85,101,102) to those of trimethyllead appears to be consistent and apt in most respects. As yet, however, few reports exist in the literature for comparison with the results detailed in this chapter. Table 1 listed only two other determinations of $K_1$ (in both cases reported as the $K_a$ of aquated $(CH_3)_3Pb^+$), both of which can be considered somewhat unreliable. The first value listed, $3.5 \times 10^4$, was determined under conditions of unknown temperature and ionic strength (32). The second value, $5.0 \times 10^5$ was determined at 25°C and in 0.1 M $KNO_3$ (72), but is in doubt as well. The source of this reference, Chemical Abstracts, quotes what appears to be the $K_a$ of aquated trimethyllead as 8.70. This is presumably a misprint or a misinterpretation of the original paper; it is assumed here that this value is actually log $K_a$. The value of $5.0 \times 10^5$ for $K_1$ was calculated on this premise and is therefore questionable. Nonetheless, the value determined for $K_1$ in this chapter is intermediate to the two previously reported values. Other

than that paper in which the work described in this paper is outlined (62), no report of $K_2$ is known to exist in the literature.

# CHAPTER IV

# THE TRIMETHYLLEAD COMPLEXES OF SELECTED THIOLS AND AMINO ACIDS

## A. Introduction

This chapter presents the results of a series of experiments designed to investigate and quantify the binding of trimethyllead by certain organic ligands. The complexation of trimethyllead by glycine, cysteine and glutathione was studied to partially elucidate the behaviour of trimethyllead in physiological systems, where these ligands are commonly present. To further increase our understanding of sulfhydryl-bound trimethyllead, the complexes of 2-mercaptoethanol, N-acetylpenicillamine and penicillamine were also considered.

In each section, the determinations of the appropriate acid dissociation constants are followed by calculations of the complex formation constants from chemical shift vs. pH measurements. The discussion examines correlations and trends in the calculated formation constants and chemical shifts, and also presents species distribution curves of the trimethyllead-complexed systems.

B. Results

1. 2-Mercaptoethanol Complexes

(a) The Acid Dissociation Constant of 2-Mercaptoethanol. As pH increases, fully protonated 2-mercaptoethanol will lose a proton as shown by Equation 27.

$$HOCH_2CH_2SH \rightleftarrows HOCH_2CH_2S^- + H^+ \qquad (27)$$

The acid dissociation constant which quantifies this equilibrium is defined by Equation 28.

$$K_a = \frac{a_{H^+}\,[HOCH_2CH_2S^-]}{[HOCH_2CH_2SH]} \qquad (28)$$

This is a mixed acid dissociation constant: both concentrations and activities are included in the definition. All $K_a$'s used in this thesis for $K_f$ calculation are of this form. It should also be noted that at very high pH, the species $HOCH_2CH_2S^-$ will deprotonate at the alcohol group. However, this doubly deprotonated species was found to have no significance in this study because such extreme conditions were never employed. For the purposes of this work, the acid-base chemistry of 2-mercaptoethanol is completely described by Equations 27 and 28.

The acid dissociation constant, $K_a$, was determined by pH titration as described in Chapter II. Temperature was maintained at 25°C and ionic strength was controlled at 0.3 M with $NaClO_4$. The value of the $pK_a$ determined

from four replicates (corrected for hydroxide ion bias as recommended by Albert and Serjeant (97)) was 9.57 ± 0.02, where the error factor indicates the spread of the values obtained. This was in good agreement with the $pK_a$ values of 9.5 obtained by Calvin at 25°C in 0.15 M NaCl (103) and 9.52 obtained by Schwarzenbach and Schellenberg at 20°C in 0.1 M $KNO_3$ (102).

A value of the $pK_a$ was also determined using the nmr chemical shift vs pH method outlined in Chapter II and detailed below. The observed chemical shift of the two methylene groups of $HOCH_2CH_2SH$ are the average of the corresponding shifts of the protonated and deprotonated species, weighted according to their populations. (In the interests of brevity, $HOCH_2CH_2SH$ and $HOCH_2CH_2S^-$ hereafter will be represented by RSH and $RS^-$, respectively.)

$$\delta_{OBS} = P_{RSH}\delta_{RSH} + P_{RS^-}\delta_{RS^-} \qquad (29)$$

Both $P_{RSH}$ and $P_{RS^-}$ will be shown to be functions of $K_a$; hence, solution of Equation 29 enables the determination of the $pK_a$ of 2-mercaptoethanol.

The values of $\delta_{RSH}$ and $\delta_{RS^-}$ were taken to be the limiting chemical shifts of the appropriate resonances at low and high pH, respectively. The fractional populations are defined as

$$P_{RSH} = [RSH]/[R]_{TOT} \qquad (30)$$

$$P_{RS^-} = [RS^-]/[R]_{TOT} \quad (31)$$

where $[R]_{TOT}$ is the total concentration of 2-mercaptoethanol in all forms. The summation of the fractional populations is unity:

$$1 = P_{RSH} + P_{RS^-} \quad (32)$$

Appropriate substitution of Equations 30 and 31 into Equation 28 results in an expression of $K_a$ in terms of the fractional populations defined above.

$$K_a = (a_{H^+} \cdot P_{RS^-})/ P_{RSH} \quad (33)$$

Appropriate substitution and rearrangement of Equations 32 and 33 gives expressions of the fractional populations in terms of hydrogen ion activity and $K_a$ alone.

$$P_{RSH} = a_{H^+}/(K_a + a_{H^+}) \quad (34)$$

$$P_{RS^-} = K_a/(K_a + a_{H^+}) \quad (35)$$

Substitution of these equations into Equation 29 results in an equation for the observed chemical shift in terms of known experimental parameters and only one unknown, $K_a$.

$$\delta_{OBS} = (a_{H^+} \cdot \delta_{RSH} + K_a \cdot \delta_{RS^-})/(K_a + a_{H^+}) \quad (36)$$

With this equation, $pK_a$ was determined from chemical shift vs. pH titration data.

The pmr spectrum of 2-mercaptoethanol consists of two multiplets of approximately equal intensity. The methylene protons nearest the alcohol group ($-OCH_2-$) give rise to the multiplet further upfield, while those nearest the sulfhydryl ($-CH_2S-$) cause the downfield multiplet. Figure 5 shows the pH dependence of these two resonances.

$K_a$ was evaluated with Equation 36 using the non-linear least-squares curve-fitting program KINET (94) described earlier in this thesis. Each curve in Figure 5 was considered separately, over the pH range 5.9 to 13.0. Total 2-mercaptoethanol concentration was 0.139 M, temperature was 25°C and ionic strength was maintained at 0.3 M with $NaClO_4$. Using the limiting chemical shift values of 3.706 ppm vs. DSS for $\delta_{RSH}$ and 3.537 ppm vs. DSS for $\delta_{RS^-}$, the $-CH_2S-$ data gave a value for $K_a$ of 2.47 ($\pm$ 0.04) x $10^{-10}$ M. Similarly, using 2.683 ppm vs. DSS for $\delta_{RSH}$ and 2.566 ppm vs. DSS for $\delta_{RS^-}$, the $-OCH_2-$ data resulted in a $K_a$ of 2.31 ($\pm$ 0.04) x $10^{-10}$ M. The averaged result gave the final $pK_a$ of 9.62 $\pm$ 0.02. The conditions and methods employed in the determination closely match those used in the determination of the formation constants of the 2-mercaptoethanol-trimethyllead complexes described later in this section; therefore, the value used for the $pK_a$ of 2-mercaptoethanol in this study was 9.62 $\pm$ 0.02 rather than the value of 9.57 obtained by pH titration.

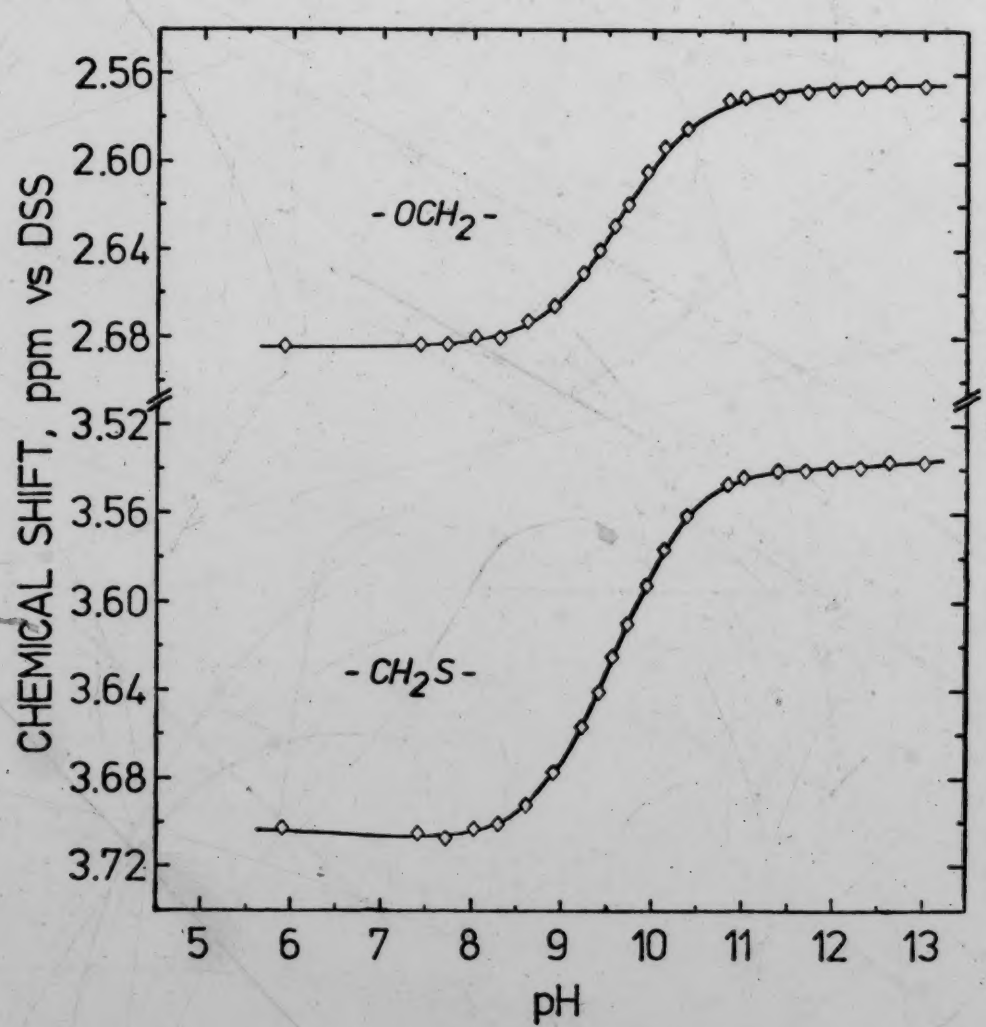


Figure 5. pH dependence of the chemical shift of the $-OCH_2-$ and the $-CH_2S-$ multiplet resonances for a 0.139 M solution of 2-mercaptoethanol at 25°C and 0.3 M ionic strength (maintained with $NaClO_4$).

(b) The 2-Mercaptoethanol Complexes of Trimethyllead. The binding of trimethyllead by 2-mercaptoethanol was investigated by monitoring the chemical shift of the methyl protons of trimethyllead as a function of pH and also as a function of the trimethyllead to 2-mercaptoethanol concentration ratio.

*(i) Qualitative Observations*

The chemical shift of the methyl protons of trimethyllead is presented in Figure 6 as a function of pH for three solutions containing trimethyllead and 2-mercaptoethanol and for one solution of trimethyllead alone. The curves for the solutions containing 2-mercaptoethanol approach the curve for the solution containing only trimethyllead at the extremes of pH. These results indicate that, at low pH, protons compete with the trimethyllead for the ligand sulfhydryl group, while at high pH, hydroxide ions compete effectively with the ligand for the available trimethyllead cations. The attainment of maximum complexation is indicated by the plateaux in the intermediate pH range, where both competing ions are at low concentrations.

A mole ratio experiment was performed to determine the coordination numbers of these complexes. The results of this experiment, in which the chemical shift of trimethyllead was measured as a function of the ligand to metal ratio, are shown in Figure 7. The observed chemical shift varies with increasing proportion of ligand until a

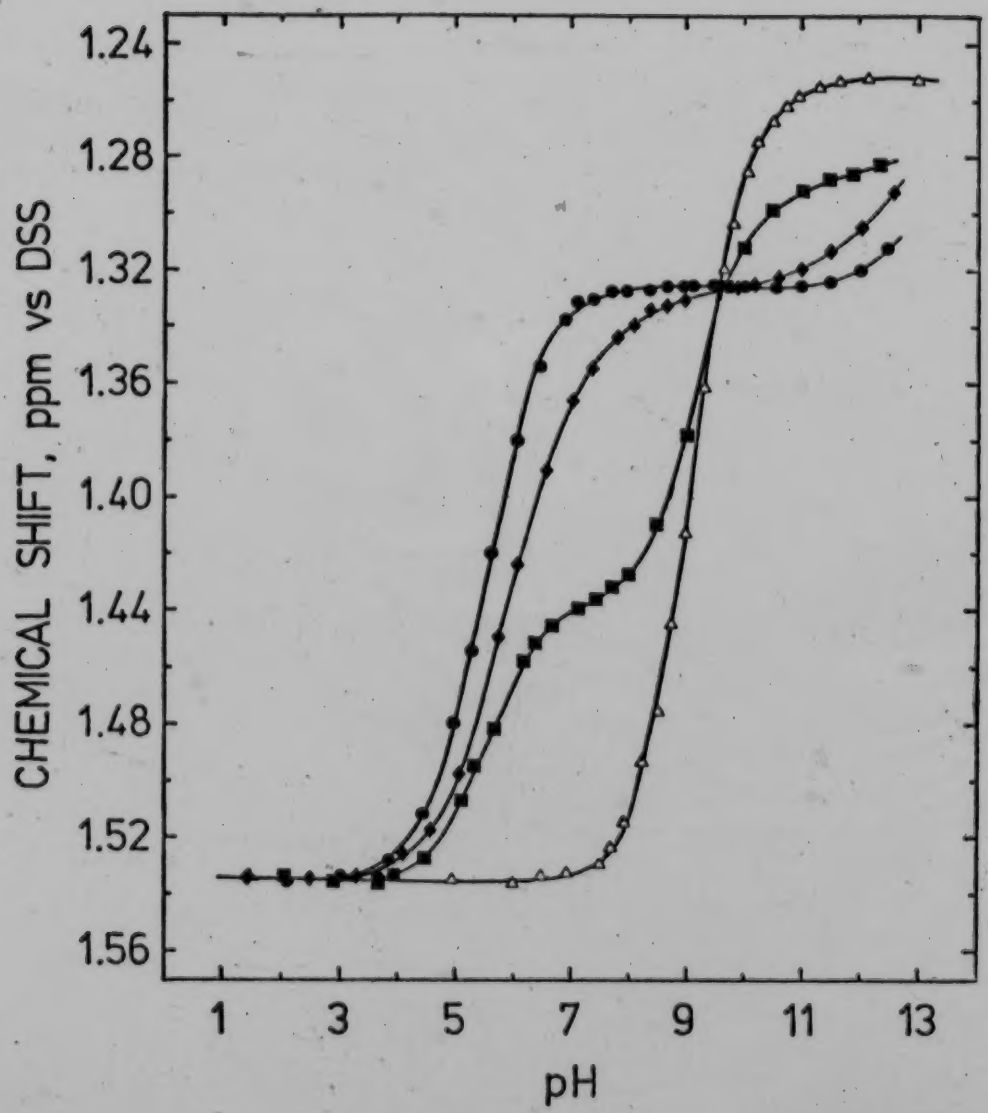


Figure 6. pH dependence of the chemical shift of trimethyllead in a sulfhydryl-free 0.0100 M aqueous solution (△) and in solutions of 0.0100 M trimethyllead and 0.0200 M 2-mercaptoethanol (●), 0.0100 M trimethyllead and 0.00970 2-mercaptoethanol (◆), and 0.0200 M trimethyllead and 0.0100 M 2-mercaptoethanol (■). Ionic strength was controlled at 0.3 M with $NaClO_4$ and temperature was 25°C.

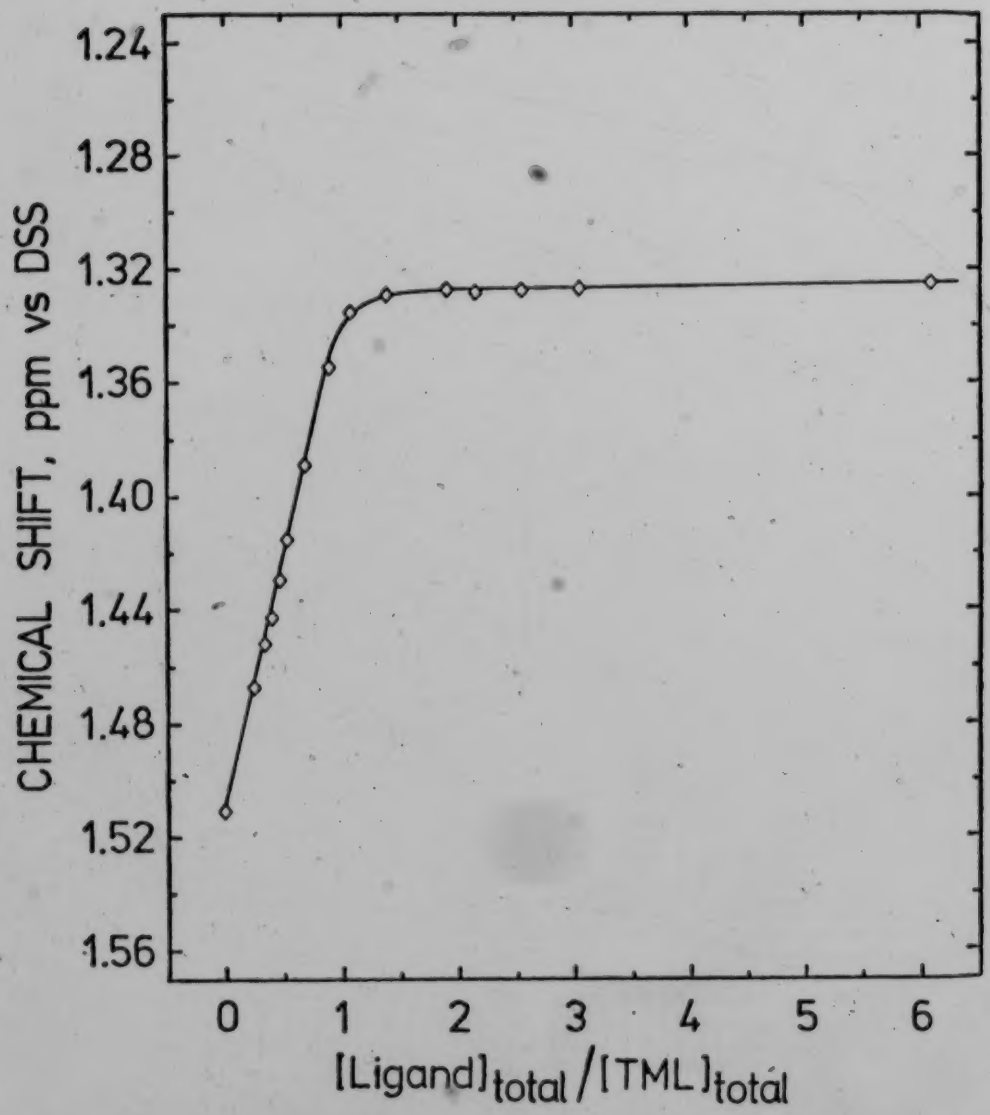


Figure 7. The dependence of the chemical shift of trimethyllead upon the ratio of 2-mercaptoethanol to trimethyllead in solution at pH 8.0. The concentration of ligand was 0.00887 M except at the ratio of zero to one. The ionic strength was maintained at 0.3 M with $NaClO_4$ and the temperature was 25°C.

one-to-one ratio is reached, after which the chemical shift remains constant even with a several-fold excess of ligand. This indicates that the major complex at all measured ratios is the one-to-one ligand-to-metal complex, $(CH_3)_3PbSCH_2CH_2OH$. No evidence was found for any complex of greater ligand to metal ratio. However, the deviation from linearity in the low ligand to metal portion of the curve was attributed to the presence of a weak 1 to 2 ligand to metal complex, most likely $((CH_3)_3Pb)_2SR^+$. This was confirmed by studies described later in this section.

*(ii) Derivation of a Mathematical Model for the 2-Mercaptoethanol-Trimethyllead System*

Separate pmr signals are not observed for the different trimethyllead species, indicating that exchange of the trimethyllead moiety among its various forms is fast on the nmr time scale (62). The chemical shift of the observed resonance is an average of the chemical shifts of the various trimethyllead species present in solution, weighted according to their populations. Formation constants and chemical shifts for the metal-ligand complexes were calculated by fitting proposed models of the complexation equilibria to the observed chemical shift data, using the curve-fitting computer program KINET (94) described earlier in this thesis. The best fit to the observed data was obtained for a model which included one to one and two to one trimethyllead to 2-mercaptoethanol complexes.

The aim in this section of the thesis is to derive a mathematical model for the observed trimethyllead chemical shift behaviour; this model will be used in the next section to calculate the unknown parameters for the metal-ligand complexes.

The derivation of the model of any chemical system requires the initial definition of equations which quantify the component equilibria of the system. The equilibria of trimethyllead in aqueous solutions are described by Equations 9 through 12 in Chapter III; those of 2-mercaptoethanol are given by Equations 27 and 28 in this chapter. Equations 37 through 40 describe the equilibria of the trimethyllead-2-mercaptoethanol complexes which resulted in the model most closely fitting the observed chemical shift data.

$$TML^+ + RS^- \rightleftarrows TMLSR \tag{37}$$

$$K_{fS} = \frac{[TMLSR]}{[TML^+][RS^-]} \tag{38}$$

$$TML^+ + TMLSR \rightleftarrows (TML)_2SR^+ \tag{39}$$

$$K_{fD} = \frac{[(TML)_2SR^+]}{[TML^+][TMLSR]} \tag{40}$$

TMLSR and $(TML)_2SR^+$ refer to $(CH_3)_3PbSCH_2CH_2OH$ and $((CH_3)_3Pb)_2SCH_2CH_2OH^+$, respectively, and $K_{fS}$ and $K_{fD}$ are

the formation constants of these complexes. The exchange-averaged chemical shift of this system is given by Equation 41; this equation is the fundamental chemical shift relation of this model.

$$\delta_{OBS} = P_{TML}\delta_{TML} + P_{TMLOH}\delta_{TMLOH} + P_{TMLD}\delta_{TMLD} + P_{TMLSR}\delta_{TMLSR} + P_{(TML)_2SR^+}\delta_{(TML)_2SR^+} \quad (41)$$

The first three terms are defined as for Equations 13 through 16 in Chapter III. The fractions of the remaining species are defined as follows:

$$P_{TMLSR} = [TMLSR]/TMLT \quad (42)$$

$$P_{(TML)_2SR^+} = 2[(TML)_2SR^+]/TMLT \quad (43)$$

where TMLT is the total concentration of the trimethyllead moiety in solution. Appropriate substitution into Equation 41 results in Equation 44.

$$\delta_{OBS} = P_{TML}\delta_{TML} + K_1 a_{OH^-} P_{TML}\delta_{TMLOH} + 2K_1K_2 a_{OH^-}(TMLT)P_{TML}^2\delta_{TMLD} + K_{fS}[RS^-]P_{TML}\delta_{TMLSR} + 2K_{fD}K_{fS}[RS^-](TMLT)P_{TML}^2\delta_{(TML)_2SR^+} \quad (44)$$

where

$$P_{TML} = [TML^+]/TMLT \quad (45)$$

All that remains is to solve for $[TML^+]$ and $[RS^-]$

in terms of known parameters. The mass balance equations for total trimethyllead and total 2-mercaptoethanol provide the necessary relations:

$$TMLT = [TML^+] + [TMLOH] + 2[TMLD] + [TMLSR] + 2[(TML)_2SR^+] \quad (46)$$

$$RSHT = [RS^-] + [RSH] + [TMLSR] + [(TML)_2SR^+] \quad (47)$$

where RSHT is the total concentration of the 2-mercaptoethanol moiety.

By appropriate substitution of Equations 10, 12, 28, 38 and 40, the mass balance equations can be written as two equations in two unknowns, $[TML^+]$ and $[RS^-]$. These can be manipulated to give a polynomial in $[TML^+]$ only, the solution of which allows the determination of both $[TML^+]$ and $[RS^-]$ if TMLT, RSHT and pH are known. This derivation is outlined below.

The mass balance equation for the ligand, expressed as a function of $[TML^+]$ and $[RS^-]$ only, is equation 48.

$$RSHT = [RS^-] + \frac{a_{H^+}[RS^-]}{K_a} + K_{fS}[TML^+][RS^-] + K_{fD}K_{fS}[TML^+]^2[RS^-] \quad (48)$$

Rearrangement of this gives Equation 49:

$$[RS^-] = RSHT/(1 + a_{H^+}/K_a + K_{fS}[TML^+] + K_{fD}K_{fS}[TML^+]^2) \quad (49)$$

Similar substitution into the mass balance equation for trimethyllead (Equation 46) results in Equation 50:

$$TMLT = [TML^+] + K_1 a_{OH^-}[TML^+] + 2K_1K_2 a_{OH^-}[TML^+]^2 + K_{fS}[TML^+][RS^-] + 2K_{fD}K_{fS}[TML^+]^2[RS^-] \quad (50)$$

Substitution of the right hand side of Equation 49 for $[RS^-]$ in Equation 50 gives an expression for the mass balance of trimethyllead in terms of $[TML^+]$ alone.

$$TMLT = [TML^+] + K_1 a_{OH^-}[TML^+] + 2K_1K_2 a_{OH^-}[TML^+]^2 + K_{fS}[TML^+]\{RSHT/(1 + a_{H^+}/K_a + K_{fS}[TML^+] + K_{fD}K_{fS}[TML^+]^2)\} + 2K_{fD}K_{fS}[TML^+]^2\{RSHT/(1 + a_{H^+}/K_a + K_{fS}[TML^+] + K_{fD}K_{fS}[TML^+]^2)\} \quad (51)$$

A rearrangement of this expression gives a polynomial in decreasing powers of $[TML^+]$:

$$\{2K_1K_2 a_{OH^-}K_{fD}K_{fS}\}[TML^+]^4 + \{2K_1K_2 a_{OH^-}K_{fS} + (1 + K_1 a_{OH^-})K_{fD}K_{fS}\}[TML^+]^3 + \{2K_1K_2 a_{OH^-}\cdot(1 + a_{H^+}/K_a) + (1 + K_1 a_{OH^-})K_{fS} + 2K_{fD}K_{fS}(RSHT) - K_{fD}K_{fS}(TMLT)\}[TML^+]^2 + \{(1 + K_1 a_{OH^-})(1 + a_{H^+}/K_a) + K_{fS}(RSHT) - K_{fS}(TMLT)\}[TML^+] - \{(1 + a_{H^+}/K_a)(TMLT)\} = 0 \quad (52)$$

The coefficients of this polynomial are functions of $K_1$, $K_2$, $K_a$ (known constants), RSHT, TMLT, $a_{H^+}$ and $a_{OH^-}$ (known experimental parameters) and the formation constants $K_{fS}$ and $K_{fD}$, the values of which were initially estimated but later optimized by computer calculations. Given this information, Equation 52 can be solved for $[TML^+]$; hence, the concentration of all the above-mentioned metal and ligand species can be determined. Finally, the substitution of the calculated values of $[TML^+]$ from Equation 52 and $[RS^-]$ from Equation 49 allows the calculation of the observed chemical shift for any reasonable set of solution conditions, including those given in Figure 6.

*(iii) Computer Optimization of Formation Constants and Chemical Shifts of Trimethyllead Complexes*

Due to the complexity of the equations derived above, the determinations of $K_{fS}$, $K_{fD}$, $\delta_{TMLSR}$ and $\delta_{(TML)_2SR^+}$ were accomplished with the digital computer program KINET (94), described earlier in this thesis. A flow chart summarizing this optimization procedure is shown in Figure 8. Initially, the program was supplied the known values of $K_1$, $K_2$, $K_a$, $\delta_{TML}$, $\delta_{TMLOH}$ and $\delta_{TMLD}$. Experiments carried out at various metal to ligand ratios (as plotted in Figure 6) provided the required chemical shift vs. pH, TMLT and RSHT data. In addition, initial estimates were introduced for the formation constants and limiting chemical shifts of the trimethyllead complexes.

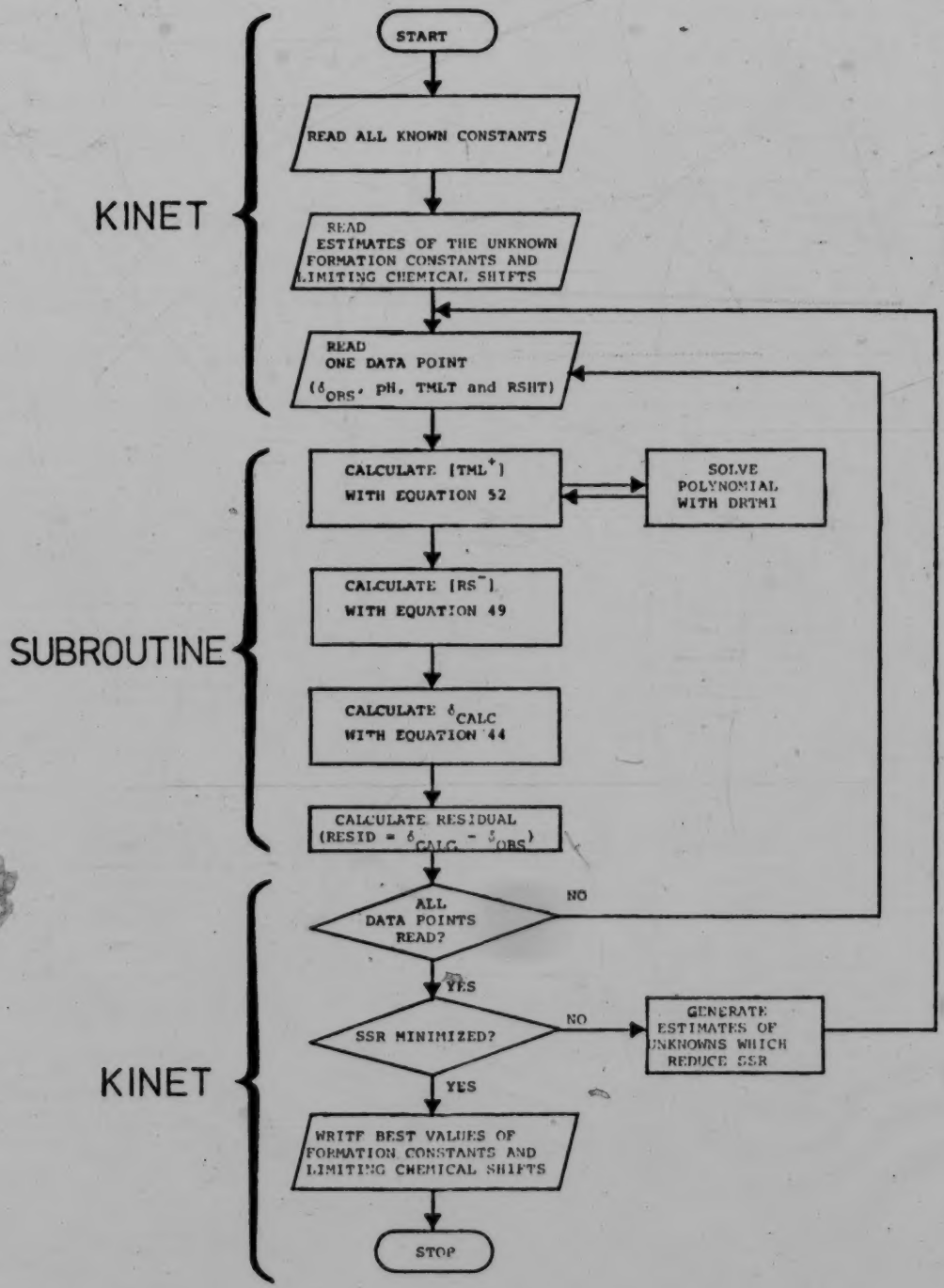


Figure 8. Flow chart of the computer procedure employed to optimize the formation constants and chemical shifts of the 2-mercaptoethanol complexes of trimethyllead.

The mathematical model (Equation 44), along with all preliminary calculations, was supplied to KINET in a subroutine (hereafter called EQN). At each data point, the subroutine EQN calculated the coefficients of Equation 52 and supplied them to the IBM SSP Library Subroutine DRTMI, which solved the polynomial for a value of $[TML^+]$ between zero and TMLT. This enabled the successive solution of Equations 45, 49 and 44, thereby providing a value for the averaged chemical shift, $\delta_{CALC}$, of the trimethyllead protons for one data point and a particular set of estimated parameters. The residual, which is the difference between this calculated shift and the experimentally observed shift, was determined for these conditions. This process was repeated until the residual at every data point had been calculated. KINET then computed the sum of the squares of the residuals (SSR) as defined by Equation 26 in Chapter III. After each such calculation, KINET altered the values of the estimated parameters such that SSR would be less in the following calculation. The best values for $K_{fS}$, $K_{fD}$, $\delta_{TMLSR}$ and $\delta_{(TML)_2SR^+}$ were attained when the minimum in the SSR was reached. At this time, KINET also provided error estimates for these parameters based on the quality of the fit between the observed and calculated chemical shift curves.

*(iv) Computed Results*

The value of $K_{fS}$ was computed to be 9.05 ($\pm$ 0.11) x $10^5$, using all the data in Figure 6 over the pH range 1.5 to 12.5 simultaneously. Similarly, the best values of $K_{fD}$, $\delta_{TMLSR}$ and $\delta_{(TML)_2SR^+}$ were calculated to be 14.0 $\pm$ 8.8, 1.3245 $\pm$ 0.0002 and 1.454 $\pm$ 0.007 respectively, where the chemical shifts are in units of ppm vs. DSS. The uncertainties are linear estimates of the standard deviations as determined by KINET.

No other determinations of these quantities are available in the literature for comparison. However, the good quality of the fit of this model calculation to the observed data tends to support the accuracy of the optimized parameters, as the calculated error estimates are a fair measure of the precision and accuracy of these results. All are of reasonably low magnitude except for that of $K_{fD}$; this large relative error is due in part to the low magnitude of $K_{fD}$. The concentration of $(TML)_2SR^+$ is always a small fraction of the total concentration and consequently $K_{fD}$ cannot be determined with a high degree of precision. The fraction of $(TML)_2SR^+$ is reduced further by the unfavorable ratios of metal to ligand employed for some of the experimental solutions.

No evidence was found to indicate the presence of measurable quantities of any species in solution other than those described above.

## 2. Glycine Complexes

The binding of trimethyllead by glycine was studied as a model for complexation by the amino and carboxylate groups in the sulfhydryl-containing amino acids and peptides studied later in this thesis.

### (a) The Acid Dissociation Constants of Glycine.

Fully protonated glycine is a dibasic acid, dissociating as follows:

$$H_3^+NCH_2COOH \rightleftarrows H_3^+NCH_2COO^- + H^+ \quad (53)$$

$$H_3^+NCH_2COO^- \rightleftarrows H_2NCH_2COO^- + H^+ \quad (54)$$

The corresponding acid dissociation constants are defined below:

$$K_{a1} = \frac{[HL]a_{H^+}}{[H_2L^+]} \quad (55)$$

$$K_{a2} = \frac{[L^-]a_{H^+}}{[HL]} \quad (56)$$

where $H_2L^+$, HL and $L^-$ represent the fully protonated, zwitterionic and doubly deprotonated species respectively. The numerical values for $K_{a1}$ and $K_{a2}$ were determined by monitoring the chemical shift of the glycine methylene protons as a function of pH at 25°C in a 0.100 M glycine solution, controlled at 0.3 M ionic strength with $NaClO_4$. The resultant curve is plotted in Figure 9.

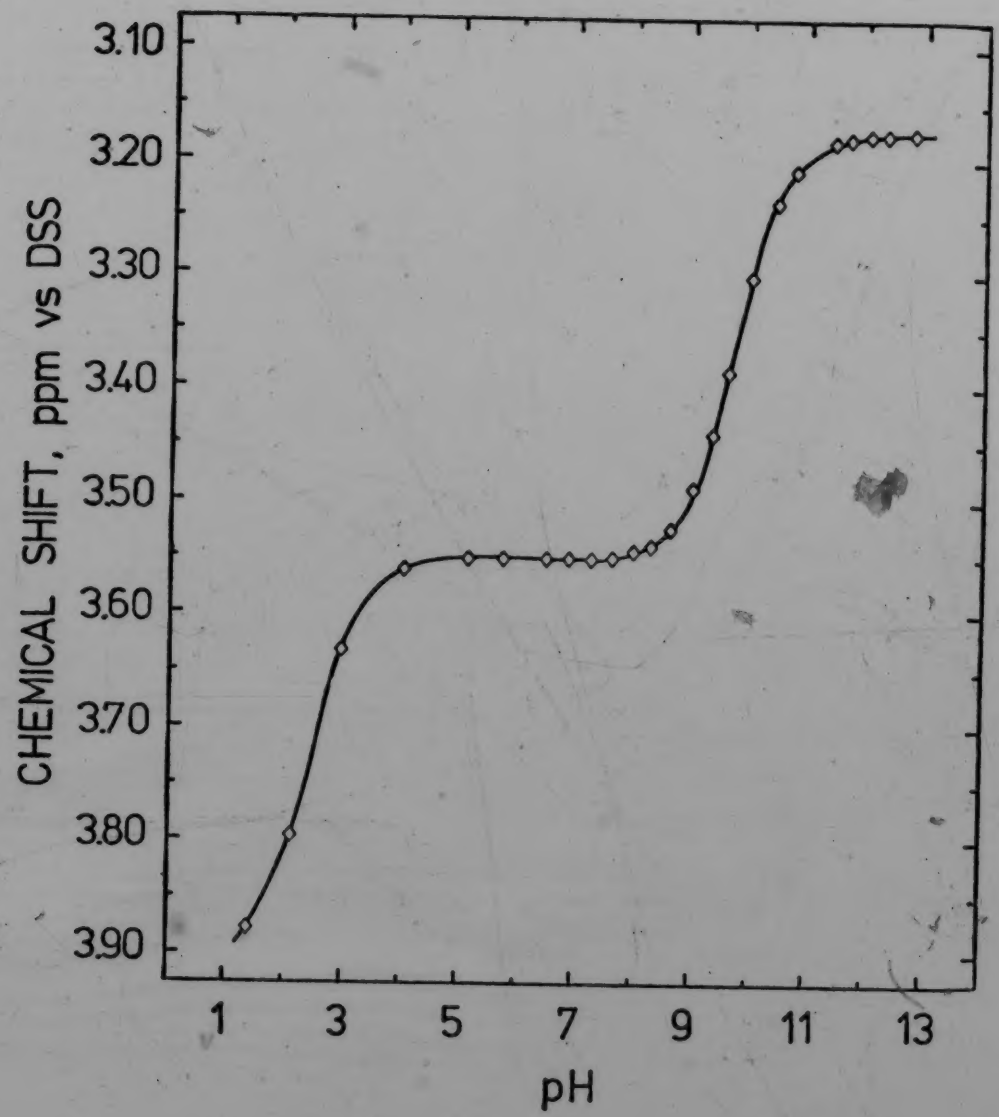


Figure 9. pH dependence of the chemical shift of the methylene protons of glycine in a 0.100 M solution at 25°C and 0.3 M ionic strength (maintained with $NaClO_4$).

The mathematical model of glycine acid dissociation was derived in a manner quite analogous to that of 2-mercaptoethanol, except that two acidic protons were considered rather than just one. The values of $pK_{a1}$ and $pK_{a2}$ are sufficiently separated that the first ionization is essentially complete before the second ionization begins to occur. This enables the calculation of both these constants as simple independent ionizations in the same run of the curve-fitting computer program KINET. Using chemical shifts of 3.552 ppm vs. DSS for zwitterionic glycine and 3.175 ppm vs. DSS for doubly deprotonated glycine, values of 3.44 ($\pm$ 0.06) x $10^{-3}$ and 1.90 ($\pm$ 0.01) x $10^{-10}$ were obtained for $K_{a1}$ and $K_{a2}$, respectively, and a value of 3.906 $\pm$ 0.001 ppm vs. DSS was obtained for the chemical shift of fully protonated glycine. From these values, $pK_{a1}$ is calculated to be 2.46 and $pK_{a2}$ to be 9.72, which compare favorably with the recently-published (104) $pK_{a1}$ of 2.34 and $pK_{a2}$ of 9.69, determined under conditions of 0.2 to 0.3 M ionic strength and 25°C temperature. Other values of these constants found in the literature include a $pK_{a1}$ of 2.45 and $pK_{a2}$ of 9.75, determined spectrophotometrically at 25°C in 1 M $NaClO_4$ (105); and a $pK_{a1}$ of 2.47 and $pK_{a2}$ of 9.68, determined using a glass electrode at 25°C in 0.2 M KCl (106). The values determined by this pmr technique were used in the following computation of the formation constants of

the glycine carboxyl complexes of trimethyllead.

(b) The Glycine Complexes of Trimethyllead.

The formation constants and chemical shifts of the glycine complexes of trimethyllead were determined by measuring the chemical shift of the methyl protons of trimethyllead as a function of pH. The chemical shift vs. pH curve resulting from a solution having a metal to ligand ratio of one to ten is compared to that of a simple trimethyllead solution in Figure 10. Ratios other than one to ten were attempted, using both the trimethyllead methyl and the glycine methylene proton chemical shifts as functions of pH. However, due to the low degree of complexation of trimethyllead by glycine, only the most extreme ratio of metal to ligand resulted in a curve measurably different from that for a solution free of metal-ligand complex. Therefore, the program KINET could calculate formation constants only with the data shown in Figure 10.

The following reaction scheme was found to give the best fit to the observed chemical shift data:

$$\begin{array}{ccccc} H_3^+NCH_2COOH & \overset{K_{a1}}{\rightleftharpoons} & H_3^+NCH_2COO^- & \overset{K_{a2}}{\rightleftharpoons} & H_2NCH_2COO^- \\ & & \updownarrow K_{f1} & & \updownarrow K_{f2} \\ & & H_3^+NCH_2COOPb(CH_3)_3 & \overset{K_{a3}}{\rightleftharpoons} & H_2NCH_2COOPb(CH_3)_3 \end{array} \qquad (57)$$

where $K_{f1}$ and $K_{f2}$ are the formation constants of the complexes of trimethyllead with monoprotonated and fully

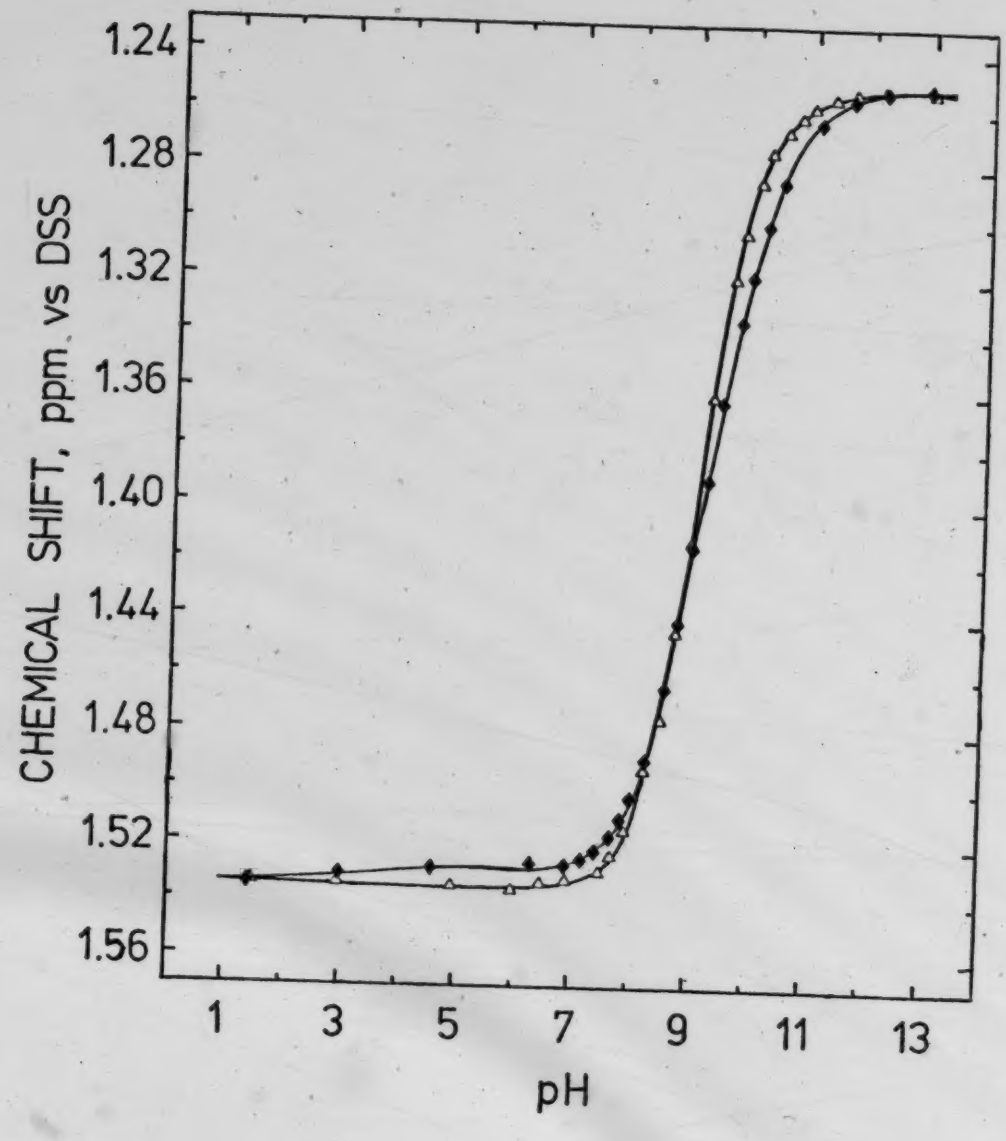


Figure 10. pH dependence of the chemical shift of trimethyllead at 25°C and 0.3 M ionic strength (maintained with $NaClO_4$) in a solution of 0.0100 M trimethyllead only (Δ) and in a solution containing 0.0100 M trimethyllead and 0.100 M glycine (◆).

deprotonated glycine, respectively. The binding site in both cases is assumed to be the carboxyl group (as discussed in part C of this chapter). Using the aforementioned abbreviations:

$$K_{f1} = \frac{[TML \cdot LH^+]}{[TML^+][HL]} \quad (58)$$

$$K_{f2} = \frac{[TML \cdot L]}{[TML^+][L^-]} \quad (59)$$

$$K_{a3} = \frac{[TML \cdot L]a_{H^+}}{[TML \cdot LH^+]} \quad (60)$$

The formation constants $K_{f1}$ and $K_{f2}$, as well as the associated chemical shifts, were determined by a computation quite similar to that described for the 2-mercaptoethanol complexes of trimethyllead. Using the appropriate constants detailed earlier in this thesis, Equation 61 was solved by KINET for the optimum values of these formation constants and chemical shifts.

$$\delta_{OBS} = P_{TML}\delta_{TML} + P_{TMLOH}\delta_{TMLOH} + P_{TMLD}\delta_{TMLD} + P_{TML.LH^+}\delta_{TML.LH^+} + P_{TML.L}\delta_{TML.L} \quad (61)$$

The values which resulted in the best fit were 1.26 ± 0.58 for $K_{f1}$, 1.481 ± 0.020 ppm vs. DSS for $\delta_{TML.LH^+}$, 29.5 ± 3.8 for $K_{f2}$ and 1.433 ± 0.016 ppm vs. DSS for $\delta_{TML.L}$.

No previously determined values for these constants

were available for comparison, but the fit to the observed data is reasonably good. The relative errors estimated here by KINET are larger than those found for the 2-mercaptoethanol results, but this is because the competition by protons and hydroxide ions precludes the formation of the weak glycine complexes through most of the experimental pH range. All the glycine results are known with a lesser degree of confidence due to the relative scarcity of complex, which in turn causes a higher error in the chemical shift data from which the results must be calculated. Nonetheless, this model still provides the best fit of the various types investigated.

The small size of the formation constant $K_{f2}$ is of immediate practical use. This constant is negligible compared to the $K_{fS}$ ($9.05 \times 10^5$) of the 2-mercaptoethanol sulfhydryl complex of trimethyllead. In sulfhydryl-containing amino acids and peptides, the amino and the sulfhydryl groups ionize more or less simultaneously; assuming a similar large difference in $K_{fS}$ and $K_{f2}$, the effect of the latter may be neglected in all solutions of low metal to ligand ratios. In addition, no evidence of amino group complexation has been observed; such complexes may therefore be neglected as well. These assumptions result in a considerable simplification of the computer calculations in the following sections, without decreasing the accuracy of the determinations of

$K_{fS}$ values and the associated chemical shifts for the trimethyllead-amino acid complexes. These simplifications were employed as required in the remainder of this chapter.

The value of $K_{a3}$ was calculated to be $4.4 \times 10^{-9}$ ($pK_{a3} = 8.35$), using the relation which states that the product of $K_{f1}$ and $K_{a3}$ equals the product of $K_{f2}$ and $K_{a2}$. This relation results from the properties of the cyclic system (118) and is hence exactly analogous to Equation 91, described and justified in detail in section 4(b) of this chapter.

3. N-Acetyl-D,L-Penicillamine Complexes

(a) The Acid Dissociation Constants of N-Acetyl-D,L-Penicillamine. The structural formula of fully protonated N-acetylpenicillamine is given by I:

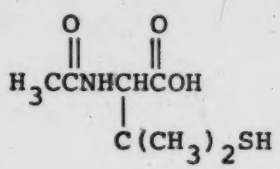

I

hereafter represented by $H_2A$ or by a shorthand version of the structure showing only the proton and metal binding sites. As pH is increased, first the carboxyl and then the sulfhydryl protons are removed. The equilibria involved are described by Equations 62 and 63; the corresponding acid dissociation constants are defined by Equations 64 and 65.

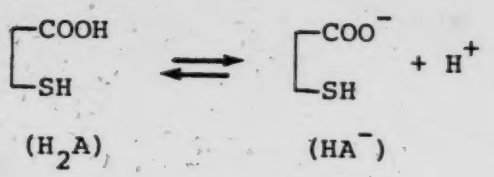

$(H_2A)$ $(HA^-)$ (62)

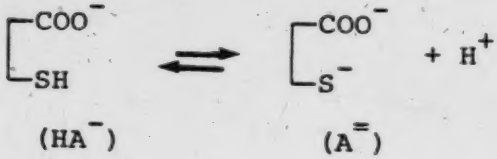

$(HA^-)$ $(A^=)$ (63)

$$K_{a1} = \frac{[HA^-]a_{H^+}}{[H_2A]} \quad (64)$$

$$K_{a2} = \frac{[A^=]a_{H^+}}{[HA^-]} \quad (65)$$

The values of $K_{a1}$ and $K_{a2}$ were determined by pH titration as described in Chapter II. The ionic strength of the solution was maintained at 0.3 M with $NaClO_4$ and temperature was controlled at 25°C. The values obtained for $K_{a1}$ and $K_{a2}$ were corrected for the interference of protons and hydroxide ions, respectively, using the methods of calculation detailed by Albert and Serjeant (97). Four replicates gave numerical values of 3.48 ± 0.01 for $pK_{a1}$ and 10.28 ± 0.05 for $pK_{a2}$, where the uncertainty is the maximum deviation from the average. Wilson and Martin (107) obtained the $pK_a$ values of this ligand by a similar pH titration. In 0.15 M KCl at 25°C, they determined a $pK_{a1}$ of 3.3 and a $pK_{a2}$ of 9.9; these compare reasonably well with the results given above, considering the dif-

ferences in ionic strength and in calculations. There is no indication that these authors performed the recommended (97) corrections for proton and hydroxide ion concentration in their $pK_a$ calculations. Furthermore, the use of only two significant figures probably indicates their level of confidence in the accuracy of the results. It was confirmed, however, that no evidence exists for amide hydrogen ionization below pH 11 (107); such a possibility is neglected henceforth.

The determination of $pK_a$ values using nmr titrations of pH vs. chemical shift was not successful due to the low solubility of the ligand under the required experimental conditions, combined with the limited usefulness of the broad, low amplitude nmr resonances of the ligand. This lack of sharpness is most likely related to the presence of the asymmetric center near the methyl groups of the ligand penicillamine residue: the low broad resonances are probably unresolved multiplets (108). The combination of poor spectral and solubility characteristics was such that the accurate measurement of the chemical shifts of the ligand resonances as a function of pH was not possible with the nmr instrument used in this research.

(b) <u>The N-Acetyl-D,L-Penicillamine Complexes of Trimethyllead</u>. The pH vs. chemical shift behaviour of the methyl protons of trimethyllead in solutions of excess

N-acetylpenicillamine was studied to determine the type and the extent of metal-ligand complexation in this system. Excess ligand was employed to ensure accurate results for the strong complexes with minimal interference from any weak complexes occurring in the same pH range. Low experimental signal amplitudes precluded the study of the pH vs. chemical shift behaviour of the various N-acetyl-penicillamine protons.

The results of experiments at metal to ligand ratios of one to two and one to four are presented in Figure 11. The plateaux between pH 8 and 11 indicate the formation of a strong complex of shift intermediate to those of the uncomplexed and the hydroxyl complexed trimethyllead cations. The difference in the breadth of these plateaux is due to the differences in total ligand concentration: a higher concentration of ligand drives the complexation equilibria towards increased formation of metal-ligand complexes over a wider pH region, despite the competition of protons and hydroxyl ions mentioned previously.

The model found to generate the best fit with the observed chemical shift data was derived using the following system of equilibria:

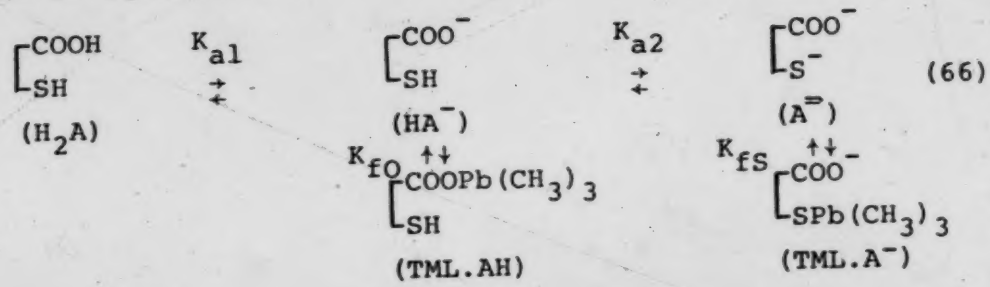


(66)

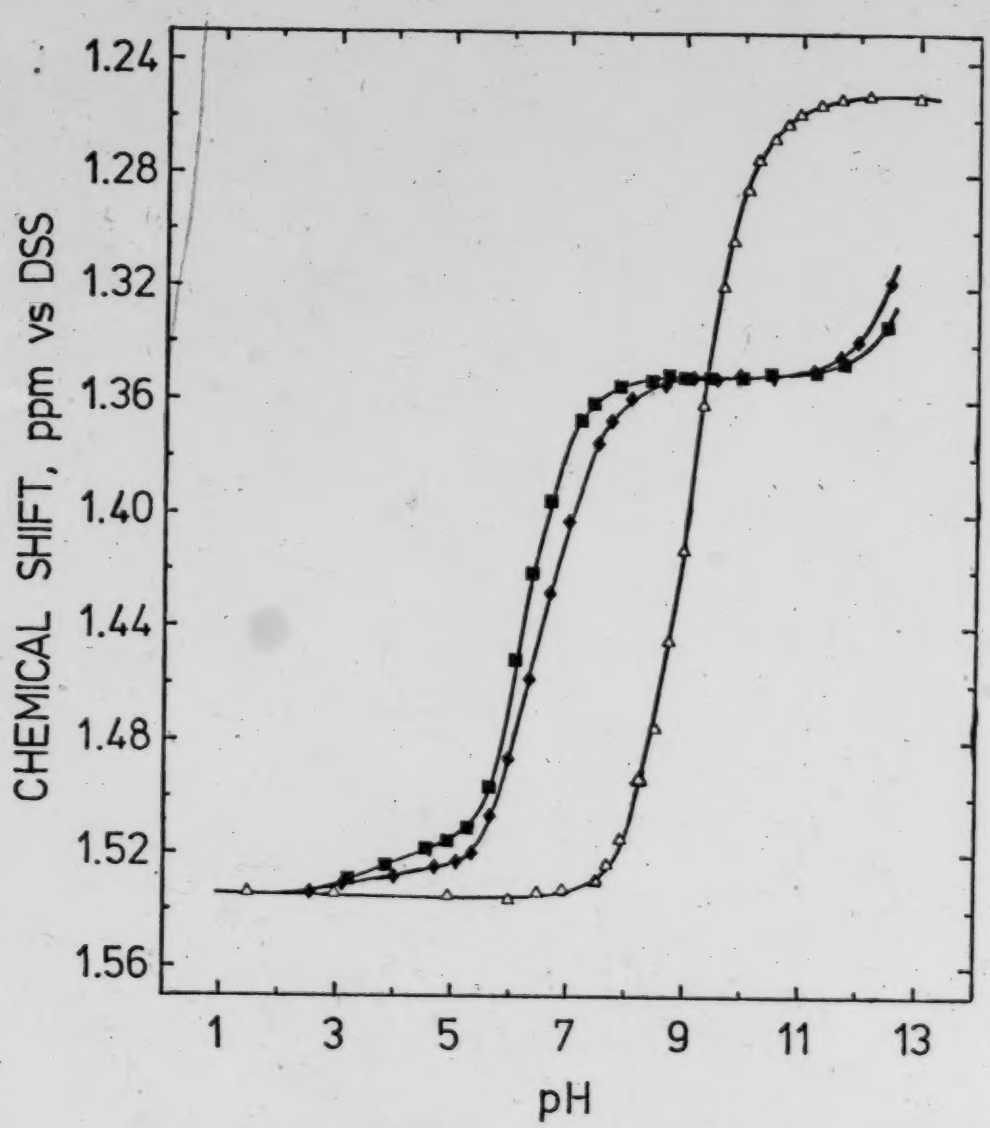


Figure 11. pH dependence of the chemical shift of trimethyllead at 25°C and 0.3 M ionic strength (maintained with $NaClO_4$) in solutions of 0.0100 M trimethyllead only (△), 0.0100 M trimethyllead and 0.0198 M N-acetyl-D,L-penicillamine (◆), and 0.0100 M trimethyllead and 0.0395 M N-acetyl-D,L-penicillamine (■).

where the species TML.AH and $TML.A^-$ are the only two trimethyllead-N-acetylpenicillamine complexes present in measurable amounts. The formation constants $K_{fO}$ and $K_{fS}$ are defined in Equations 67 and 68:

$$K_{fO} = \frac{[TML.AH]}{[TML^+][HA^-]} \tag{67}$$

$$K_{fS} = \frac{[TML.A^-]}{[TML^+][A^=]} \tag{68}$$

No higher order complexes containing more than one metal or ligand moiety per molecule of complex were detected. However, at different concentration ratios, this model may require modification to include possibilities such as $(TML)_2A$.

The derivation and calculation of the model was performed quite analogously to that described for 2-mercaptoethanol earlier in this chapter. The basic relation describing the observed chemical shift behaviour is Equation 69:

$$\delta_{OBS} = P_{TML}\delta_{TML} + P_{TMLOH}\delta_{TMLOH} + P_{TMLD}\delta_{TMLD} + P_{TML.AH}\delta_{TML.AH} + P_{TML.A^-}\delta_{TML.A^-} \tag{69}$$

Using the values of $K_{a1}$ and $K_{a2}$ calculated in the previous subsection, the computer program KINET solved this equation for the best-fitting values of $K_{fO}$, $K_{fS}$ and the trimethyllead pmr chemical shifts of the corresponding complexes,

i.e., $\delta_{TML.AH}$ and $\delta_{TML.A^-}$. These are 4.0 ± 2.1 for $K_{fO}$, 1.465 ± 0.030 ppm vs. DSS for $\delta_{TML.AH}$, 4.07 (± 0.21) x $10^5$ for $K_{fS}$ and 1.351 ± 0.0005 ppm vs. DSS for $\delta_{TML.A^-}$, where the uncertainties are linear estimates of the standard deviation provided by KINET. The larger relative errors calculated for $K_{fO}$ and $\delta_{TML.AH}$ are functions of the scarcity of complex giving rise to the original data. Nonetheless, some carboxyl-complexed trimethyllead must be present because omission of this species from the model results in a poorer fit to the observed data. Furthermore, the values of $K_{fO}$ and $\delta_{TML.AH}$ are reasonably consistent with previously published data (62,77) concerning the trimethyllead complexes of certain carboxylic acids. Acids of $pK_a$ similar to $pK_{a1}$ of this ligand, such as acetylglycine ($pK_a$ 3.40), have quite similar formation constants of the trimethyllead complex (the $K_{fO}$ is 6.6) as well as similar chemical shifts (the $\delta_{COMPLEX}$ is 1.479). These similarities will be discussed in more detail later in this chapter.

The large value obtained for $K_{fS}$ is similar to that calculated for the formation of the 2-mercaptoethanol complex of trimethyllead (the $K_{fS}$ of which is 9.05 (± 0.11) x $10^5$); the deprotonated sulfhydryl group binds the trimethyllead cation in both cases. The slightly lower magnitude of the N-acetylpenicillamine binding constant relative to that of 2-mercaptoethanol is presumably due to steric factors: the presence of the bulky β-methyl

and N-acetyl groups near the sulfhydryl binding site reduces the frequency of successful complexation with the relatively bulky trimethyllead cation, compared to that of the small 2-mercaptoethanol molecule. Other factors, such as the larger $pK_a$ of the N-acetylpenicillamine sulfhydryl group as well as the additional electrostatic attraction of the deprotonated carboxyl group, tend to ameliorate the binding of trimethyllead somewhat. These effects will be discussed in more detail in a later section.

4. D,L-Penicillamine Complexes

(a) The Macroscopic Acid Dissociation Constants of D,L-Penicillamine. Fully protonated D,L-penicillamine has the structural formula shown by II:

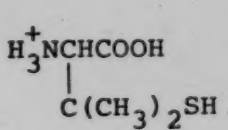

II

This structure will be symbolized by $H_3P^+$ or by an abbreviated structural formula which portrays only the active binding sites.

Increasing the pH of a solution containing $H_3P^+$ first causes deprotonation at the carboxyl group. The mixed acid dissociation constant, $K_{a1}$, quantifies the extent of this deprotonation at a given pH.

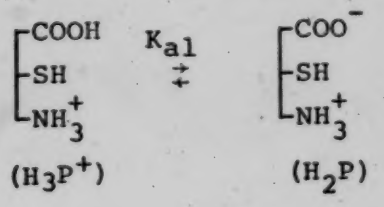

(70)

$$K_{a1} = \frac{[H_2P]a_{H^+}}{[H_3P^+]} \qquad (71)$$

The deprotonation of the carboxyl group is complete well before the deprotonation of the sulfhydryl and amino groups occurs. However, the sulfhydryl and amino deprotonations are not similarly distinct: simultaneous proton dissociation occurs at these sites over a significant pH range. It is not possible to determine the individual acid dissociation constants of such coincident deprotonations by normal pH titration techniques. Nevertheless, the pH titration curve of penicillamine exhibits separate inflection points corresponding to the titration of two acidic protons in this pH region. A portion of both acidic groups are titrated at the first inflection, resulting in stronger binding of the remaining proton. The final proton, irrespective of location, is removed at significantly higher pH. The positions of these inflection points are used to determine the macroscopic acid dissociation constants $K_{a2}$ and $K_{a3}$ (97), but only the overall degree of protonation is considered, with no regard for the states of the individual deprotonation sites.

$$H_2P \overset{K_{a2}}{\rightleftarrows} HP^- + H^+ \qquad (72)$$

$$HP^- \overset{K_{a3}}{\rightleftarrows} P^= + H^+ \qquad (73)$$

$$K_{a2} = \frac{[HP^-]a_{H^+}}{[H_2P]} \qquad (74)$$

$$K_{a3} = \frac{[P^{=}]a_{H^+}}{[HP^{-}]} \qquad (75)$$

Monoprotonated (site unspecified) and fully deprotonated penicillamine are represented by $HP^-$ and $P^=$, respectively.

In the chemical literature of the last two decades, the acid-base chemistry of D,L-penicillamine is usually characterized in terms of the macroscopic ionization constants obtained from pH data. A survey of the literature located a number of articles in which values for these constants had been reported. Several of these were rejected due to inadequate experimental descriptions, suspected technical errors or the employment of temperatures other than 25°C for the determinations. The remainder are presented in Table II.

All of the listed values were determined by pH titration at 25°C, but at different ionic strengths. This invalidates direct comparison of the various ionization constants reported in the literature, because the values are dependent on the ionic strength. A set of corresponding constants, corrected to an ionic strength of 0.3 M (as employed in the experiments described in this thesis), are also presented in Table II. This correction was done using the modified Davies Equation (109) described in King (110) and Robinson and Stokes (111):

$$-\log \gamma_i = \frac{A\, z_1 z_2\, \mu^{1/2}}{1 + \mu^{1/2}} - 0.1\, z_1 z_2 \mu \qquad (76)$$

TABLE II

SELECTED MACROSCOPIC $K_a$ VALUES OF D,L-PENICILLAMINE[a]

| $pK_{a1}$[b] (lit) | $pK_{a1}$[c] (corr) | $pK_{a2}$[b] (lit) | $pK_{a2}$[c] (corr) | $pK_{a3}$[b] (lit) | $pK_{a3}$[c] (corr) | $\mu$[d] (lit) | REFERENCE |
|---|---|---|---|---|---|---|---|
| --- | --- | 7.95 | 7.93 | 10.45 | 10.39 | 0.16 M ($KNO_3$) | 107 |
| 1.90 | 1.94 | 7.932 | 7.89 | 10.658 | 10.54 | 0.10 M (KCl) | 113 |
| --- | --- | 7.88 | 7.84 | 10.43 | 10.32 | 0.10 M ($KNO_3$) | 114 |
| 2.44 | 2.46 | 7.97 | 7.95 | 10.46 | 10.39 | 0.15 M ($KNO_3$) | 115 |
| 2.0[e] | 2.0 | 8.01 | 8.02 | 10.62 | 10.65 | 0.8 M ($KNO_3$) | 116[f] |
| BEST VALUES: | 1.94 | | 7.93 | | 10.39 | 0.3 | |

(a) At 25°C; except where noted, all values are mixed concentration-activity constants.
(b) Values reported in the literature at the ionic strengths listed in this table.
(c) Values corrected to correspond to 0.3 M ionic strength as described in text.
(d) Ionic strength and inert electrolyte of the solutions used in each $pK_a$ determination reported in the literature.
(e) Reference 117.
(f) Calculated using hydrogen ion concentrations rather than activities - correction for this difference does not alter the $pK_a$ values chosen in this table.

The value of A at 25°C was taken to be 0.5115 from Bates (112).

Activity coefficients were calculated using Equation 76 for each charged species in the expression for the macroscopic ionization constants, both at the reported ionic strength and at 0.3 M. This determination of the various activity coefficients enabled the conversion of the reported ionization constants to the corresponding values of those constants at 0.3 M ionic strength. An example of this procedure is outlined below.

$K_{a3}$, as expressed in Equation 75, is a mixed concentration-activity ionization constant. The corresponding thermodynamic ionization constant $K^T_{a3}$, is defined by Equation 77:

$$K^T_{a3} = \frac{a_{P^=} a_{H^+}}{a_{HP^-}} \tag{77}$$

Appropriate substitution of the general definition of activity, Equation 78, into the expression for the thermodynamic ionization constant results in Equation 79:

$$a_i = \gamma_i [i] \tag{78}$$

$$K^T_{a3} = \frac{\gamma_{P^=} [P^=] a_{H^+}}{\gamma_{HP^-} [HP^-]} \tag{79}$$

Recognizing the right hand side of Equation 75 as a factor of Equation 79, Equation 80 can be written:

$$K_{a3}^{T} = \frac{\gamma_{P=}}{\gamma_{HP^-}} K_{a3} \qquad (80)$$

Since $K_{a3}^{T}$ is a constant, independent of the ionic strength of experimental solutions, it follows that Equation 81 expresses correctly the relationship between values of $K_{a3}$ obtained at different ionic strengths:

$$\frac{\gamma_{P=(1)}}{\gamma_{HP^-(1)}} K_{a3(1)} = \frac{\gamma_{P=(2)}}{\gamma_{HP^-(2)}} K_{a3(2)} \qquad (81)$$

The bracketted subscripts 1 and 2 indicate the values determined at the first and second ionic strengths, respectively. As stated earlier, the activity coefficients at both ionic strengths were calculated with Equation 76. Substitution of the literature value of $K_{a3}$ (at the first ionic strength) for $K_{a3(1)}$ allowed the calculation of $K_{a3(2)}$ (the value corrected to an ionic strength of 0.3 M). Similar calculations were performed to obtain corrected values of $K_{a1}$ and $K_{a2}$; the results are presented in Table II as $pK_a$ values.

Only two values for $pK_{a1}$ were found in the literature, together with an unpublished value (117) obtained using the pmr chemical shift vs. pH technique. The $pK_{a1}$ value of 1.94 was determined to be the better for several reasons: it was the nearest to the value of 2.0 obtained by the pmr technique, the paper provided a much greater quantity of experimental detail and the publication was

the more recent by a full decade. The best values of $pK_{a2}$ and $pK_{a3}$ were chosen by selecting the median of each set of corrected values. The median values so obtained were the $pK_{a2}$ and $pK_{a3}$ corrected from the results published by Wilson and Martin (107).

(b) The Microscopic Acid Dissociation Constants of D,L-Penicillamine. The ionizations of the sulfhydryl and amino groups of penicillamine occur simultaneously; the macroscopic constants $K_{a2}$ and $K_{a3}$ described in the previous subsection are composites of the microscopic ionization constants. These microscopic constants, denoted by lower case "k", quantify the extent of deprotonation of the individual sulfhydryl and amino groups as described in the accompanying scheme. The subscripts 1, 2 and 3 refer to the deprotonated carboxylic acid, sulfhydryl and amino groups, respectively.

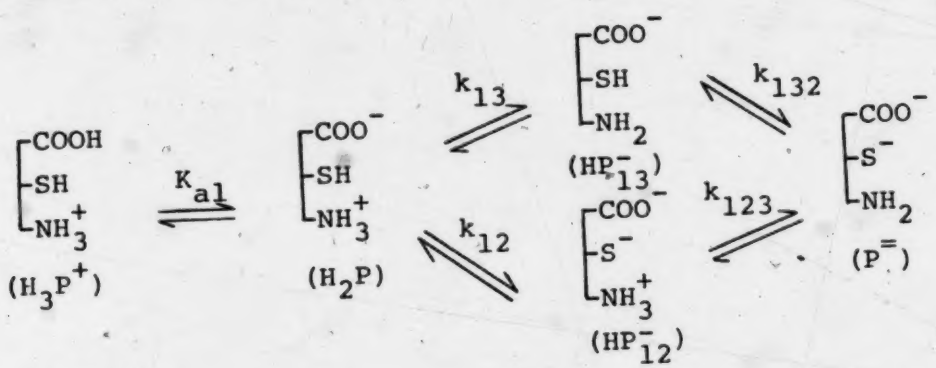


(82)

The microconstants defined by the above scheme are related to the macroconstants determined by pH titration:

$$K_{a2} = k_{12} + k_{13} \tag{83}$$

$$K_{a3}^{-1} = k_{123}^{-1} + k_{132}^{-1} \tag{84}$$

Rearrangement of Equation 84 gives Equation 85:

$$K_{a3} = k_{123} \cdot k_{132} / (k_{123} + k_{132}) \tag{85}$$

Due to the properties of a cyclic system, we also have

$$K_{a2}K_{a3} = k_{12}k_{123} = k_{13}k_{132} \tag{86}$$

The derivations of these equations are given in Edsall and Wyman (118).

Only three independent equations relate to four microconstants; the value of at least one microconstant is required to solve these equations for the remaining microconstants. Using a spectrophotometric method, Wilson and Martin (107) determined a value for $pk_{12}$ of 8.05 at 25°C and 0.16 M ionic strength. This was corrected to 8.03 at 25°C and 0.3 M ionic strength with the method of calculation described in the previous subsection. Equations 83, 85 and 86 were then employed to determine the remaining microconstants. At 25°C and 0.3 M ionic strength, the $pk_a$ values of penicillamine were calculated to be 8.03 for $pk_{12}$, 8.61 for $pk_{13}$, 10.29 for $pk_{123}$ and 9.70 for $pk_{132}$.

These constants, together with the $pK_{a1}$ value of 1.94 obtained earlier, completely characterize the acid-base behaviour displayed by D,L-penicillamine under the experimental conditions employed in the study detailed by the next subsection.

(c) The D,L-Penicillamine Complexes of Trimethyllead.

The binding of trimethyllead by D,L-penicillamine was investigated by observing the chemical shift of the trimethyllead protons as a function of pH. As before, two-fold and four-fold excesses of ligand were employed to ensure accurate determinations of the constants of the strong sulfhydryl complexes. The results of these experiments are presented in Figure 12.

In addition to the trimethyllead resonances, signals were observed for the methyl protons of D,L-penicillamine. Separate resonances were detected for each methyl group, due to the asymmetry of the neighboring α-carbon atom. At any instant, the two methyl groups are exposed to dissimilar molecular environments, causing their resonances to occur at different chemical shifts regardless of the rate of rotation about the hindered $C_\alpha - C_\beta$ bond. The variation of the resultant chemical shifts with pH is nearly identical for the 1 to 2 and 1 to 4 metal to ligand solutions; hence, only the former is shown in Figure 13. The methyl resonances, though well separated at all pH

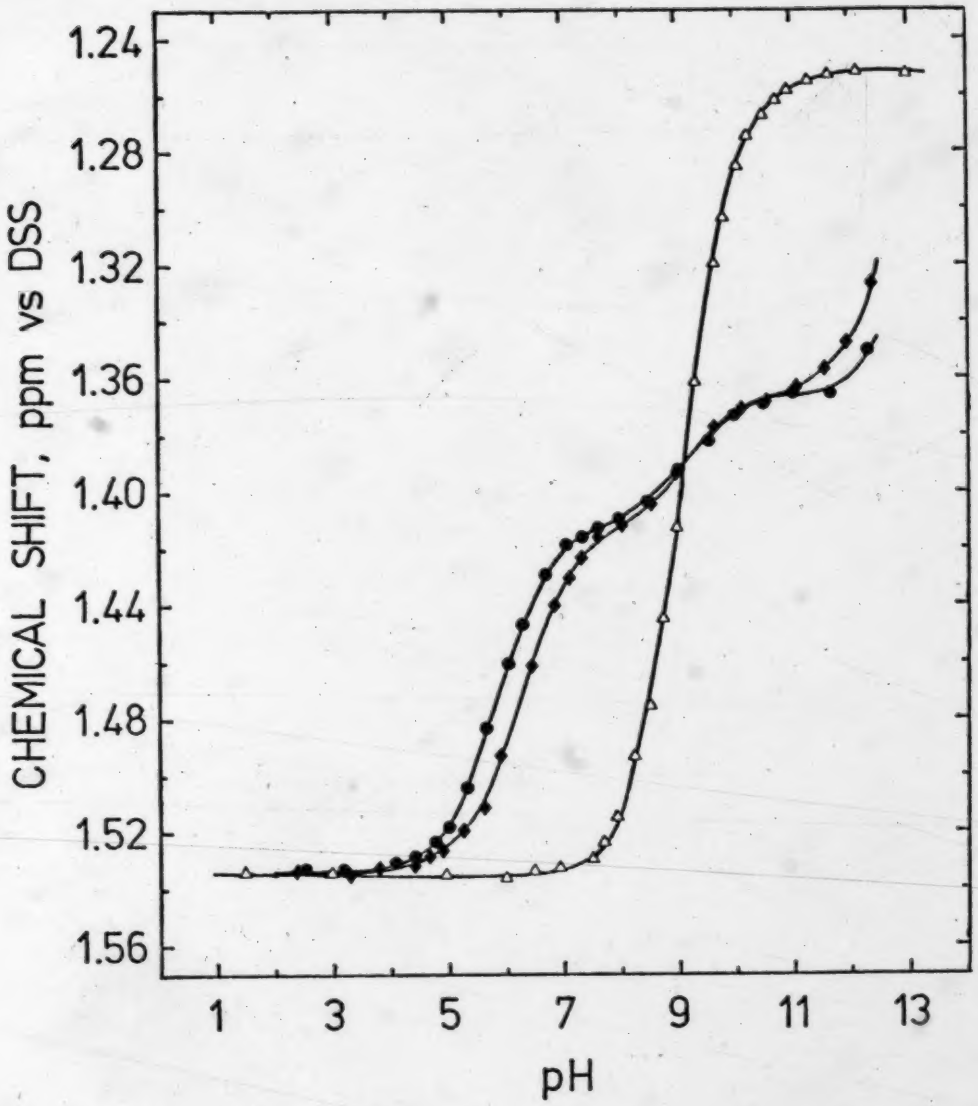


Figure 12. pH dependence of the chemical shift of trimethyllead at 25°C and 0.3 M ionic strength (maintained with $NaClO_4$) in solutions of 0.0100 M trimethyllead only (△), 0.00498 M trimethyllead and 0.00996 M D,L-penicillamine (◆), and 0.00500 M trimethyllead and 0.0199 M D,L-penicillamine (●).

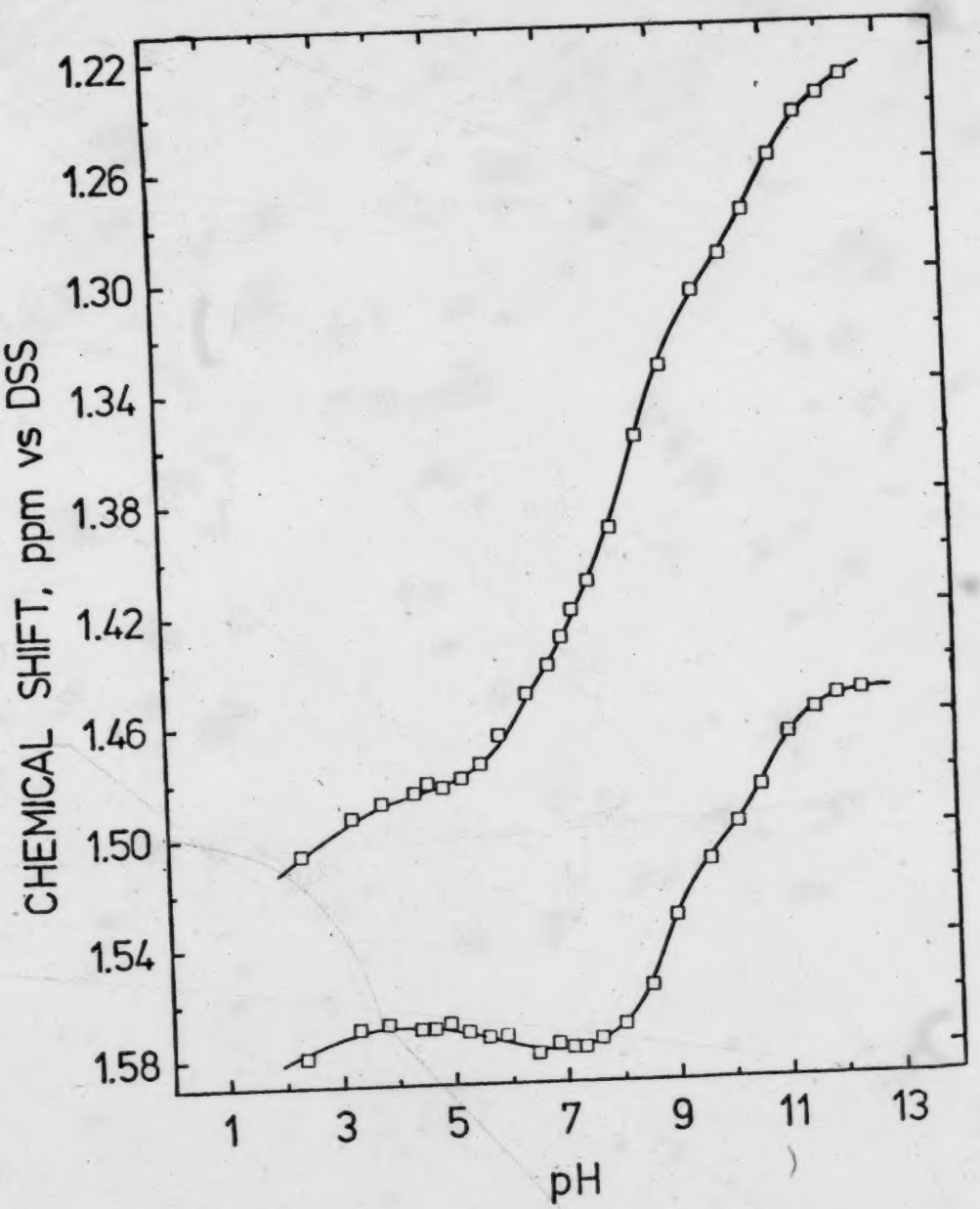


Figure 13. pH dependence of the chemical shift of the methyl protons of D,L-penicillamine at 25°C and 0.3 M ionic strength (maintained with $NaClO_4$) in a solution of 0.00498 M trimethyllead and 0.00996 M D,L-penicillamine.

levels, were rather broad and low in intensity. Therefore, the measurement errors inherent in this data set were much higher than those of the sharp, intense trimethyllead resonances. In addition, excess ligand was employed in all these experiments, resulting in a smaller proportion of the observed ligand chemical shift being due to the shift of metal-ligand complexes. For these reasons, the ligand resonance data was poorly suited for the accurate calculation of formation constants. The marked changes in chemical shift seen in Figure 13 are for the most part due to deprotonation of the functional groups of penicillamine; the effects of complexation by trimethyllead are much less distinct.

The best fit to the chemical shift data for solutions containing trimethyllead and penicillamine was obtained with the model which considered complexation at the sulfhydryl group only. An expanded model which also included a carboxyl complex of trimethyllead resulted in a poorer fit. All models which included 2:1 trimethyllead: ligand complexes resulted in no positive real values for the associated constants. This was at least partially attributable to the experimental conditions, which were such as to minimize the formation of $(TML)_2P$ type complexes. In addition, space-filling models indicate that the formation of such 2:1 complexes with the penicillamine sulfhydryl group is very unlikely due to steric inter-

actions of the trimethyllead cations with the ligand β-methyl groups. On the other hand, trimethyllead-carboxyl complexes are within the realms of possibility, but are not observed in these data. This is likely a result of the low basicity of the ligand carboxylic acid group; a correlation between $pK_a$ and the carboxylate complex formation constant has been observed for trimethyllead (62,77). These points will be discussed later in this chapter.

The most successful model is depicted by Equation 87.

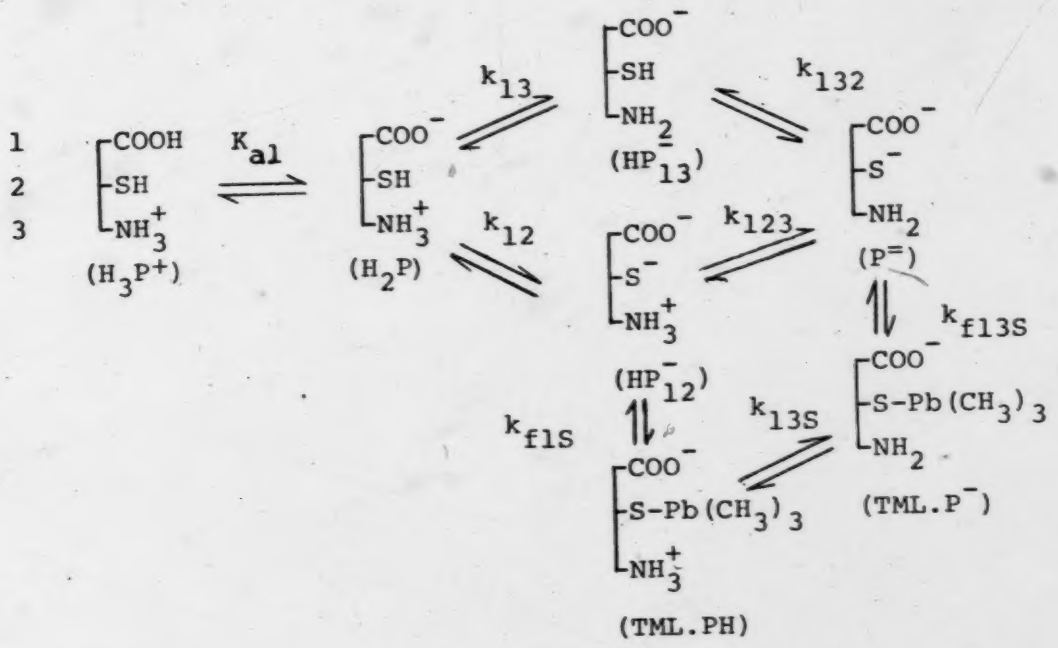


(87)

The subscripts 1, 2 and 3 indicate that the product is deprotonated and uncomplexed at the carboxyl, sulfhydryl and amino groups, respectively. A subscript f indicates

a formation constant and a subscript S signifies that a trimethyllead cation is bound to the sulfhydryl group of the product. The formation constants $k_{f1S}$ and $k_{f13S}$ are thus defined as follows:

$$k_{f1S} = \frac{[TML.PH]}{[HP_{12}^{-}][TML^{+}]} \tag{88}$$

$$k_{f13S} = \frac{[TML.P^{-}]}{[P^{=}][TML^{+}]} \tag{89}$$

The model for the observed chemical shift of penicillamine was derived using Equation 90:

$$\delta_{OBS} = P_{TML}\delta_{TML} + P_{TMLOH}\delta_{TMLOH} + P_{TMLD}\delta_{TMLD} + P_{TML.PH}\delta_{TML.PH} + P_{TML.P^{-}}\delta_{TML.P^{-}} \tag{90}$$

This model and the appropriate data were supplied to the curve-fitting computer program KINET (94), which optimized the values of $k_{f1S}$, $\delta_{TML.PH}$, $k_{f13S}$ and $\delta_{TML.P^{-}}$. The procedure employed here was quite analogous to that described for the metal-ligand systems discussed previously in this chapter. These calculations yielded the following optimal values: 1.13 ($\pm$ 0.05) x $10^4$ for $k_{f1S}$, 1.414 ($\pm$ 0.001) for $\delta_{TML.PH}$, 4.22 ($\pm$ 0.32) x $10^5$ for $k_{f13S}$ and 1.373 ($\pm$ 0.001) for $\delta_{TML.P^{-}}$, where the chemical shifts are in units of ppm vs. DSS. As before, the uncertainties are linear estimates of the standard deviation, calculated

by KINET. These results compare quite well with the other determinations in this chapter, given the differences in steric and electrostatic interactions of the various ligands with trimethyllead cations. Correlation of these effects will be discussed later in this chapter.

The value of $k_{13S}$, the ionization constant of the trimethyllead-complexed species TML.PH, was calculated using the relationship:

$$k_{f1S} \cdot k_{13S} = k_{123} \cdot k_{f13S} \qquad (91)$$

which is analogous to Equation 86 and is derived in a similar manner (118). However, it must be realized that Equation 86 is defined for dissociation constants only; hence, the inverse of each of the formation constants, $k_{f1S}$ and $k_{f13S}$, is used in the derivation of Equation 91. The value of $k_{13S}$ was found to be $1.93 \times 10^{-9}$, giving a $pk_{13S}$ value of 8.71. This is considerably less than the value of 10.29 determined for $pk_{123}$, but quite similar to the $pk_{13}$ of 8.61. Thus it may be inferred that a trimethyllead cation complexed to the sulfhydryl group of a penicillamine molecule closely mimics a similarly bonded hydrogen ion, in terms of their effects on the acid strengths of neighboring functional groups. The electrostatic, inductive and steric factors involved will be discussed later in this work.

5. L-Cysteine Complexes

(a) The Macroscopic Acid Dissociation Constants of L-Cysteine. At low pH, L-cysteine assumes the fully protonated form shown by III:

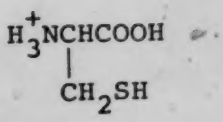

III

hereafter symbolized by $H_3C^+$ or by an abbreviated structural formula identical to that used for D,L-penicillamine, since the functional groups are similarly situated. The structure of III differs only in the substitution of hydrogen atoms for the methyl groups adjacent to the sulfhydryl in structure II. This apparently minor dissimilarity leads to significant differences in the acid-base and complexation behaviour of these compounds.

The macroscopic ionization constants of L-cysteine are defined by the following reaction scheme and equations:

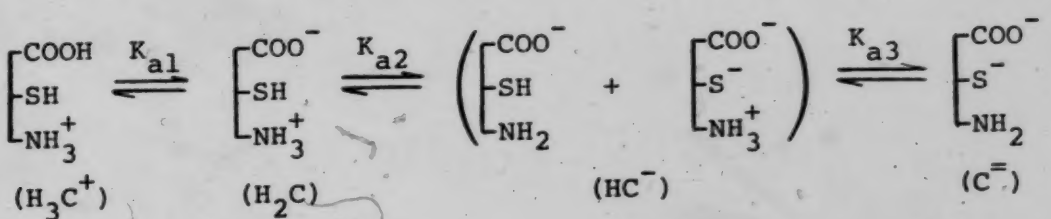

$(H_3C^+)$ $(H_2C)$ $(HC^-)$ $(C^=)$

(92)

$$K_{a1} = \frac{[H_2C]a_{H^+}}{[H_3C^+]} \qquad (93)$$

$$K_{a2} = \frac{[HC^-]a_{H^+}}{[H_2C]} \qquad (94)$$

$$K_{a3} = \frac{[C^{=}]a_{H^+}}{[HC^{-}]} \qquad (95)$$

where $[HC^{-}]$ is the sum of the concentrations of the two possible monoprotonated species shown in Equation 92.

The rationale for this treatment of the macroscopic acid-base chemistry of cysteine is identical to that of the previous section regarding penicillamine. Using the procedure detailed therein, a series of values for $K_{a1}$, $K_{a2}$, and $K_{a3}$ were collected from the literature and the corresponding values of these constants at 0.3 M ionic strength were calculated. The original constants and those corrected to an ionic strength of 0.3 M are presented in Table III. The median of each set of corrected ionization constants was used in the calculations described later in this section. The most recent and trustworthy value of $K_{a1}$ (113) was found to be $1.17 \times 10^{-2}$, when corrected to an ionic strength of 0.3 M. The median values of $K_{a2}$ and $K_{a3}$ were $6.03 \times 10^{-9}$ and $5.62 \times 10^{-11}$, both of these calculated from the published values of Coates, Marsden and Rigg (119).

(b) The Microscopic Acid Dissociation Constants of L-Cysteine. The microscopic ionization scheme of L-cysteine has been determined (119,122) to be similar to that of D,L-penicillamine, discussed in the previous section.

TABLE III

SELECTED MACROSCOPIC $K_A$ VALUES OF L-CYSTEINE[a]

| $pK_{a1}$[b] (lit) | $pK_{a1}$[c] (corr) | $pK_{a2}$[b] (lit) | $pK_{a2}$[c] (corr) | $pK_{a3}$[b] (lit) | $pK_{a3}$[c] (corr) | μ (lit) | REFERENCE |
|---|---|---|---|---|---|---|---|
| --- | --- | 8.37 | 8.22 | 10.70 | 10.25 | 0.00[d] | 119 |
| 1.896 | 1.93 | 8.178 | 8.14 | 10.361 | 10.25 | 0.10 (KCl) | 113 |
| --- | --- | 8.13 | 8.09 | 10.11 | 10.00 | 0.10 ($KNO_3$) | 114 |
| --- | --- | 8.30 | 8.28 | 10.40 | 10.33 | 0.15 (NaCl) | 120 |
| --- | --- | 8.48 | 8.46 | 10.55 | 10.48 | 0.15 ($KNO_3$) | 121 |
| BEST VALUES: | 1.93 | | 8.22 | | 10.25 | 0.3 | |

(a) At 25°C; all values are mixed concentration-activity constants.
(b) Values reported in the literature at the ionic strengths listed in this table.
(c) Values corrected to 0.3 M ionic strength as described in the text.
(d) Corrected to zero ionic strength using a Debye-Huckel type equation and other detailed calculations as found in reference 97. No inert electrolyte was added.

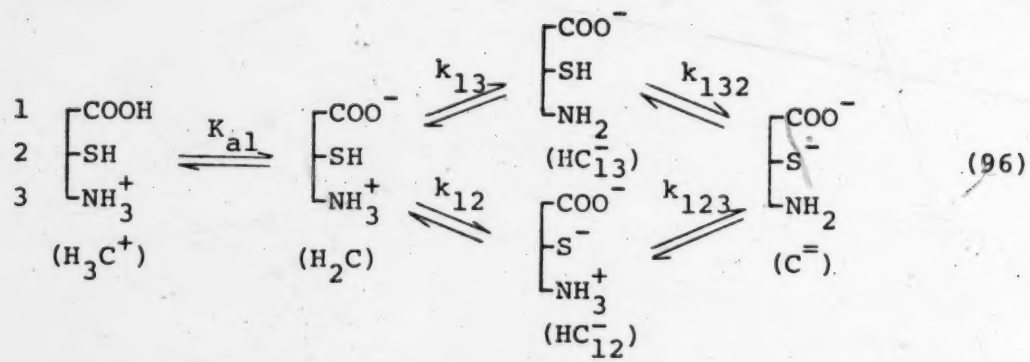

(96)

Equations 83 through 86 thus apply for the L-cysteine system of equilibria as well as for that of D,L-penicillamine. As before, these equations cannot be solved without additional information.

Coates, Marsden and Rigg (122) obtained the required data using a spectrophotometric method, and calculated a value of 8.53 ± 0.01 for $pk_{12}^{T}$ at 25°C. This corresponds to a $pk_{12}$ of 8.38 at 0.3 M ionic strength and 25°C. Based on this result, values of 8.73 for $pk_{13}$, 10.09 for $pk_{123}$ and 9.74 for $pk_{132}$ were computed. The previously determined value of 1.93 for $pK_{a1}$ completes the quantification of the acid-base equilibria described by Equation 96.

A comparison of the cysteine and penicillamine microconstants indicates that the sulfhydryl group of the latter is significantly more acidic than that of cysteine. The ratio of the monoprotonated penicillamine species, $[HP_{12}^{-}]/[HP_{13}^{-}]$, is thus greater than the corresponding cysteine ratio, $[HC_{12}^{-}]/[HC_{13}^{-}]$. The calculated values of

these ratios are 3.8 and 2.2, respectively.

(c) The L-Cysteine Complexes of Trimethyllead.

As in the earlier studies, the complexation of trimethyllead by L-cysteine was studied by observing the pH dependence of the proton chemical shift of trimethyllead in appropriate solutions. Two-fold and four-fold excesses of ligand were employed to increase the sensitivity of the method to the formation of strong sulfhydryl complexes, at the expense of the less important, weaker complexes occurring at other functional groups. The results of these experiments are presented in Figure 14.

The model which best fits the observed data was derived from a scheme of equilibria identical to that of penicillamine (Equation 87), except for the inclusion of a carboxyl complex of trimethyllead.

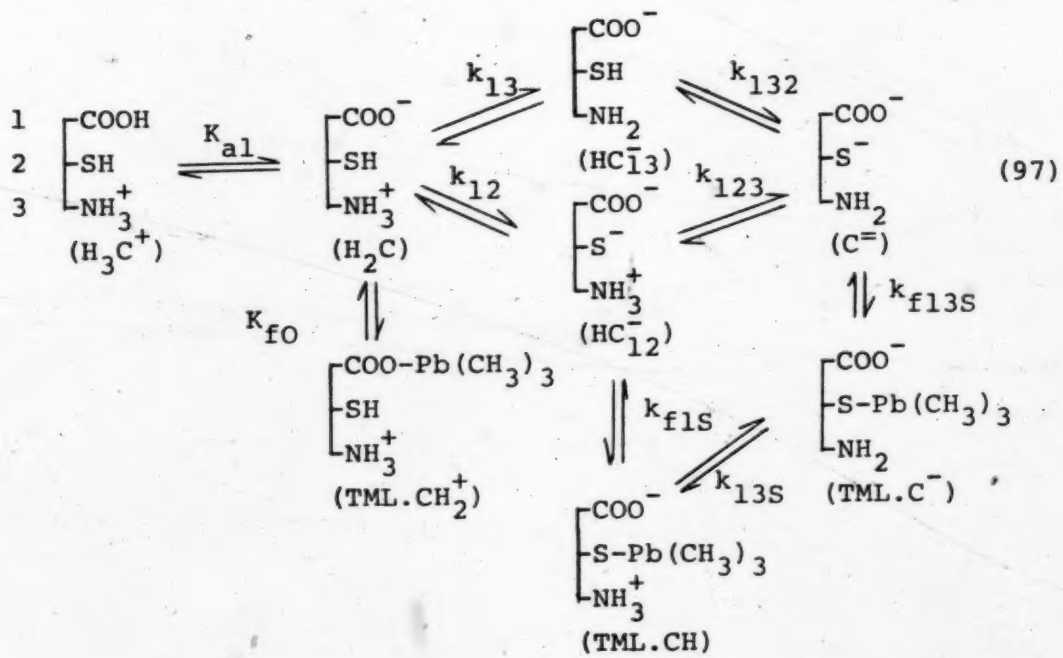

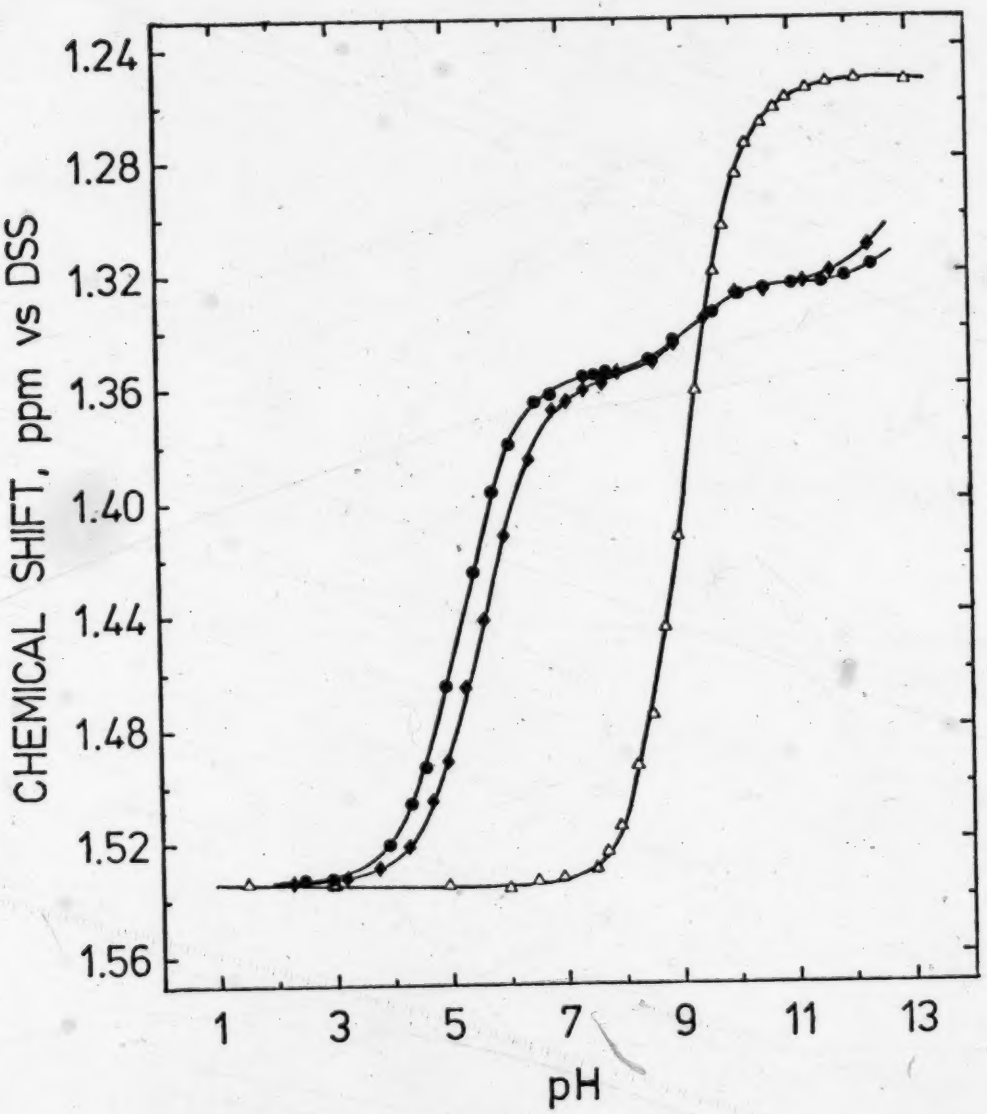


Figure 14. pH dependence of the chemical shift of trimethyllead at 25°C and 0.3 M ionic strength (maintained with $NaClO_4$) in solutions of 0.0100 M trimethyllead only (△), 0.00499 M trimethyllead and 0.00949 M L-cysteine (◆) and 0.00502 M trimethyllead and 0.0190 M L-cysteine (●).

All symbols are defined as in the penicillamine section of this chapter, except that the "P" of penicillamine is replaced with the "C" of cysteine. In addition, the subscript "O" in $K_{fO}$ indicates that the trimethyllead cation is bound to the oxygen atom of the deprotonated carboxyl group.

In contrast to the penicillamine case, space-filling models indicated that an additional species, having two trimethyllead cations bound to the cysteine sulfhydryl, was not prevented by steric interactions. However, while a doubly coordinated sulfhydryl group is sterically possible, 2:1 trimethyllead-cysteine complex formation is not favored at the low metal-to-ligand ratios used in this work. Incorporation of this 2:1 species into Equation 97 resulted in untenable values for the corresponding formation constant and chemical shift, indicating that the contribution of this species to the observed chemical shift was too low to measure accurately. With higher metal to ligand ratios, such two to one complexes could be considerably more important. This speculation is reinforced by studies of other workers (123) which indicate that two or more of the analogous (although less bulky) methylmercury cations can bond to one sulfhydryl group. In any case, under the conditions chosen for this trimethyllead study, Equation 97 best represents the detectable species and equilibria in solution.

The model of the trimethyllead chemical shift in the system given by Equation 97 is the following:

$$\delta_{OBS} = P_{TML}\delta_{TML} + P_{TMLOH}\delta_{TMLOH} + P_{TMLD}\delta_{TMLD} + P_{TML.CH_2^+}\delta_{TML.CH_2^+} + P_{TML.CH}\delta_{TML.CH} + P_{TML.C^-}\delta_{TML.C^-} \quad (98)$$

This model, together with the appropriate data, was fitted to the observed chemical shift curve using the computer program KINET as described previously. The optimum values of the formation constants and the associated chemical shifts are 2.2 ± 2.0 for $K_{fO}$, 1.426 ± 0.089 for $\delta_{TMLCH_2^+}$, 9.67 (± 0.27) x $10^4$ for $k_{f1S}$, 1.356 ± 0.0005 for $\delta_{TMLCH}$, 9.24 (± 0.50) x $10^5$ for $k_{f13S}$ and 1.325 ± 0.0005 for $\delta_{TMLC^-}$, where the chemical shifts are in ppm vs. DSS. The inaccuracies are linear estimates of the standard deviations as calculated by KINET.

The large error estimates for $K_{fO}$ and $\delta_{TMLCH_2^+}$ result directly from the low concentrations of the carboxyl complex: such low concentrations contribute relatively little to the averaged trimethyllead chemical shift, from which $K_{fO}$ and $\delta_{TML.CH_2^+}$ are calculated. However, exclusion of $TMLCH_2^+$ from the model gives a much poorer fit. In addition, the calculated values of $K_{fO}$ and $\delta_{TML.CH_2^+}$ correlate reasonably well with other carboxylate complex data discussed in this chapter. For these reasons, the

carboxyl complex parameters were accepted in spite of the poor precision observed. Better measurements may be possible at higher metal to ligand ratios.

The value of $k_{13S}$ was calculated to be $7.83 \times 10^{-10}$ ($pk_{13S} = 9.11$) using Equation 91. This is much closer to the $pk_{13}$ value of 8.73 than to the $pk_{123}$ of 10.09, due to the same factors which govern the analogous penicillamine deprotonations. However, the trimethyllead cation mimics the behaviour of a proton much less closely for cysteine than for penicillamine, probably due to the differences in steric interactions and in inductive effects in the two ligands.

6. Glutathione Complexes

(a) The Acid Dissociation Constants of Glutathione.

When fully protonated, the tripeptide glutathione (γ-L-glutamyl-L-cysteinylglycine) has the structural formula given by IV:

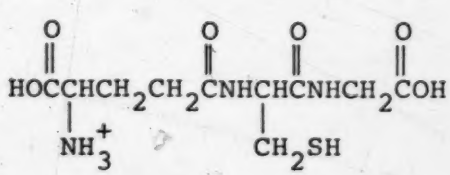

IV

This molecule possesses two pairs of acidic groups which ionize simultaneously: the two carboxylic acid groups which ionize in the pH range 0.5 to 6.0 and the sulfhydryl

and ammonium groups which ionize in the pH range 7 to 12. The determination of the microscopic ionization constants of all these groups was accomplished with studies of the nmr chemical shifts of selected carbon-bonded protons as a function of pH (124). The resultant microscopic ionization scheme is given by Figure 15. The ionization reaction to which a given microconstant refers is given by the subscripts: the last number in the subscript denotes the group involved in the ionization step under consideration, while the preceding numbers denote the groups from which protons have already ionized. The L-glutamyl carboxylic acid group is denoted by the number 1, the glycyl carboxylic acid group by 2, the sulfhydryl group by 3 and the ammonium group by 4, as indicated near $H_4G^+$ in Figure 15. However, in the case of the macroscopic constants mentioned below, the subscripts refer only to the total number of protons removed from the product of the equilibrium, regardless of the sites of deprotonation.

The macroscopic ionization constants exhibited by glutathione were calculated (124) using equations analogous to Equations 83 through 86 of the present work. The micro- and macroconstants of glutathione were presented (124) as both $p_cK_a$ and $pK_a$ values; only the latter were used in this thesis and are listed in Table IV.

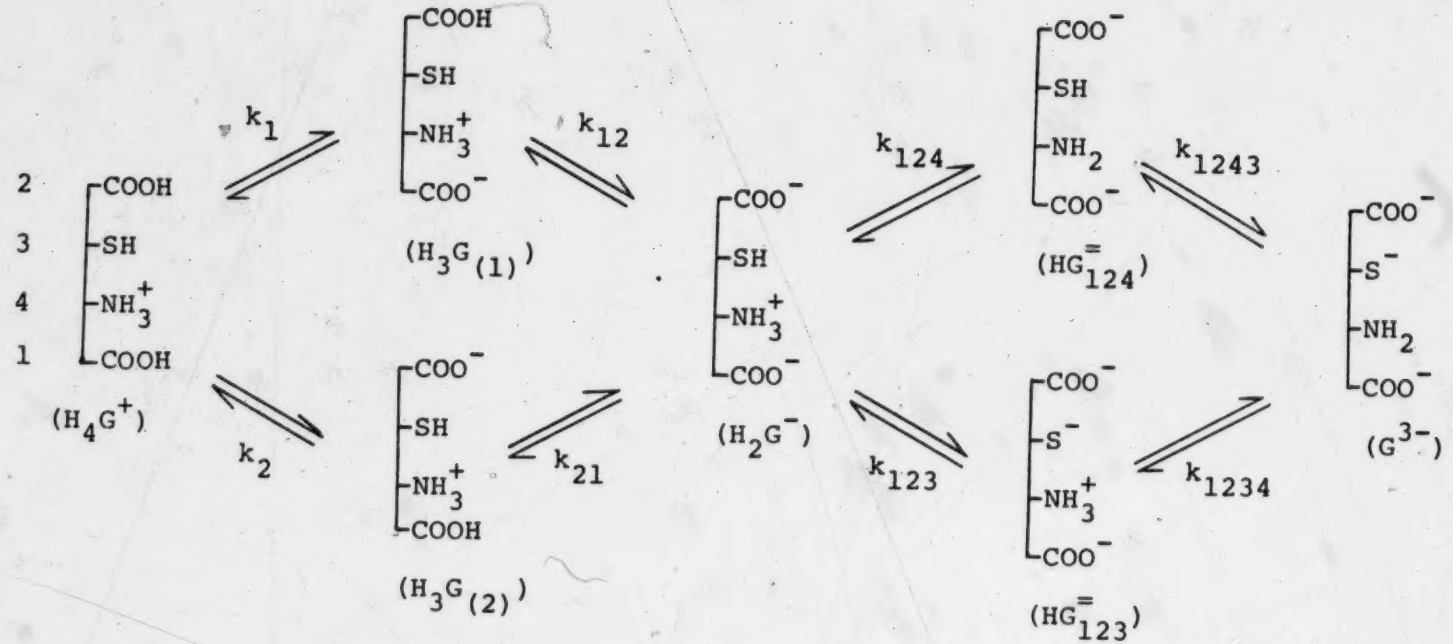


Figure 15. Microscopic ionization scheme for glutathione, considering only the predominant species present (124). See text for labelling of the acid groups and definition of the subscripts.

TABLE IV

IONIZATION CONSTANTS OF GLUTATHIONE (124)

| MACROSCOPIC[a,b,c] | | MICROSCOPIC[a,b] | |
|---|---|---|---|
| $pK_{a1}$ | 2.15 | $pk_1$ | 2.19 ± 0.04 |
| | | $pk_2$ | 3.22 ± 0.04 |
| $pK_{a2}$ | 3.49 | $pk_{12}$ | 3.45 ± 0.10 |
| | | $pk_{21}$ | 2.42 ± 0.01 |
| $pK_{a3}$ | 8.76 | $pk_{123}$ | 8.97 ± 0.04 |
| | | $pk_{124}$ | 9.17 ± 0.04 |
| $pK_{a4}$ | 9.56 | $pk_{1234}$ | 9.35 ± 0.10 |
| | | $pk_{1243}$ | 9.08 ± 0.02 |

(a) Mixed constants calculated in terms of the hydrogen ion activities, using the pH meter readings directly.

(b) At 25°C and 0.31 to 0.42 M ionic strength.

(c) Calculated from the microscopic ionization constants.

(b) Glutathione Complexes of Trimethyllead

*(i) Proton NMR Results*

The complexation equilibria of trimethyllead and glutathione were studied using measurements of the chemical shift of the trimethyllead protons as a function of pH. To obtain a greater precision for the large formation constants, two- and fourfold excesses of ligand were maintained in solution. The results of three experiments are presented in Figure 16.

The model of metal-ligand interaction based on the large number of different protonated forms shown in Figure 15 is exceedingly complex, involving simultaneous complexation at two pairs of deprotonated functional groups. It was determined that this model exceeded the computational capabilities of the curve-fitting program KINET (94). In addition, the above-mentioned low metal to ligand ratios reduced the already small contributions of the various weak carboxyl and 2:1 complexes to the observed chemical shift. These considerations necessitated the simplification of the scheme presented in Figure 15. The replacement of the microionization scheme of the carboxylic acid groups with two successive macroionizations affects the sulfhydryl results minimally, since both carboxylates were found to complex trimethyllead quite weakly. In addition, complexation of the amino group by trimethyllead was considered negligible for

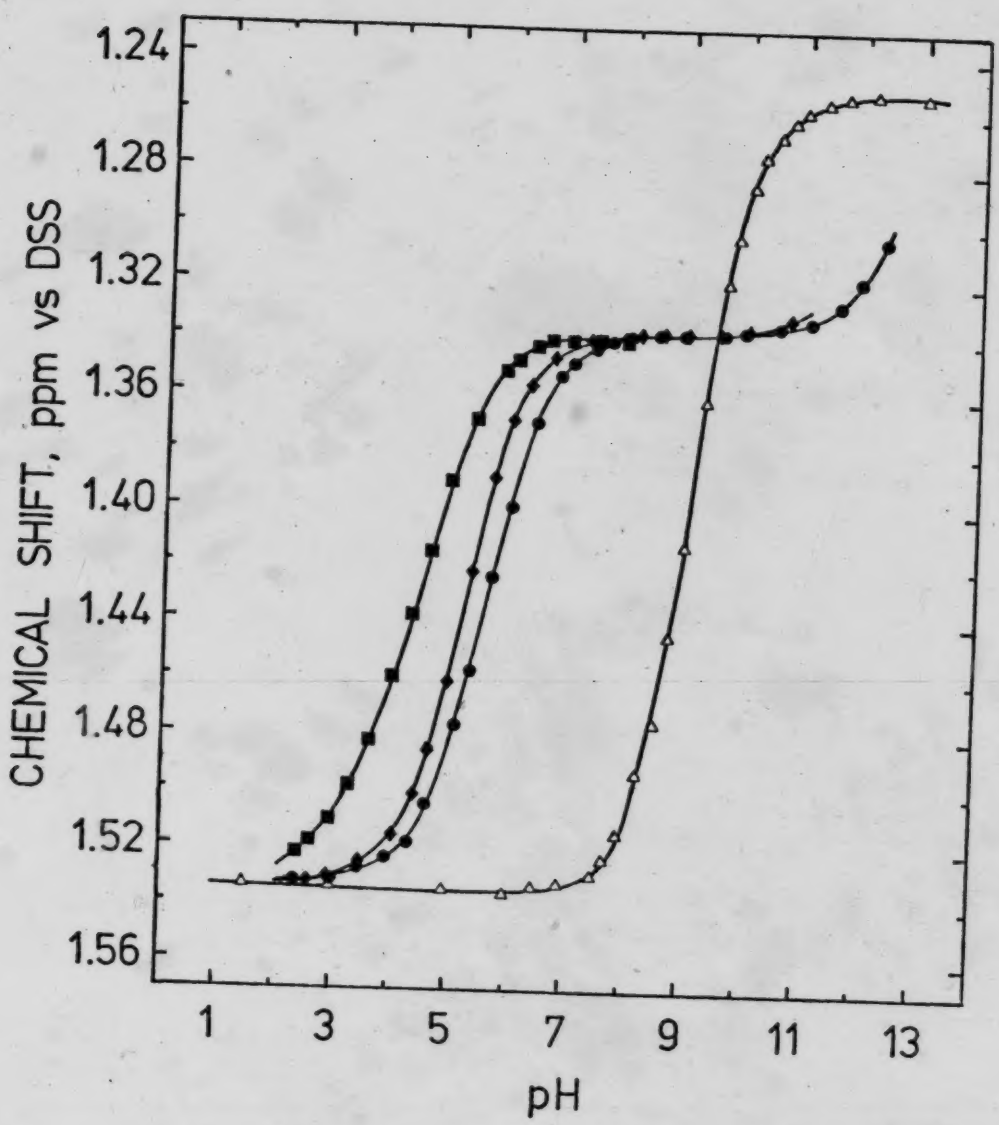


Figure 16. pH dependence of the chemical shift of trimethyllead at 25°C and 0.3 M ionic strength (maintained with $NaClO_4$) in solutions of 0.0100 M trimethyllead only (△), 0.00501 M trimethyllead and 0.00973 M glutathione (●), 0.00501 M trimethyllead and 0.0194 M glutathione (◆) and 0.0749 M trimethyllead and 0.146 M glutathione (■).

reasons detailed earlier in this chapter.

The simplified model which resulted in the best fit to the observed data is given by Figure 17. All previous model systems can be considered as subsets of this system of equilibria. In this figure, all subscripts are defined as for Equation 97 and Figure 15. In addition, the subscript "D" indicates the formation of a two to one metal to ligand complex, with both trimethyllead cations binding to the sulfhydryl group simultaneously. The use of brackets indicates that the model makes no distinction between the species so enclosed.

The model of the chemical shift behaviour of this system is given by Equation 99:

$$\delta_{OBS} = P_{TML}\delta_{TML} + P_{TMLOH}\delta_{TMLOH} + P_{TMLD}\delta_{TMLD} + P_{TML.GH_3^+}\delta_{TML.GH_3^+} + P_{TML.GH_2}\delta_{TML.GH_2} + P_{TML.GH^-}\delta_{TML.GH^-} + P_{TML.G^=}\delta_{TML.G^=} + P_{TML_2.GH}\delta_{TML_2.GH} \quad (99)$$

where $P_{TML_2.GH}$ is defined by Equation 100:

$$P_{TML_2.GH} = 2[TML_2.GH]/TMLT \quad (100)$$

and all other parameters are defined analogously to those of models described earlier in this chapter.

Despite the simplifications outlined above, the model

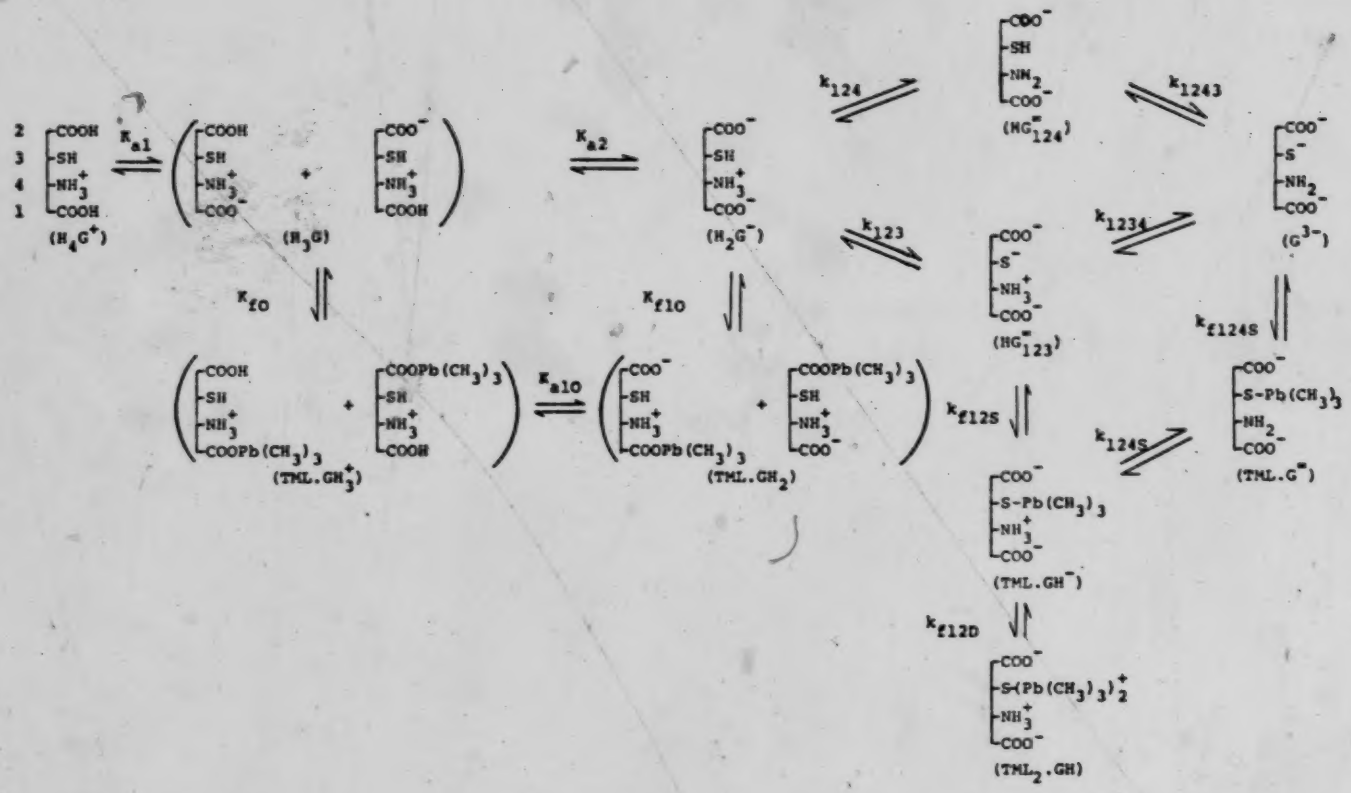

Figure 17. Microscopic ionization and trimethyllead complexation scheme for glutathione in solutions of low metal to ligand ratios.

given in Figure 17 resulted in an exceptionally good fit to the observed data. The optimized values of the unknown parameters were the following: 4.23 (± 0.26) x $10^5$ for $k_{f124S}$, 1.335 ± 0.0005 for $\delta_{TML.G^=}$, 3.47 (± 0.05) x $10^5$ for $k_{f12S}$, 1.338 ± 0.0005 for $\delta_{TML.GH^-}$, 10.8 ± 1.7 for $K_{f1O}$, 1.455 ± 0.012 for $\delta_{TML.GH_2}$, 1.2 ± 1.1 for $K_{fO}$, 1.433 ± 0.076 for $\delta_{TML.GH_3^+}$, 17.4 ± 4.9 for $k_{f12D}$ and 1.351 ± 0.011 for $\delta_{TML_2.GH}$, where all the chemical shifts are in ppm vs. DSS. The inaccuracies quoted are the linear estimates of the standard deviations calculated by KINET. The large relative errors of the formation constants and chemical shifts of the weak complexes result from the low concentration of these complexes in the experimental solutions. As is the case with weak complexes of other ligands described earlier in this chapter, the scarcity of such species hinders accurate determination of the associated parameters. However, the small relative errors computed for the sulfhydryl complexes indicate that these are not similarly afflicted nor are they significantly prejudiced by the large errors of other constants.

The value of $k_{124S}$, calculated using an equation analogous to Equation 91, was found to be 5.45 x $10^{-10}$ ($pk_{124S}$ is 9.26). $pk_{124S}$ does not differ significantly from the value of 9.35 for $pk_{1234}$; this is reasonable, since the spatial separation of the ionizing amino group

and the sulfhydryl complexation site is relatively large.

By a similar method, $K_{al0}$ was calculated to be approximately $2.9 \times 10^{-3}$ ($pK_{al0}$ equals 2.54). However, this calculation involves $K_{f0}$ and $K_{f10}$, both of which are of limited precision, and does not take into account the microionization scheme of the carboxyl groups shown in Figure 15. Therefore, the accuracy of this $K_{al0}$ value is probably much less than that of $k_{124S}$ above.

*(ii) Carbon-13 NMR Results*

To corroborate the results obtained above with pmr techniques, the chemical shifts of the carbon-13 resonances of glutathione and trimethyllead were studied as functions of pH. The experimental conditions were similar to those employed for the pmr studies, but the extraction of quantitative data was prevented by the formation of small quantities of a white precipitate above pH 5.5 for solutions containing 0.0947 M trimethyllead and 0.146 M glutathione. This precipitate turned brown and then black over a period of several days. Such phenomena have been consistently observed for solutions composed of trimethyllead and sulfhydryl-containing ligands in relatively high concentrations at high pH. In the present study, the degree of precipitation was small enough that qualitative interpretation was still possible.

The results for several of the carbon-13 resonances

of glutathione and of trimethyllead are presented in Figures 18, 19 and 20. The assignments of the glutathione resonances are those favored by several authors (125-127). The carbon atoms are identified by Glu, Cys or Gly, to indicate the amino acid residue in which the carbon is located, and $C_\alpha$, $C_\beta$, $C_\gamma$, CONH or COOH, to indicate the particular carbon of that residue. The glutathione resonances omitted from Figures 18 and 19 did not differ significantly from the pH vs. cmr chemical shift curves reported by Fairhurst (128) for pure glutathione in solution.

No similar data were available for comparison with Figure 20; nevertheless, the glutathione cmr data provided confirming evidence for the model depicted in Figure 17. Above pH 3, the observed cmr chemical shift curves for the Cys-$C_\alpha$ and Cys-$C_\beta$ atoms are well displaced from those of pure glutathione solutions, indicating strong complexation at the sulfhydryl group down to fairly low pH values. This is consistent with the large formation constants of the glutathione sulfhydryl complexes quantified in the previous section. The curves for the Glu-COOH and the Gly-COOH carbon atoms are not displaced significantly in the region between pH 2 and 6 where maximum carboxyl complexation is calculated to occur (vide infra: Figure 32). (The deviations observed for the solutions of highest pH coincide with precipitate formation.) This is consistent with the small formation constants measured

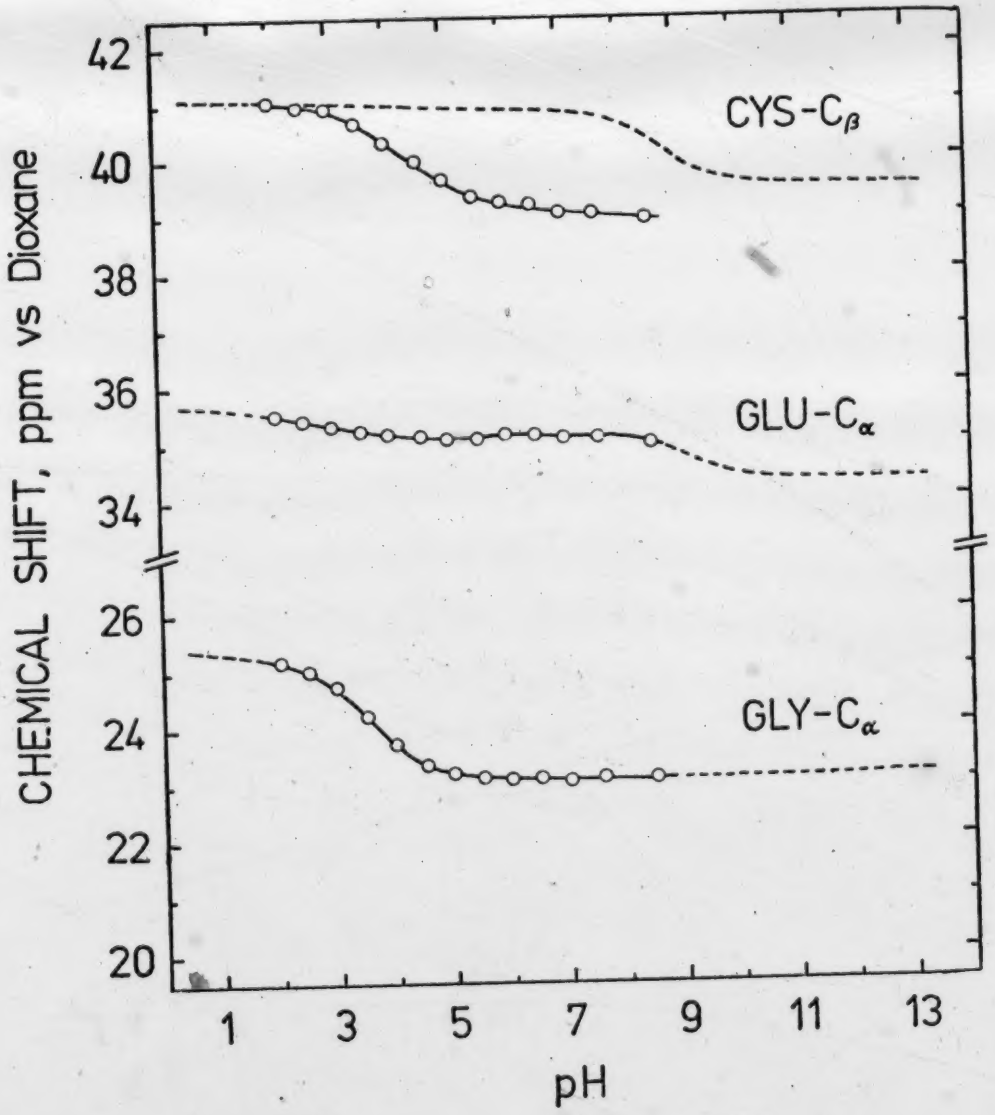


Figure 18. pH dependence of the carbon-13 chemical shift of selected carbons of glutathione at 25°C in a solution (117,128) of 0.21 M glutathione only (dashed lines) and at 0.4 M ionic strength (maintained with $NaClO_4$) in a solution of 0.146 M glutathione and 0.0947 M trimethyllead (circles). Positive chemical shifts indicate the resonances are upfield of dioxane.

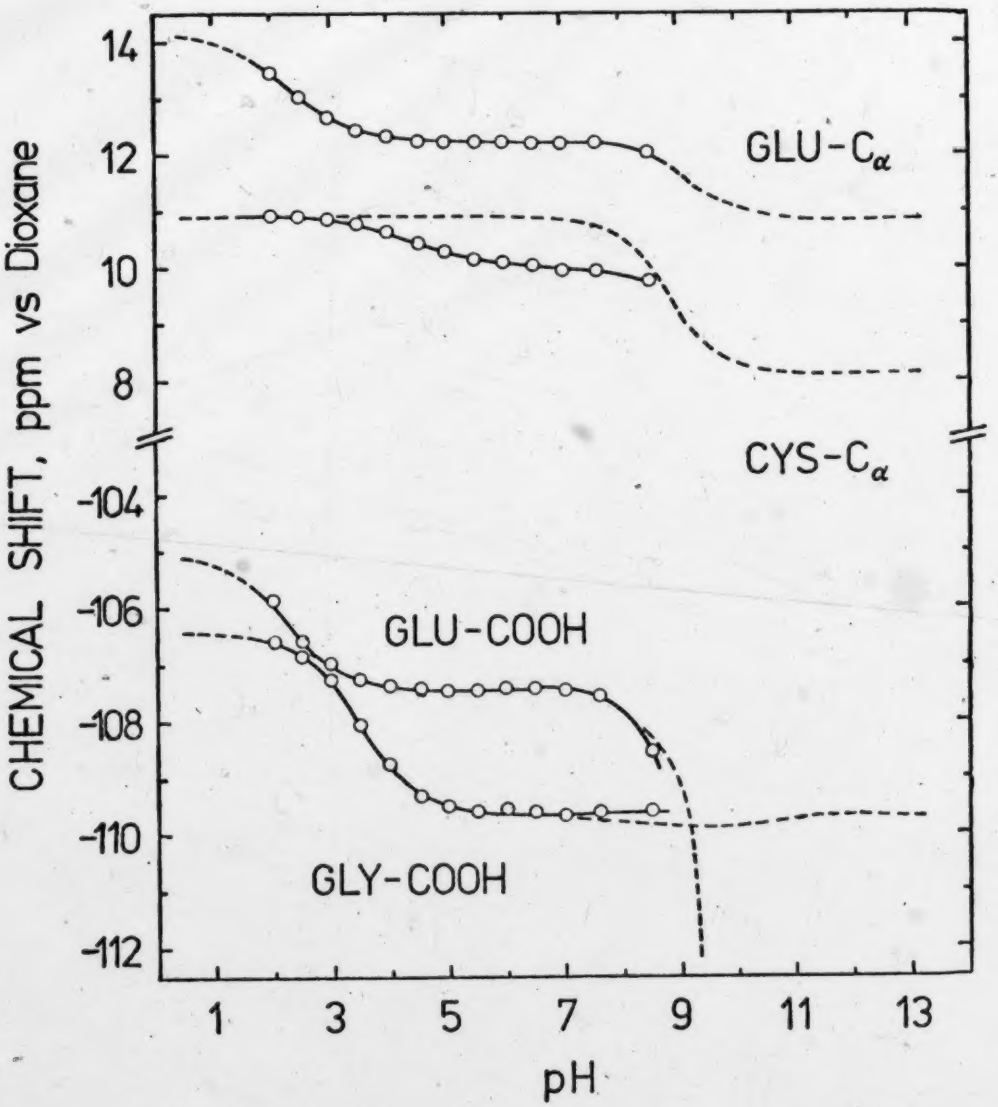


Figure 19. pH dependence of the carbon-13 chemical shift of selected carbons of glutathione at 25°C in a solution (117,128) of 0.21 M glutathione only (dashed lines) and at 0.4 M ionic strength (maintained with $NaClO_4$) in a solution of 0.146 M glutathione and 0.0947 M trimethyllead (circles). Positive chemical shifts indicate the resonances are upfield of dioxane.

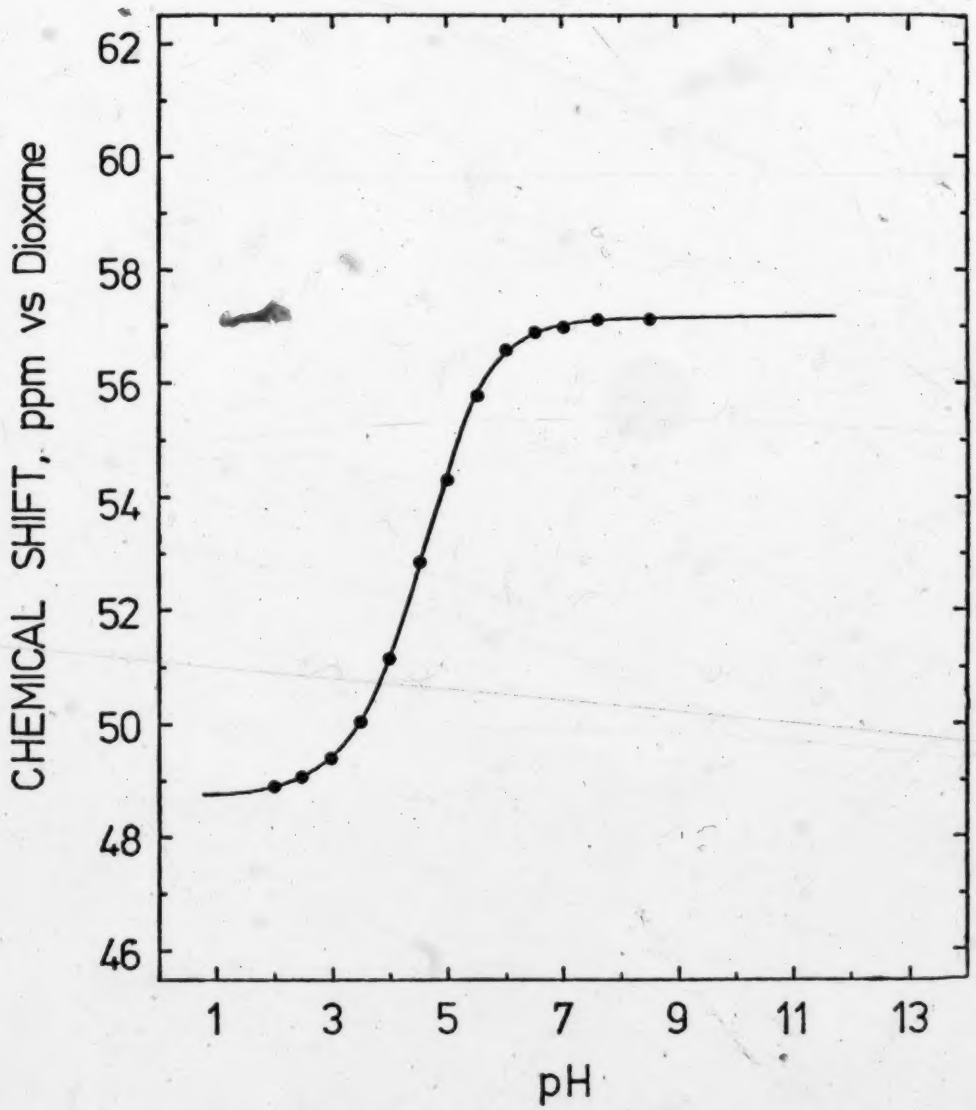


Figure 20. pH dependence of the carbon-13 chemical shift (vs. dioxane) of 0.0947 M trimethyllead in solution with 0.146 M glutathione at 25°C and 0.4 M ionic strength (maintained with $NaClO_4$). Positive chemical shifts indicate the resonances are upfield of dioxane.

for the glutathione carboxyl complexes of trimethyllead. The assumption that the amine group of glutathione does not complex detectably with trimethyllead is borne out by the coincidence of the Glu-$C_\alpha$ curves of pure glutathione and trimethyllead-complexed glutathione. Similarly, the complexation of glutathione by trimethyllead does not measurably enhance the acidity of the amide nitrogens of glutathione. Thus, the cmr data tends to confirm the model postulated above for the complexation of trimethyllead by glutathione.

Also obtained in this study was a value for the lead-207:carbon-13 coupling constant, which was 308.8 Hz at pH 5.00 in the solution described in this subsection. This is in the vicinity of $^{207}Pb$ - $^{13}C$ coupling constants reported for a number of similar trialkyllead compounds under a variety of conditions (81-83).

## C. Discussion

A variety of ligands were selected for the present study to permit the observation of the effects of various ligand parameters upon the formation of trimethyllead complexes. Tables V and VI provide summaries of the formation constants and the chemical shifts of the various ligand-trimethyllead complexes described in this Chapter, along with some corresponding proton, inorganic lead and

TABLE V

FORMATION CONSTANTS OF THE TRIMETHYLLEAD, PROTON, $Pb^{++}$ AND METHYLMERCURY COMPLEXES OF THE SULFHYDRYL GROUPS OF SEVERAL ORGANIC LIGANDS AND THE CHEMICAL SHIFTS VS. DSS OF THE TRIMETHYLLEAD COMPLEXES

| Ligand | $\log\left(\frac{[(CH_3)_3PbL]}{[(CH_3)_3Pb^-][L]}\right)$ [a,b] | $\log\left(\frac{[HL]}{a_{H^+}[L]}\right)$ [a] | $\log\left(\frac{[PbL]}{[Pb^{++}][L]}\right)$ [e] | $\log\left(\frac{[CH_3HgL]}{[CH_3Hg^+][L]}\right)$ [e] | $\delta_{(CH_3)_3PbL}$ [a,b,c] |
|---|---|---|---|---|---|
| 2-mercaptoethanol | 5.96 ± 0.01 | 9.62 | --- | 16.12 (102) | 1.3245 ± 0.0002 |
| N-acetyl-D,L-penicillamine | 5.61 ± 0.02 | 10.28 | --- | --- | 1.351 ± 0.0005 |
| D,L-Penicillamine | | | | | |
| - Monoprotonated Complex[d] | 4.05 ± 0.02 | 8.03 | 12.37 (114) | --- | 1.414 ± 0.001 |
| - Fully deprotonated complex | 5.63 ± 0.04 | 9.70 | | | 1.373 ± 0.001 |
| L-Cysteine | | | | | |
| - Monoprotonated Complex[d] | 4.99 ± 0.02 | 8.38 | 11.39 (114) | 15.7 (130) | 1.356 ± 0.0005 |
| - Fully deprotonated complex | 5.97 ± 0.03 | 9.74 | | | 1.325 ± 0.0005 |
| Glutathione | | | | | |
| - Monoprotonated Complex[d] | 5.54 ± 0.01 | 8.97 | 10.60 (121) | 15.9 (130) | 1.338 ± 0.0005 |
| - Fully deprotonated complex | 5.63 ± 0.03 | 9.08 | | | 1.335 ± 0.005 |

(a) At 25°C and 0.3 M ionic strength.
(b) Errors are linear estimates of the standard deviation.
(c) ppm vs. DSS.
(d) Protonated at the amino group.
(e) Reference numbers in brackets.

TABLE VI

FORMATION CONSTANTS, $pK_a$ VALUES AND CHEMICAL SHIFTS OF THE CARBOXYLATE COMPLEXES AND THE TWO TO ONE SULFHYDRYL COMPLEXES OF TRIMETHYLLEAD[a,b]

| Ligand | $K_f$ $((CH_3)_3PbL)$ | $pK_a$ [d] | $\delta_{(CH_3)_3PbL}$ [c] | $K_f$ $((CH_3)_3Pb)_2L)$ | $\delta_{(CH_3)_3Pb)_2L}$ [c] |
|---|---|---|---|---|---|
| 2-Mercaptoethanol | --- | --- | --- | 14.0 ± 8.8 | 1.454 ± 0.007 |
| Glycine | | | | | |
| - Monoprotonated | 1.26 ± 0.58 | 2.46 | 1.481 ± 0.020 | --- | --- |
| - Fully deprotonated | 29.5 ± 3.8 | 4.43[e] | 1.433 ± 0.016 | --- | --- |
| N-acetyl-D,L-Penicillamine | 4.0 ± 2.1 | 3.48 | 1.465 ± 0.030 | --- | --- |
| D,L-Penicillamine | --- | 1.94 | --- | --- | --- |
| Cysteine | 2.2 ± 2.0 | 1.93 | 1.426 ± 0.089 | --- | --- |
| Glutathione | | | | | |
| - Triprotonated | 1.2 ± 1.1 | 2.15 | 1.433 ± 0.076 | --- | --- |
| - Diprotonated | 10.8 ± 1.7 | 3.49 | 1.455 ± 0.012 | --- | --- |
| - Monoprotonated | --- | --- | --- | 17.4 ± 4.9 | 1.351 ± 0.011 |

(a) At 25°C and 0.3 M ionic strength.
(b) Errors are linear estimates of the standard deviation.
(c) ppm vs. DSS.
(d) Carboxylic acid deprotonation.
(e) $pK_a$ of the ionization: $H_2NCH_2COOH \rightleftharpoons H_2NCH_2COO^- + H^+$, from reference 118, page 486.

methylmercury data for comparison. A later section will present qualitative explanations of the trends and apparent anomalies in the tabulated data concerning trimethyllead complexes.

The results presented in this chapter also demonstrate that the carboxyl, sulfhydryl and trimethyllead-complexed sulfhydryl groups of the selected organic ligands are all potential binding sites for $(CH_3)_3Pb^+$, and that the amount of complexation at a particular site is strongly pH-dependent.

1. The pH Dependence of the Complexation of Trimethyllead by Organic Ligands

(a) Conditional Formation Constants as Functions of pH. The pH dependence of complex formation may be illustrated using conditional formation constants; these will be distinguished from the formation constants described earlier by a subscript c. A conditional formation constant, $K_{f,c}$ is defined as the pH dependent equilibrium constant for the reaction:

$$[TML]_{free} + [LIGAND]_{free} \rightleftharpoons [TML.LIGAND]_{total} \quad (101)$$

$$K_{f,c} = \frac{[TML.LIGAND]_{total}}{[TML]_{free} \cdot [LIGAND]_{free}} \quad (102)$$

where $[TML]_{free}$ and $[LIGAND]_{free}$ include all free forms of

trimethyllead and ligand, respectively, and $[TML.LIGAND]_{total}$ includes all forms (protonated and deprotonated) of the particular complex under study (131).

Although a number of the formation constants given earlier in this chapter are large, the corresponding conditional formation constants can be quite small due to competing reactions with proton or hydroxide ions. The conditional formation constants of the trimethyllead complexes with the ligands discussed in this work are presented as functions of pH in Figures 21 through 26. Each $K_{fc}$ is almost always somewhat smaller than the corresponding $K_f$, and its magnitude is strongly pH-dependent. The changes in slope evident in the tails of a few of these curves result from additional protonation or deprotonation at other functional groups on the ligand. The differences in amplitude of the curves of corresponding complexes are functions of the differences in the magnitudes of the various complex formation constants as well as of the effects of the competing reactions, i.e., ligand protonation and trimethyllead complexation with hydroxide ions. These differences will be explained in a later section.

These Figures indicate that the one to one trimethyllead to sulfhydryl complex is the strongest complex in the pH range of approximately 6 to 12. At high pH, there is some dissociation of the complexes due to hydroxide ion competition for the $(CH_3)_3Pb^+$ cation. At intermediate

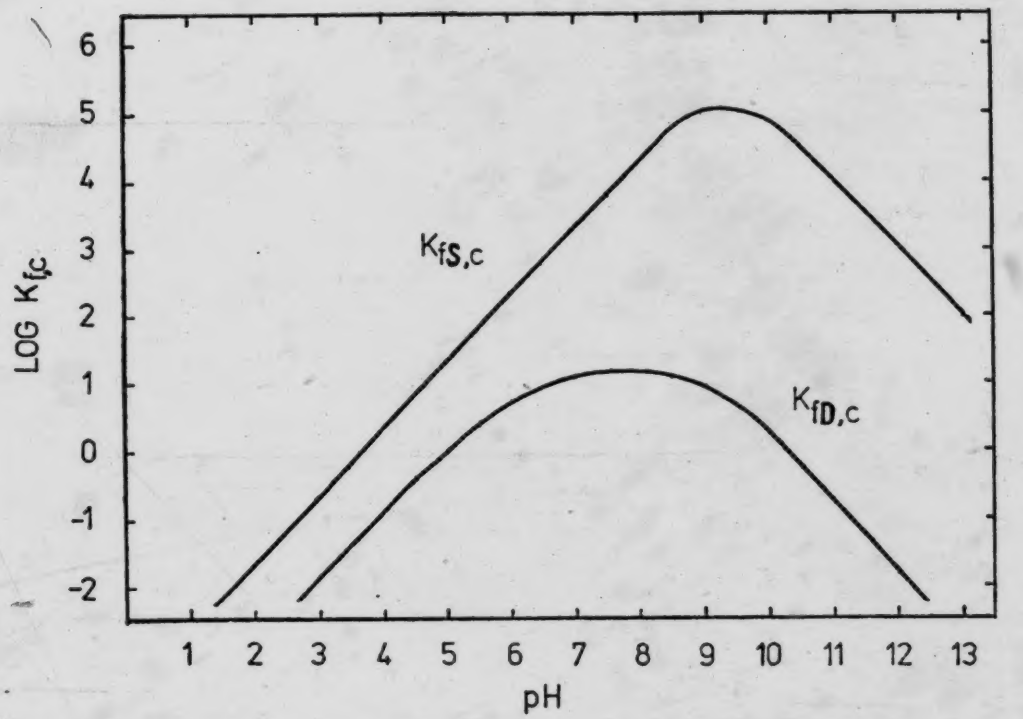


Figure 21. Conditional formation constants of the 2-mercaptoethanol complexes of trimethyllead as functions of pH at 25°C and 0.3 M ionic strength.

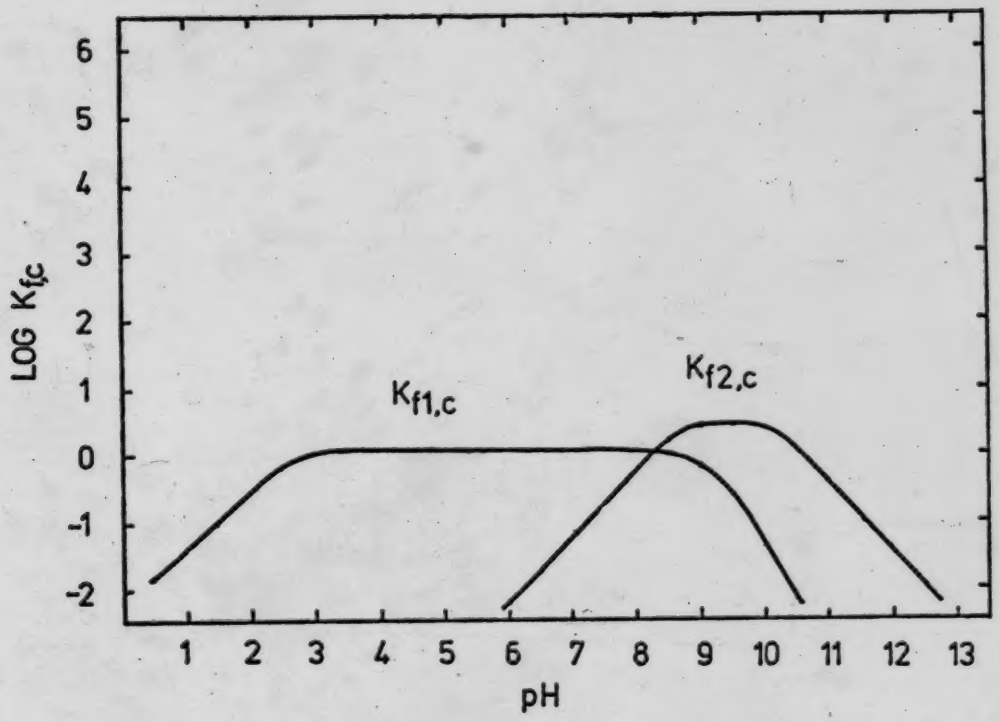


Figure 22. Conditional formation constants of the glycine complexes of trimethyllead as functions of pH at 25°C and 0.3 M ionic strength.

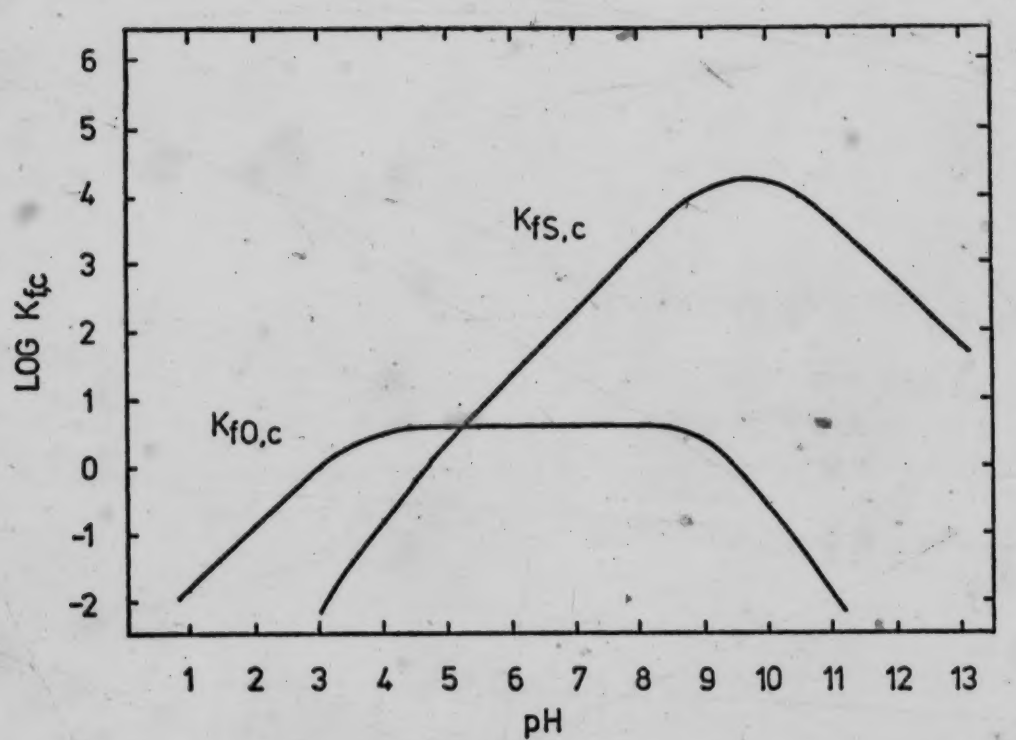


Figure 23. Conditional formation constants of the N-acetyl-D,L-penicillamine complexes of trimethyllead as functions of pH at 25°C and 0.3 M ionic strength.

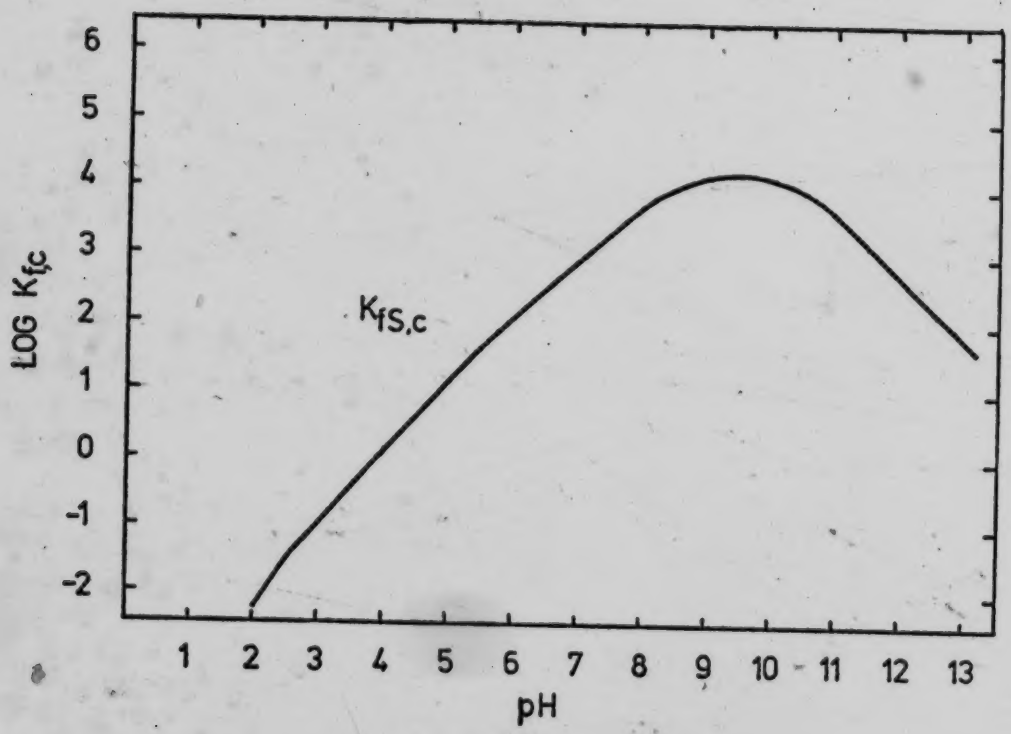


Figure 24. Conditional formation constants of the D,L-penicillamine complexes of trimethyllead as functions of pH at 25°C and 0.3 M ionic strength.

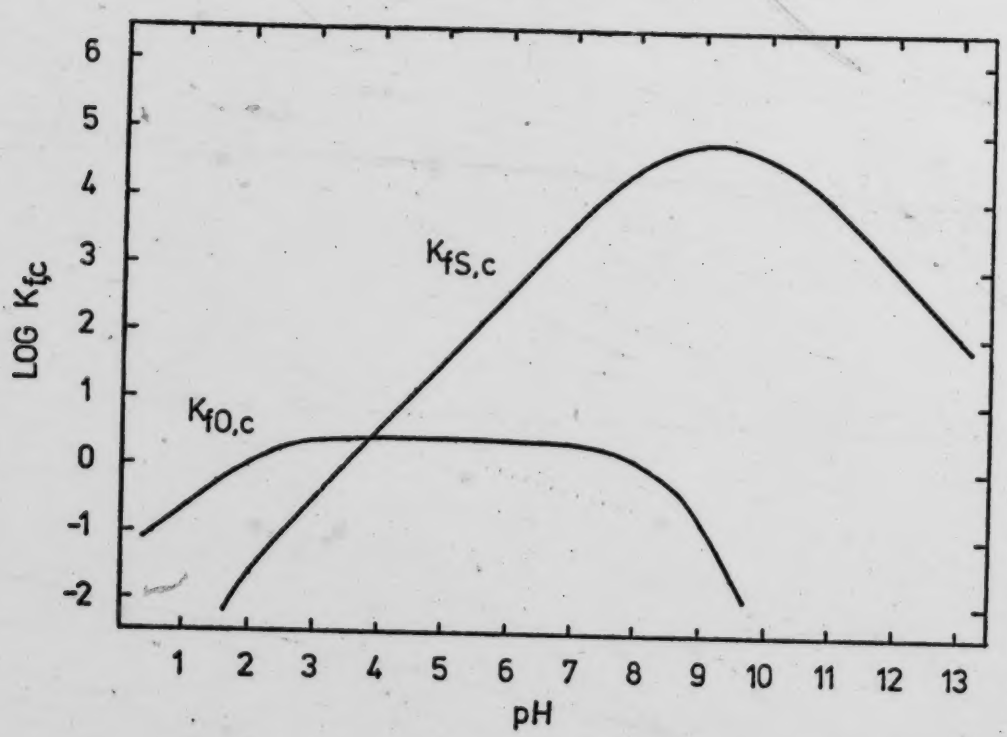


Figure 25. Conditional formation constants of the L-cysteine complexes of trimethyllead as functions of pH at 25°C and 0.3 M ionic strength.

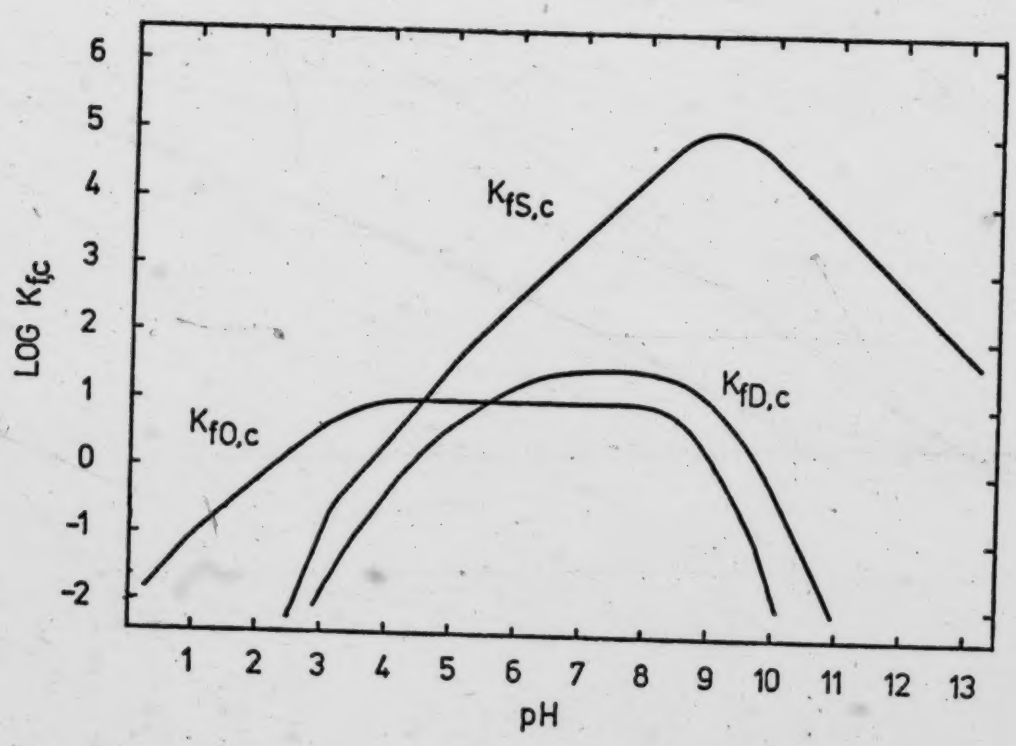


Figure 26. Conditional formation constants of the glutathione complexes of trimethyllead as functions of pH at 25°C and 0.3 M ionic strength.

pH, the sulfhydryl complexes dissociate due to competitive protonation of the sulfhydryl group. For 2-mercaptoethanol and glutathione, small amounts of the two to one trimethyllead to sulfhydryl complexes were also detected in this region. As shown in Figures 21 and 26, the curves of these two to one complexes approach those of the one to one complexes. This occurs because the ratio of free $(CH_3)_3Pb^+$ to deprotonated sulfhydryl is relatively high at neutral pH levels; hence, this is the most favorable region for the formation of two to one trimethyllead to ligand complexes. Such complexes were not detected for the majority of the ligands studied, due to other factors discussed later in this chapter.

At somewhat lower pH, usually between pH 2 and 4, the $K_{fC}$ values of the various carboxylate complexes exceed all others. This is due to the much higher acidity of the carboxylic acid groups. Therefore, at low pH the carboxylate complexes of trimethyllead will be the strongest in the solution, even though the carboxylate $K_f$ values are several orders of magnitude less than those of the sulfhydryl complexes. At very low pH, even the carboxylate groups become protonated and trimethyllead complexation declines rapidly.

(b) Species Distributions as Functions of pH. The formation constants of trimethyllead hydroxide complexes

discussed in Chapter III, the $pK_a$ values of the various ligand binding sites and the complex formation constants determined earlier in this Chapter were used to compute the species distribution curves shown in Figures 27 through 32. These curves illustrate the pH dependence of the fractional concentration of each species, where each fractional concentration is defined as the concentration of the relevant metal or ligand moiety found in solution as part of a particular species, divided by the total analytical concentration of the moiety. A trimethyllead to ligand ratio of one to two, common to all the binding studies described in this Chapter, was employed in the calculation of these curves. These calculations are also dependent on the actual concentrations of trimethyllead and ligand, which were 0.005 M and 0.010 M, respectively, for each case.

The upper plot in each of these figures depicts the fractional concentrations vs. pH of all the species containing trimethyllead while the lower plots refer strictly to those species containing ligand. At low pH, the primary species in solution are $(CH_3)_3Pb^+$ and fully protonated ligand. At higher pH levels, a succession of complexes form, according to the values of the various formation constants and $pK_a$'s. The proportions found at each pH value are consistent with the conditional formation constant data. In addition, these plots provide

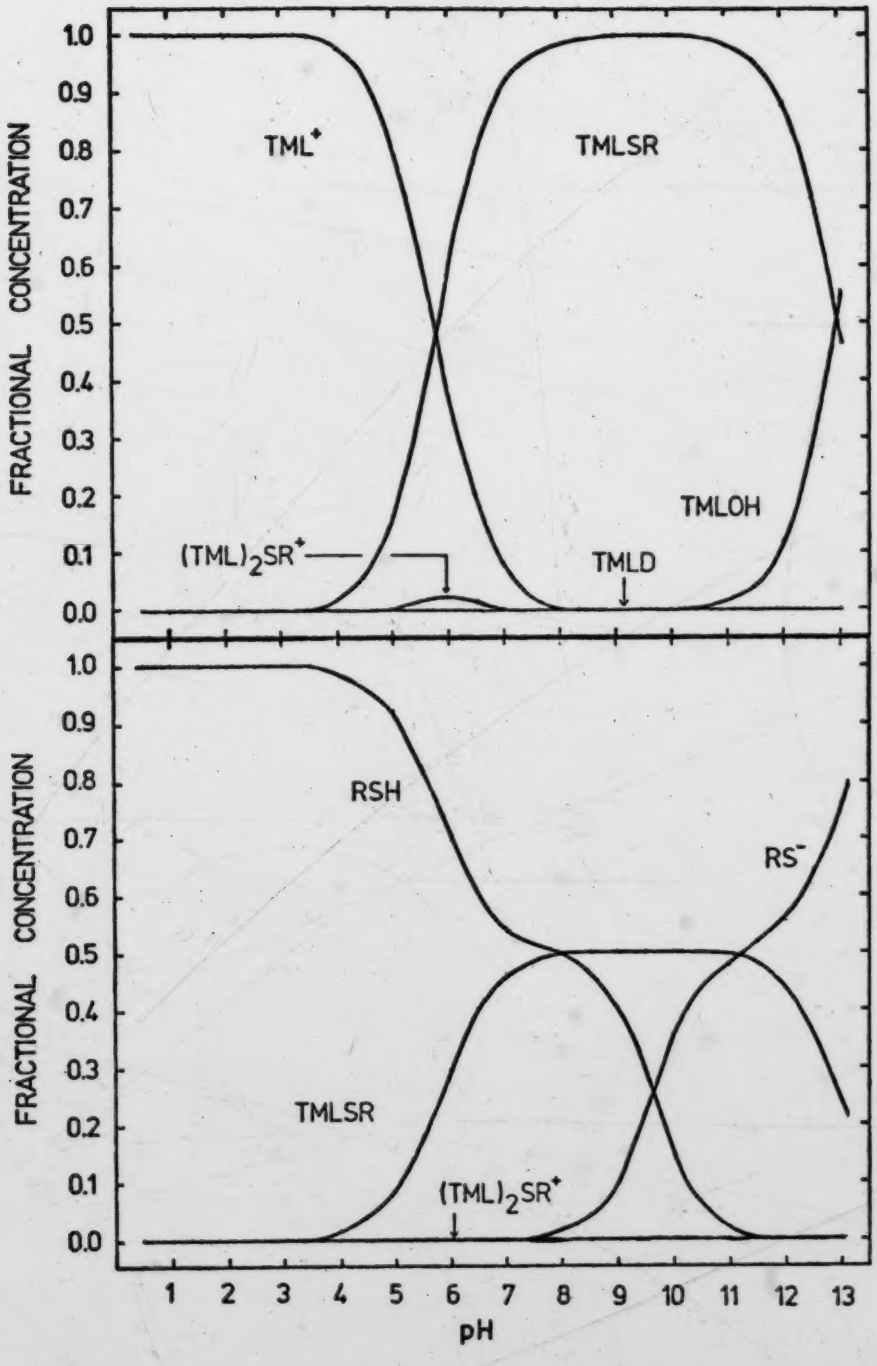


Figure 27. pH dependence of the trimethyllead (upper plot) and 2-mercaptoethanol (lower plot) species distribution in a solution containing 0.005 M trimethyllead and 0.010 M ligand at 25°C and 0.3 M ionic strength. Symbols are defined as in Equations 13 and 40.

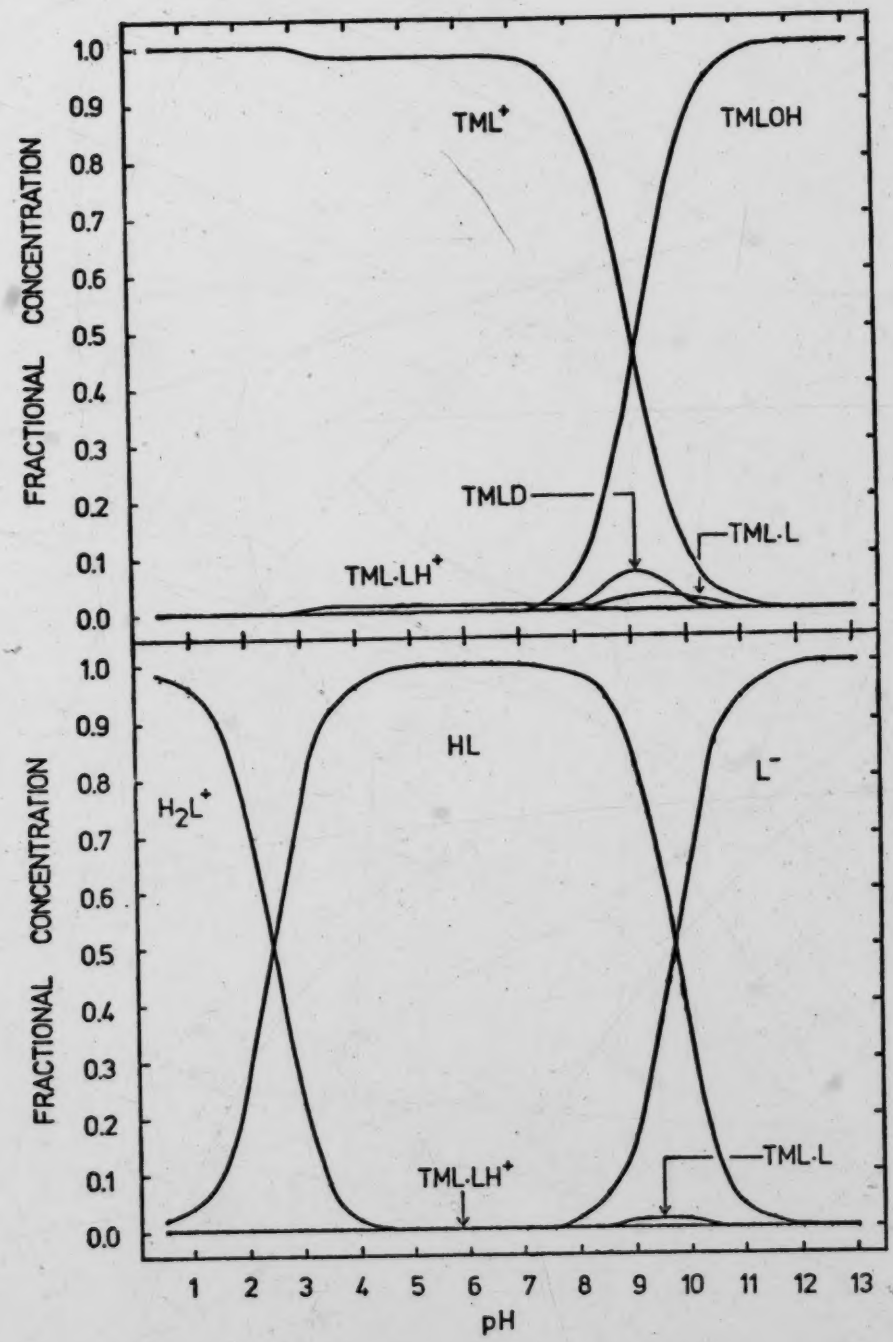


Figure 28. pH dependence of the trimethyllead (upper plot) and glycine (lower plot) species distribution in a solution containing 0.005 M trimethyllead and 0.010 M ligand at 25°C and 0.3 M ionic strength. Symbols are defined as in Equations 13 and 55 - 60.

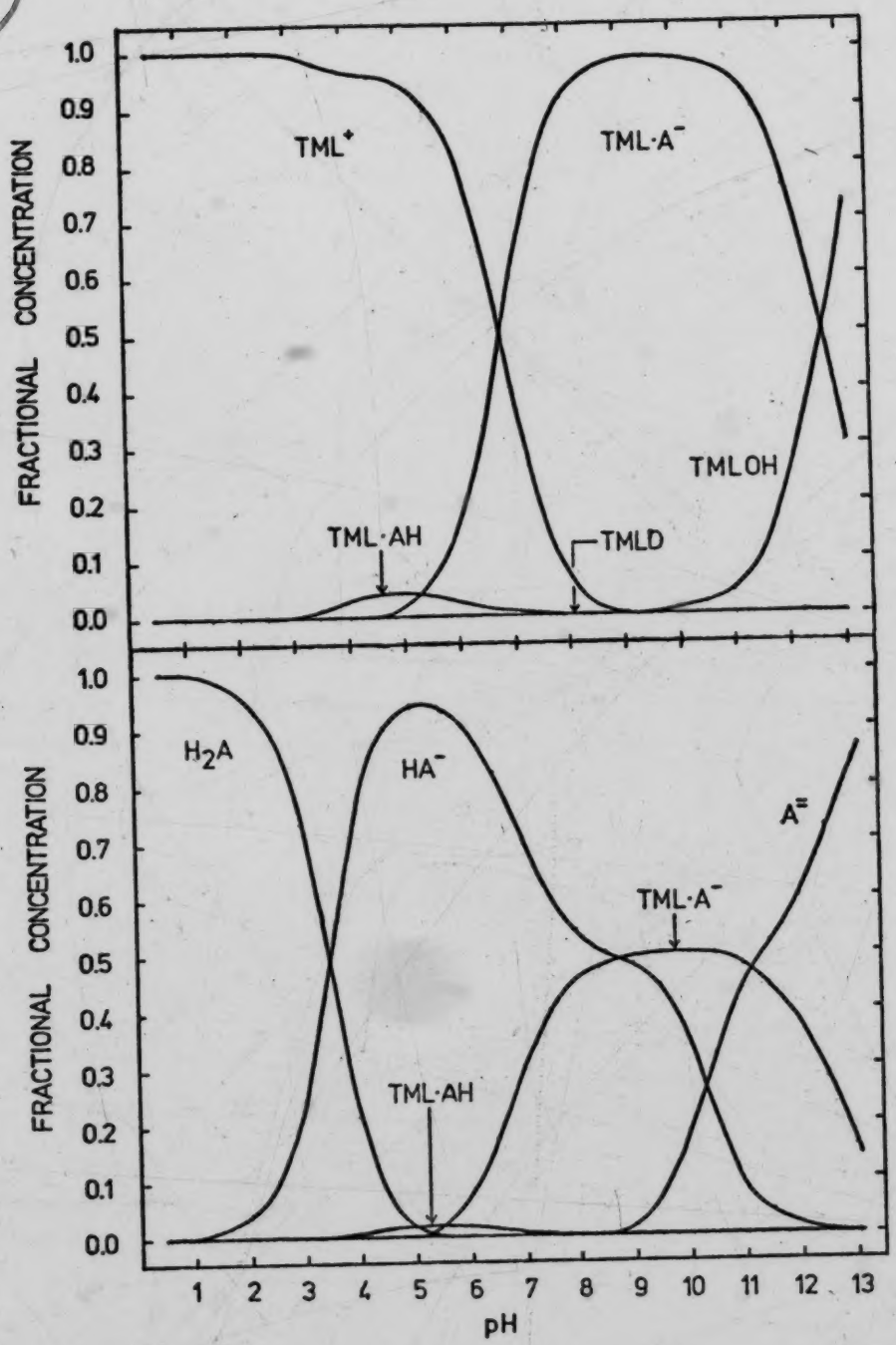


Figure 29. pH dependence of the trimethyllead (upper plot) and N-acetyl-D,L-penicillamine (lower plot) species distribution in a solution containing 0.005 M trimethyllead and 0.010 M ligand at 25°C and 0.3 M ionic strength. Symbols are defined as in Equations 13 and 66.

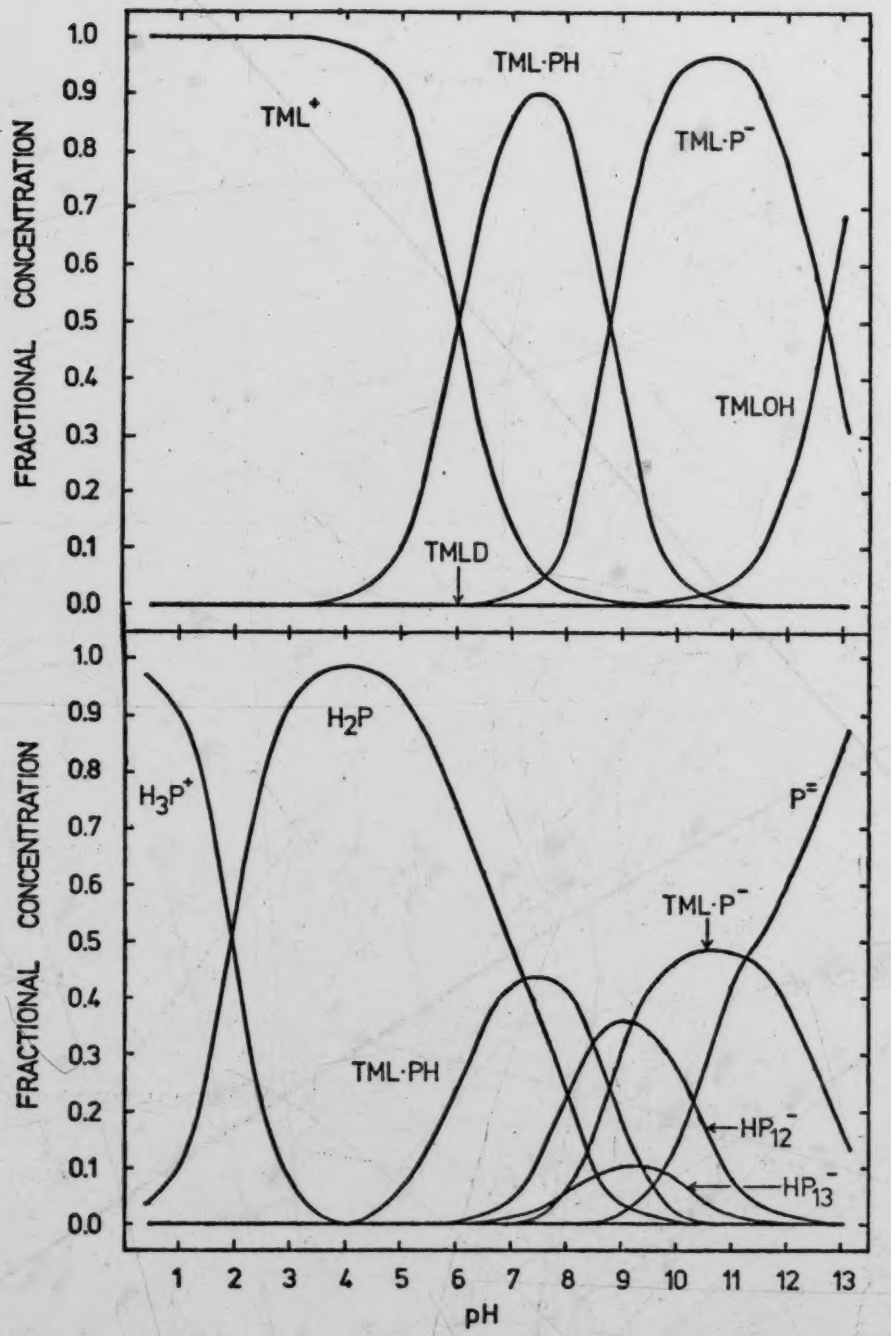


Figure 30. pH dependence of the trimethyllead (upper plot) and D,L-penicillamine (lower plot) species distribution in a solution containing 0.005 M trimethyllead and 0.010 M ligand at 25°C and 0.3 M ionic strength. Symbols are defined as in Equations 13 and 87.

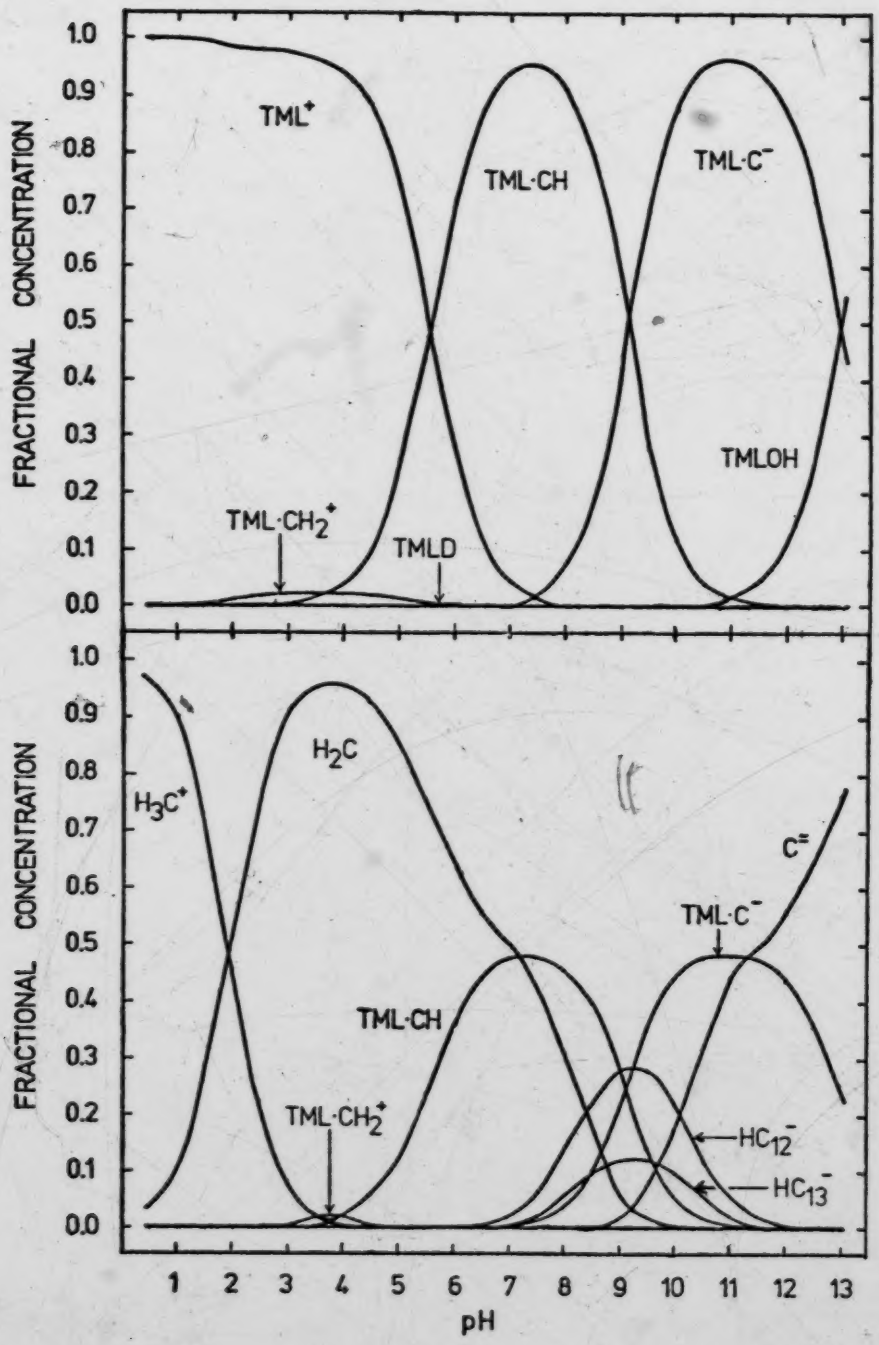


Figure 31. pH dependence of the trimethyllead (upper plot) and L-cysteine (lower plot) species distribution in a solution containing 0.005 M trimethyllead and 0.010 M ligand at 25°C and 0.3 M ionic strength. Symbols are defined as in Equations 13 and 97.

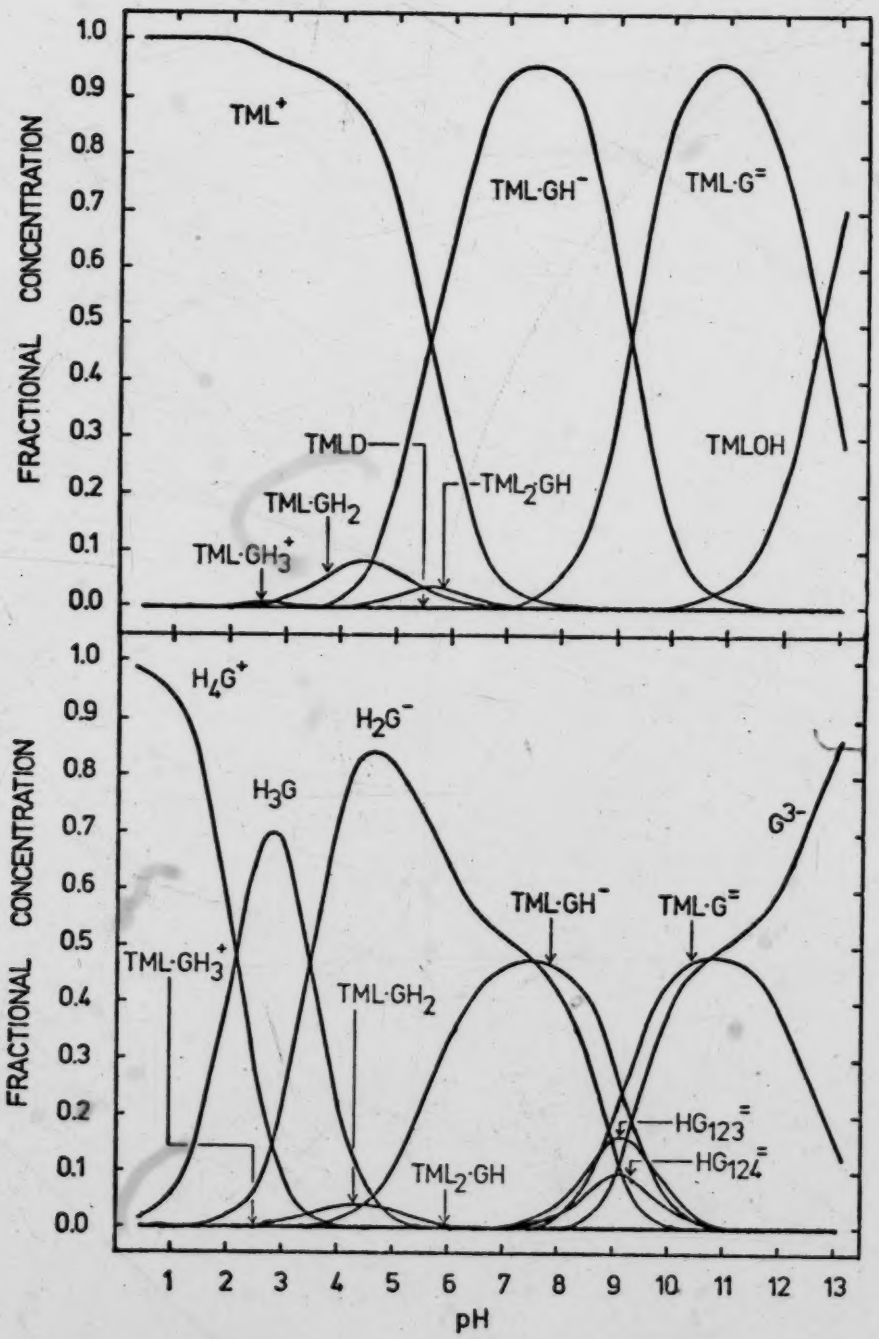


Figure 32. pH dependence of the trimethyllead (upper plot) and glutathione (lower plot) species distribution in a solution containing 0.005 M trimethyllead and 0.010 M ligand at 25°C and 0.3 M ionic strength. Symbols are defined as in Equation 13 and Figure 17.

information regarding the degree of trimethyllead complexation to certain functional groups for differing ligand protonation states. Penicillamine, cysteine and glutathione exhibit separate curves for the sulfhydryl complexes protonated and deprotonated at the amino group, as does glycine for its analogous carboxylate complexes. Glutathione also shows separate curves for the glycyl and glutamyl carboxylate complexes of trimethyllead, with the glycyl complex dominating above pH 3. (The proportion of any trimethyllead-complexed species in the lower plots is limited to a maximum of 0.5 due to the two-to-one excess of ligand over metal concentration.)

The carboxylate complex of fully deprotonated glycine with trimethyllead is shown in Figure 28 to be reduced in proportion by competition for the trimethyllead cation with the dimeric species $((CH_3)_3Pb)_2OH^+$. The contrast in total proportions between this complex and the various sulfhydryl complexes shown in the other species distribution plots is quite striking, supporting the assumption made earlier in this Chapter that the concentration of such carboxyl complexes is negligible in amino acid solutions containing an excess of sulfhydryl groups. However, under conditions of excess trimethyllead, detection and quantitation of these fully deprotonated carboxyl complexes may be possible.

The amounts of two-to-one trimethyllead-to-2-mercapto-

ethanol or glutathione complexes are also seen to be small, due to competition with several other equilibria. However, the proportion of such complexes in solution is highly dependent on the total concentration of trimethyllead: at higher metal concentrations and at appropriate pH levels, these species may become major solution components. Under such conditions, similar two-to-one complexes may also form in measurable quantities with some of the remaining sulfhydryl-containing ligands.

The composition of a trimethyllead-ligand solution can be seen in Figures 21 through 32 to be strongly pH dependent. Therefore, the control of pH enables selection of the type of trimethyllead complex occurring in solution. For example, at physiological pH values (near 7.4), the major species present under conditions of excess ligand will be the one-to-one trimethyllead-sulfhydryl complex. The two-to-one and the carboxylate complexes of trimethyllead are not likely to occur in significant proportions under these conditions, unless most of the free sulfhydryl groups are subsequently rendered relatively inactive by some other means, such as oxidation.

2. Other Factors Influencing the Complexation of Trimethyllead by Organic Ligands

The trimethyllead cation is a Lewis acid; hence, the strength of its complexes will be dependent upon the

inherent basicities of the ligand binding sites involved. The formation constants for all one-to-one complexes described in this Chapter are plotted versus this basicity (expressed in terms of $pK_a$ values) in Figure 33. Included in this plot are the formation constants for several trimethyllead-carboxylic acid complexes (62). In this Figure, reasonably strong correlation of log $K_f$ with $pK_a$ is demonstrated by the various carboxylate complexes and, to a lesser extent, by the sulfhydryl complexes as well. There are, nonetheless, a number of factors including differences in polarizability, in steric and conformational requirements and in electrostatic interactions, which cause significant deviations from linearity in the data.

Firstly, the central lead(IV) atoms of trimethyllead are much larger and more polarizable than are protons (although the polarizability of this lead species is much less than that of inorganic lead). As noted in Chapter I, the bonds of trimethyllead with polarizable ligand atoms, such as the sulfhydryl sulfur, will have significant covalent character and may include $p\Pi$-$d\Pi$ bonding as well. On the other hand, the weak bonds of trimethyllead with ligand atoms of low polarizability ("hard" Lewis bases, in the sense described by Pearson (64)) will have little covalent character and no $p\Pi$-$d\Pi$ bonding. Hence, the bonding in the weak carboxylate complexes of trimethyllead is primarily ionic. The proton is a much harder Lewis acid

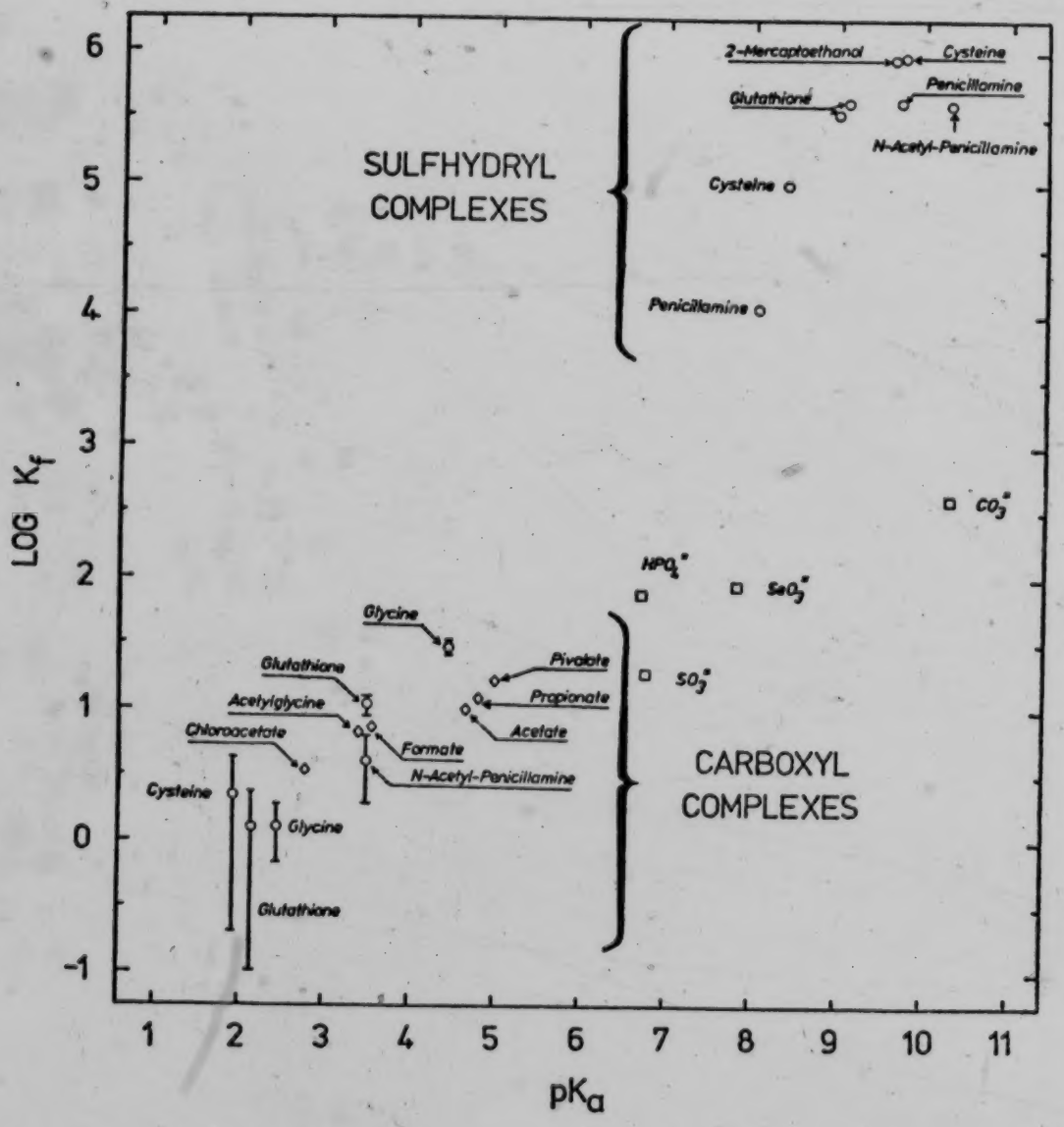


Figure 33. The dependence of the logarithm of the trimethyllead complex formation constant upon the $pK_a$ values of the respective free ligands. Complexes shown are those studied in this work (○) and in references 62 (◇) and 63 (□).

than trimethyllead, thus forming stronger ionic bonds with hard bases than does trimethyllead (64). Interestingly, the "soft" methylmercury, the "borderline" $Pb^{++}$ and the "hard" hydrogen ions all form stronger bonds with sulfhydryl and carboxyl groups than does trimethyllead, indicating the importance of factors other than hard and soft Lewis acidity and basicity in the formation of trimethyllead complexes. (However, it should be noted that the strengths of the $Pb^{2+}$ and trimethyllead complexes cannot be compared directly because the ligands studied in this work may chelate $Pb^{2+}$ using several donor groups simultaneously, whereas trimethyllead reacts as a one-coordinate species only.)

Steric factors have a sizeable influence on the complexation behaviour of trimethyllead. The presence of the three equatorial methyl groups severely reduces the probability of the formation of a chemical bond upon collision of trimethyllead and ligand molecules. Protons, lead(II) ions and even methylmercury cations are much less hindered than trimethyllead cations. Hence, it is not surprising that these form stronger complexes with the ligands of this study than does trimethyllead. This effect is amplified by the presence of bulky non-reactive groups on some ligand molecules. For example, molecular models indicate that the β-methyl groups of penicillamine and N-acetylpenicillamine interact sterically with the

trimethyllead methyl groups such that the complex formation constants are significantly lower than those of the analogous cysteine complexes. The N-acetyl group also hinders complex formation to some extent.

A complicating factor is that of electrostatic attraction and repulsion between the trimethyllead cation and the cationic or anionic ligand groups remote from the site of complexation. Such interactions are generally small, but are nonetheless noticeable if the interfering ionic group is situated quite near to the complexing functional group. This is especially true if steric factors increase the probability of these interactions. For example, the formation of the monoprotonated (protonated at the ammonium group) penicillamine complex of trimethyllead is significantly reduced due to a combination of electrostatic and steric effects. Space-filling model studies indicate that the conformations allowing closest approach of trimethyllead to the ligand are those in which the ammonium group is situated near the sulfhydryl binding site, thus optimizing the repulsive electrostatic interaction. Conversely, the monoprotonated cysteine molecule may adopt conformations minimizing electrostatic repulsion of cationic trimethyllead; the formation constant of the monoprotonated cysteine complex is much larger.

Another example of electrostatic effects is that of the monoprotonated glutathione complex. In this case,

the glutamyl ammonium group is well removed from the sulfhydryl binding site, resulting in no significant reduction of the sulfhydryl-trimethyllead complex formation constant. Similarly, the glutathione glycyl carboxylate complex of trimethyllead is well removed and immune to the effects of the ammonium group. However, the glutamyl carboxylate complex forms adjacent to the glutamyl ammonium group: this complex forms only to a very small extent.

A further example of the effect of a nearby positively charged protonated group is provided by the glycine system. The two complexes most probably involved are $(CH_3)_3Pb\text{-}O_2CCH_2NH_3^+$ and $(CH_3)_3Pb\text{-}O_2CCH_2NH_2$. The difference observed between the values of the two formation constants is due to the protonation state of the amino group.

Other examples of electrostatic interactions include the penicillamine carboxylate and the two N-acetyl-penicillamine complexes of trimethyllead. The concentration of the penicillamine complex is below experimental detection limits due to steric hindrances and the aforementioned sterically-optimized electrostatic repulsion of cationic trimethyllead. The N-acetyl-penicillamine complexes are free of electrostatic repulsion, but the acetyl blocking group causes increased steric interactions between the ligand and trimethyllead.

Steric and electrostatic interactions also affect

the formation of two-to-one trimethyllead-to-ligand complexes. Only those complexes which are relatively free of such interferences at the sulfhydryl binding site will form measurable quantities of such complexes. In this study, the only ligands found to be of this type were 2-mercaptoethanol and glutathione. No fully deprotonated two-to-one complexes were observed, due to the competition of hydroxide ion for the trimethyllead cation at the high pH values required to fully deprotonate the ligands in this study.

Table V presents overall formation constants for some complexes of inorganic lead(II). However, comparison of the trimethyllead results is somewhat misleading without a consideration of the chelation effect. Penicillamine and cysteine probably act as tridentate ligands toward $Pb^{++}$ (114,121), resulting in larger overall formation constants and more complicated behaviour than that exhibited by trimethyllead. (Glutathione, however, appears to be monodentate towards $Pb^{++}$ (125).) In contrast, it has been found in this work and in other studies (62,63, 77,129) that trimethyllead reacts as a one-coordinate species with a variety of ligands; chelation is prevented by the equatorial methyl groups. Thus, the strength of trimethyllead complexes is significantly less than the analogous $Pb^{++}$ complexes. In addition, the oxidation states of the lead atoms, the overall charges and the

steric effects are different for trimethyllead and $Pb^{++}$. The low degree of correlation observed between the formation constants of analogous complexes of trimethyllead and $Pb^{++}$ is therefore to be expected.

In contrast, the methylmercury complex formation constants shown in Table V are somewhat more easily correlated to those of trimethyllead. This is because the central Pb(IV) of trimethyllead is isoelectronic with the Hg(II) of methylmercury, the two metal ion species have identical +1 charges and both species bind to various ligand functional groups in primarily one-to-one ratios. However, steric factors are relatively unimportant in methylmercury complexation, and in addition, methylmercury is a very "soft", polarizable Lewis acid (64) compared to trimethyllead. Therefore, methylmercury binds much more strongly with a wide variety of ligands (especially "soft" Lewis bases such as sulfhydryl groups) than does trimethyllead, despite their above-mentioned similarities.

The correlation of the Lewis basicity of the ligand functional group to the nmr chemical shift of the trimethyllead protons in the complex may be examined in the plot of $\delta_{COMPLEX}$ vs. $pK_a$ shown by Figure 34. The Lewis basicity of an electron donor group is by definition a measure of its electron donating power: certain electrons of the base move towards an acidic center by an amount proportional to the strength of the bond. Increased

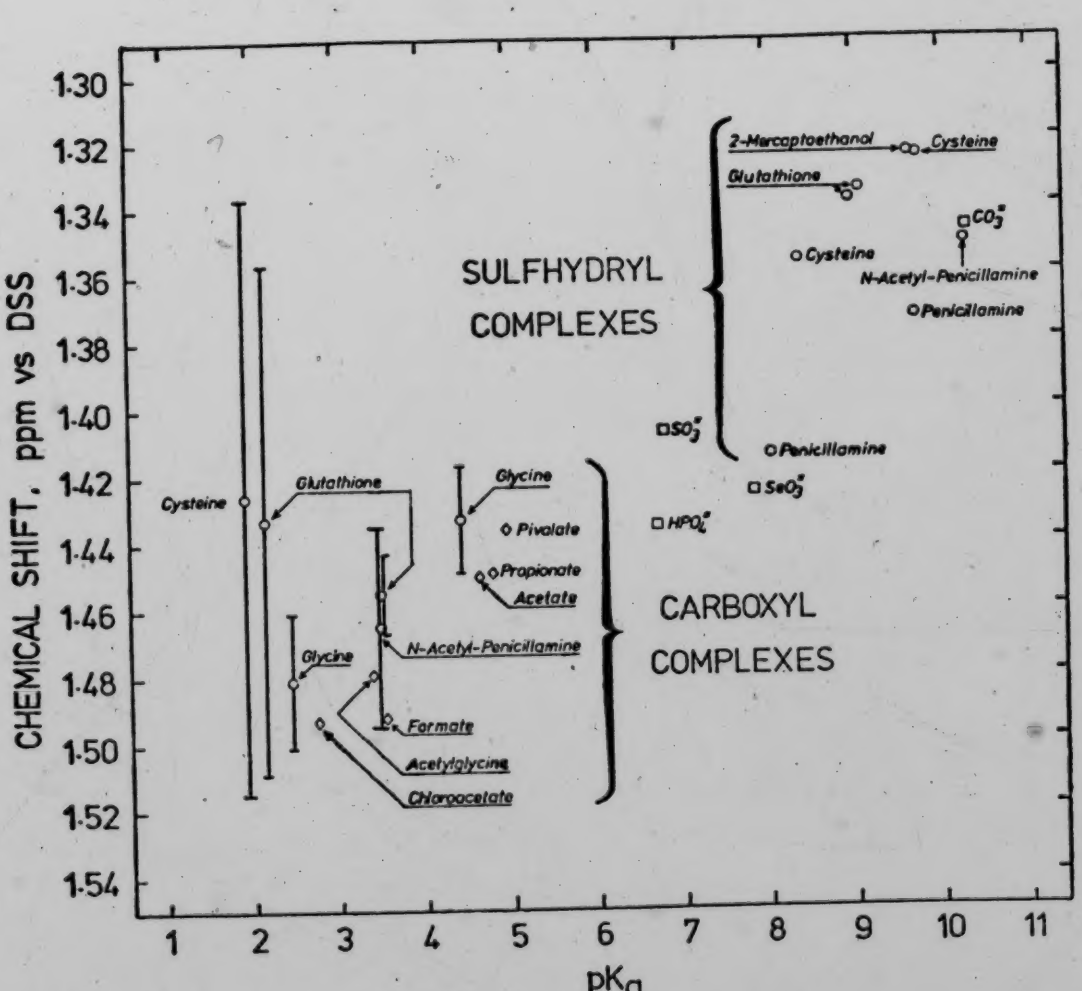


Figure 34. The dependence of the chemical shift of the trimethyllead methyl protons in certain trimethyllead complexes upon the $pK_a$ values of the respective free ligands. Complexes shown are those studied in this work (○) and in references 62 (◇) and 63 (□).

bond strength results in increased electron density near the acidic center, which in the case of trimethyllead results in increased electron density near the electron-withdrawing methyl groups. The protons of these methyl groups are therefore better shielded from the external magnetic field in an nmr experiment, causing smaller chemical shifts relative to DSS for the stronger complexes. The ligands which form stronger complexes with trimethyllead in general form stronger complexes with hydrogen ions as well, due to the greater basicity of the functional group.

A number of deviations from linearity are observed in Figure 34. Other factors, such as steric interactions, which are unrelated to the ligand basicity, can nonetheless reduce the strength of the trimethyllead complex. This reduces the shielding of the trimethyllead protons and increases the chemical shift because the average metal-ligand bond length is increased. These weaker complexes undergo a lesser degree of electron transfer from base to acid. This increase in chemical shift is observed for the sterically-hindered penicillamine and N-acetylpenicillamine sulfhydryl complexes in Figure 34. Electrostatic effects appear to be negligible.

The points presented in the above discussions are necessarily qualitative, but they nonetheless provide consistent explanations of the nature of trimethyllead

binding with the various ligands studied in this thesis.

3. Conclusions

It should be possible to use the material presented in this thesis to elucidate the behaviour of trimethyllead in biological systems. For example, at the physiological pH level of 7.4, the results of this thesis when combined with previous studies (62,63,77,129) indicate the preferred site of trimethyllead binding to be the sulfhydryl group of sulfhydryl-containing ligands. The blocking of sulfhydryl active sites on proteins of various sorts is probably a major avenue of trimethyllead poisoning, as it is with methylmercury (84). However, the evidence is not conclusive because the body of research on trimethyllead complexation by biological ligands is quite small. Studies on the binding of trimethyllead by imidazole and phenolic hydroxide groups, for example, could also shed light on the mechanisms of trimethyllead toxicity. A detailed knowledge of the complexation behaviour of trimethyllead in aqueous and non-aqueous systems will be required to develop a complete understanding of the physiological effects of trimethyllead intoxication and to optimize the design of appropriate therapeutic agents.

## BIBLIOGRAPHY


1. C. Loewig, Ann. 88, 318 (1853).
2. C. Loewig, J. Prakt. Chem., 60, 304 (1853).
3. C. Loewig, Chem. Zentr., 1852, 575.
4. J. Klippel, J. Prakt. Chem., 81, 287 (1860).
5. H. Shapiro and F. W. Frey, "The Organic Compounds of Lead", Interscience Publishers, New York, N.Y. (1968).
6. H. Shapiro and F. W. Frey, op. cit., Chap. 1.
7. B. F. Greek, Chem. and Eng. News, 48 (47), 52 (1970).
8. T. Midgley, Jr. and T. A. Boyd, Ind. Eng. Chem., 14, 894 (1922).
9. R. W. Leeper, L. Summers and H. Gilman, Chem. Rev., 54, 101 (1954).
10. B. B. Ewing and J. E. Pearson in "Advances in Environmental Science and Technology," Vol. 3, J. N. Pitts, Jr., R. L. Metcalf and A. C. Lloyd, Ed., Wiley-Interscience, New York, N.Y. (1974).
11. P. Grandjean in "Lead," T. B. Griffin and J. H. Knelson, Ed., Academic Press, New York, N.Y. (1975).
12. H. Shapiro and F. W. Frey, op. cit., Chap. 17.
13. R. S. Tobias, Organometal. Chem. Rev., 1, 93 (1966).
14. H. Shapiro and F. W. Frey, op. cit., Chap. 4.
15. R. M. Harrison and D. P. H. Laxen, Atm. Environ., 11, 201 (1977).
16. P. T. S. Wong, Y. K. Chau and P. L. Luxon, Nature, 253, 263 (1975).

17. A. W. P. Jarvie, R. N. Markall and H. R. Potter, Nature, 255, 217 (1975).

18. U. Schmidt and F. Huber, Nature, 259, 157 (1976).

19. W. P. Ridley, L. J. Dizikes and J. M. Wood, Science, 197, 329 (1977).

20. G. Ter Haar in "Lead," T. B. Griffin and J. H. Knelson, Ed., Academic Press, New York, N.Y. (1975).

21. H. Shapiro and F. W. Frey, op. cit., Chap. 5.

22. J. E. Cremer, Occup. Health Rev., 17 (3), 14 (1965).

23. J. E. Cremer, Brit. J. Ind. Med., 16, 191 (1959).

24. J. S. Thayer, J. Organomet. Chem., 76, 265 (1974).

25. W. N. Aldridge in "The Organometallic and Coordination Chemistry of Germanium, Tin and Lead," M. Gielen and P. G. Harrison, Ed., Freund Publishing House Ltd., Tel Aviv (1978).

26. J. E. Cremer, Brit. J. Ind. Med., 18, 277 (1961).

27. J. E. Cremer, Bioch. J., 68, 685 (1958).

28. W. Bolanowska and J. M. Wisniewska-Knypl, Bioch. Pharmacol., 20, 2108 (1971).

29. J. E. Casida, E. C. Kimmel and G. Widmark, Acta Chem. Scand., 25, 1497 (1971).

30. W. N. Aldridge, B. W. Street and D. N. Skilleter, Biochem. J., 168, 353 (1977).

31. R. A. Henry and K. H. Byington, Biochem. Pharmacol., 25, 2291 (1976).

32. A. Kosiara, K. Douglass and M. Beer, Proc. Ann. Meet. Electron Microsc. Soc. Am., 33, 624 (1975).

33. J. Ahlberg, C. Ramel and C. A. Wachtmeister, Ambio, 1, 29 (1972).

34. R. M. McClain and B. A. Becker, Toxicol. Appl. Pharmacol., 21, 265 (1972).

35. S. S. Epstein and N. Mantel, Experientia, 24, 580 (1968).

36. M. C. Marsh and B. T. Simpson, J. Cancer Res., 11, 417 (1927); Chem. Abst., 22, 3696 (1928).

37. N. S. Neshkov, Gig. Tr. Prof. Zabol, 15, 45 (1971); Biol. Abs., 53, 63974 (1972).

38. N. M. Bagirov, Tr. Azerb. Nauch.-Issled. Inst. Gig. Tr. Prof. Zabol., 5, 150 (1970); Chem. Abstr. 81, 67981m (1974).

39. V. Scarinci, Studi Urbinati, Fac. farm. [C], 29 (4), 102 (1955), Chem. Abs. 51, 10736b (1957); Arch. Sci. Biol. (Bologna), 44, 153 (1960), Chem. Abs., 60, 4679f (1965).

40. H. Shapiro and F. W. Frey, op. cit., Chap. 2.

41. L. C. Willemsens and G. J. M. van der Kerk in "Organometallic Compounds of the Group IV Elements, Vol. I, Part II," A. G. MacDiarmid, Ed., Dekker, New York, N.Y. (1968), p. 191.

42. R. J. H. Clark, A. G. Davies and R. J. Puddephatt, J.A.C.S., 90, 6923 (1968).

43. M. J. Janssen, J. G. A. Luijten and G. J. M. van der Kerk, Receuil, 82, 90 (1963).

44. N. Bertazzi, G. Alonzo, A. Silvestri and G. Consiglio, J. Organomet. Chem., 37, 281 (1972).

45. E. Amberger and R. Hoenigschmidt-Grossich, Chem. Ber., 98, 3795 (1965).

46. L. C. Willemsens, "Organolead Chemistry," Int. Lead and Zinc Org., New York (1964); L. C. Willemsens and G. J. M. van der Kerk, "Investigations in the Field of Organolead Chemistry," Int. Lead and Zinc Org., Utrecht (1965), cited in reference 47.

47. M. Gielen and N. Sprecher, Organomet. Chem. Rev., 1, 455 (1966).

48. Y. M. Chow and D. Britton, Acta Cryst., B27, 856 (1971).

49. M. Boleslawski, S. Pasynkiewicz and M. Harasimowicz, J. Organomet. Chem., 78, 61 (1974).

50. K. Dehnicke, R. Schmitt, A. F. Shihada and J. Pebler, Z. Anorg. Allg. Chem., 404, 249 (1974); Chem. Abs., 80, 146248k (1974).

51. T. Tanaka, Organomet. Chem. Rev. A, 5, 1 (1970).

52. H. Shapiro and F. W. Frey, op. cit., Chap. 11.

53. G. M. Sheldrick and R. Taylor, Acta Cryst., B31, 2740 (1975).

54. R. J. Puddephatt and G. H. Thistlethwaite, J. Organomet. Chem., 40, 143 (1972).

55. N. A. Matwiyoff and R. S. Drago, Inorganic Chem., 3, 337 (1964).

56. V. G. K. Das and W. Kitching, J. Organomet. Chem., 13, 523 (1968).

57. G. D. Shier and R. S. Drago, J. Organomet. Chem., 6, 359 (1966).

58. I. R. Beattie, Quart. Rev. Chem. Soc., 17, 382 (1963).

59. G. Matsubayashi , Y. Kawasaki, T. Tanaka and R. Okawara, Bull. Chem. Soc. Japan, 40, 1566 (1967).

60. I. P. Beletskaya, K. P. Rubin, A. N. Ryabtsev and O. A. Reutov, J. Organomet. Chem., 59, 1 (1973).

61. P. Goggin, D. Phil. thesis, Oxford (1960), cited in references 13 and 58.

62. T. L. Sayer, S. J. Backs, C. A. Evans, E. K. Millar and D. L. Rabenstein, Can. J. Chem., 55, 3255 (1977).

63. E. K. Millar, C. A. Evans and D. L. Rabenstein, Can. J. Chem., 56, 3104 (1978).

64. R. G. Pearson, J.A.C.S., 85, 3533 (1963).

65. G. Distefano, A. Ricci, R. Danieli, A. Foffani, G. Innorta and S. Torroni, J. Organomet. Chem., 65, 205 (1974).

66. G. Distefano, A. Ricci, F. P. Colonna, D. Pietropaulo and S. Pignatoro, J. Organomet. Chem., 78, 93 (1974).

67. J. D. Kennedy, W. McFarlane and G. S. Pyne, J. C. S. Dalton, 1977, 2322.

68. G. Guillerm, M. Lequan and M. P. Simonnin, Bull. Soc. Chim. Fr., 1973 (5), 1649.

69. M. J. Cooper, A. K. Holliday, P. K. Makin, R. J. Puddephatt and P. J. Smith, J. Organomet. Chem., 65, 377 (1974).

70. N. A. Matwiyoff and R. S. Drago, J. Organomet. Chem., 3, 393 (1965).

71. S. Sorriso, A. Ricci and R. Danieli, J. Organomet. Chem., 87, 61 (1975).

72. P. Zanella and G. Plazzogna, Ann. Chim. (Rome), 59, 1160 (1969); Chem. Abs., 72, 89615m (1970).

73. N. Bertazzi, Z. anorg. allg. Chem., 410, 316 (1974).

74. G. Pilloni and F. Magno, Inorg. Chim. Acta, 5, 30 (1971).

75. G. Pilloni and F. Magno, Inorg. Chim. Acta, 4, 105 (1970).

76. G. Pilloni and F. Milani, Inorg. Chim. Acta 3, 689 (1969).

77. T. L. Sayer, Ph.D. Thesis, University of Alberta (1976).

78. H. P. Fritz and K. Schwarzhans, Chem. Ber., 97, 1390 (1964).

79. H. P. Fritz and K. Schwarzhans, J. Organomet. Chem., 1, 297 (1964).

80. E. W. Abel and D. B. Brady, J. Organomet. Chem., 11, 145 (1968).

81. G. Singh, J. Organomet. Chem., 99, 251 (1975).

82. D. C. van Beelen, D. de Vos, G. J. M. Bots, L. J. van Doorn and J. Wolters, Inorg. Nucl. Chem. Lett.,

12, 581 (1976).

83. T. N. Mitchell, J. Gmehling and F. Huber, J.C.S. Dalton, 1978, 960.

84. D. L. Rabenstein, Acc. Chem. Res., 11, 100 (1978).

85. S. Libich and D. L. Rabenstein, Anal. Chem., 45, 118 (1973).

86. A. I. Vogel, "Quantitative Inorganic Analysis," 3rd ed., John Wiley and Sons, Inc., New York (1961), p. 931.

87. Ibid., p. 443.

88. Ibid., p. 243.

89. W. E. Harris and B. Kratochvil, "Chemical Separations and Measurements," W. B. Saunders Co., Toronto (1974), p. 24.

90. R. Benesch and R. E. Benesch, Biochim. Biophys. Acta, 23, 643 (1957).

91. A. P. Kreshkov and L. B. Oganesyan, J. Anal. Chem. (U.S.S.R.), 26, 534 (1971).

92. A. P. Kreshkov and L. B. Oganesyan, J. Anal. Chem. (U.S.S.R.), 28, 2012 (1973).

93. R. Saetre, Ph.D. Thesis, University of Alberta (1978).

94. D. L. Dye and V. A. Nicely, J. Chem. Ed., 48, 443 (1971).

95. C. S. Handloser, M. R. Chakrabarty and M. W. Mosher, J. Chem. Ed., 50, 510 (1973).

96. E. Grunwald, A. Loewenstein and S. Meiboom, J. Chem. Phys., 27, 641 (1957).

97. A. Albert and E. P. Serjeant, "The Determination of Ionization Constants," Chapman and Hall Ltd., London (1971).

98. H. J. Haupt, F. Huber and J. Gmehling, Z. Anorg. Allg. Chem., 390, 31 (1972).

99. J. Gmehling, thesis, Univ. Dortmund (1973), cited in reference 18.

100. F. Feigl and V. Anger, "Spot Tests in Inorganic Analysis," 6th English Ed., Elsevier Publishing Co., New York (1972), p. 284.

101. D. L. Rabenstein, C. A. Evans, M. C. Tourangeau and M. T. Fairhurst, Anal. Chem., 47, 338 (1975).

102. G. Schwarzenbach and M. Schellenberg, Helv. Chim. Acta, 48, 28 (1965).

103. M. Calvin in "Glutathione," S. P. Colowich et al., Eds., Academic Press Inc., New York (1954), p. 3.

104. D. L. Rabenstein, R. Ozubko, S. Libich, C. A. Evans, M. T. Fairhurst and C. Suvanprakorn, J. Coord. Chem., 3, 263 (1974).

105. R. C. Mercier, M. Bonnet and M. R. Paris, Bull. Soc. Chim. France, 1965, 2926.

106. V. S. Sharma and H. B. Mathur, Indian J. Chem., 3, 475 (1965).

107. E. W. Wilson and R. B. Martin, Arch. Biochem. Biophys.,

142, 455 (1971).

108. R. M. Silverstein and G. C. Bassler, "Spectrometric Identification of Organic Compounds," 2nd ed., John Wiley and Sons, New York (1967), p. 129.

109. C. W. Davies, J. Chem. Soc., 1938, 2093.

110. E. J. King, "Acid-Base Equilibria," Pergamon Press, Oxford (1965), p. 20.

111. R. A. Robinson and R. H. Stokes, "Electrolyte Solutions," 2nd ed., Butterworths, London (1959), pp. 231-232.

112. R. G. Bates, "Determination of pH," 2nd ed., Wiley-Interscience, New York (1973), p. 450.

113. J. H. Ritsma and F. Jellinek, Recueil, 91, 923 (1972).

114. G. R. Lenz and A. E. Martell, Biochemistry, 3, 745 (1964).

115. E. J. Kuchinskas and Y. Rosen, Arch. Biochem. Biophys., 97, 370 (1962).

116. M. T. Fairhurst, Ph.D. Thesis, University of Alberta (1975), p. 176.

117. M. T. Fairhurst, unpublished results.

118. J. T. Edsall and J. Wyman, "Biophysical Chemistry," Vol. 1, Academic Press, New York (1958), Chapter 9.

119. E. Coates, C. Marsden and B. Rigg, Trans. Faraday Soc., 65, 863 (1969).

120. M. A. Grafius and J. B. Nielands, J.A.C.S., 77, 3389 (1955).

121. N. C. Li and R. A. Manning, J.A.C.S., 77, 5225 (1955).

122. E. Coates, C. G. Marsden and B. Rigg, Trans. Faraday Soc., 65, 3032 (1969).

123. D. L. Rabenstein and M. T. Fairhurst, J.A.C.S., 97, 2086 (1975).

124. D. L. Rabenstein, J.A.C.S., 95, 2797 (1973).

125. B. J. Fuhr and D. L. Rabenstein, 95, 6944 (1973).

126. G. Jung, E. Breitmaier, W. Voelter, T. Keller and C. Taenzer, Angew. Chem., Int. Ed., Engl., 9, 894 (1970).

127. G. Jung, E. Breitmaier and W. Voelter, Eur. J. Biochem., 24, 438 (1972).

128. M. Fairhurst, Ph.D. Thesis, University of Alberta (1975), p. 94.

129. E. K. Millar, M.Sc. Thesis, University of Alberta (1978).

130. R. B. Simpson, J.A.C.S., 83, 4711 (1961).

131. H. A. Laitinen and W. E. Harris, "Chemical Analysis," 2nd ed., McGraw-Hill, Toronto (1975), p. 194.